UNIVERSIDADE DE SÃO PAULO

FACULDADE DE CIÊNCIAS FARMACÊUTICAS DE RIBEIRÃO PRETO

Isotretinoin-loaded *Delonix* polymeric nanoparticles prospects as a delivery tool in the treatment of acne

Potencial de nanopartículas poliméricas de *Delonix* contendo isotretinoína para o tratamento da acne

ABAYOMI TOLULOPE OGUNJIMI

Ribeirão Preto
2018

UNIVERSIDADE DE SÃO PAULO

FACULDADE DE CIÊNCIAS FARMACÊUTICAS DE RIBEIRÃO PRETO

ABAYOMI TOLULOPE OGUNJIMI

Isotretinoin-loaded *Delonix* polymeric nanoparticles prospects as a delivery tool in the treatment of acne

Potencial de nanopartículas poliméricas de Delonix contendo isotretinoína para o tratamento da acne

Doctoral thesis presented to the Graduate Program of School of Pharmaceutical Sciences of Ribeirão Preto/USP for the degree of Doctor in Sciences.

Concentration Area: Pharmaceutics and Cosmetics

Supervisor: Prof. Dra. Renata F.V. Lopez

Versão corrigida da Dissertação de Tese de Doutorado o apresentada ao Programa de Pós-Graduação Ciências Farmaceuticas em 16/02/2018. A versão original encontra-se disponível na Faculdade de Ciências Farmacêuticas de Ribeirão Preto/USP.

The corrected version of this Doctoral thesis was presented to the Graduate Program in Pharmaceutical Sciences on 16/02/2018. The original version is available at the Faculty of Pharmaceutical Sciences of Ribeirão Preto/USP

Ribeirão Preto
2018

Abayomi Tolulope Ogunjimi

Isotretinoin-loaded *Delonix* polymeric nanoparticles prospects as a delivery tool in the treatment of acne Ribeirão Preto, 2018.

163 p; 30cm.

Doctoral thesis presented to the Graduate Program of School of Pharmaceutical Sciences of Ribeirão Preto/USP for the degree of Doctor in Sciences. Concentration Area: Pharmaceutics and Cosmetics

Supervisor: Prof. Dra. Renata F.V. Lopez

1. Acne 2. Isotretinoin 3. Delonix polymeric nanoparticles 4. Follicular targeting 5. Topical delivery

APPROVAL PAGE

Abayomi Tolulope Ogunjimi

Isotretinoin-loaded *Delonix* polymeric nanoparticles prospects as a delivery tool in the treatment of acne

Doctoral thesis presented to the Graduate Program of School of Pharmaceutical Sciences of Ribeirão Preto/USP for the degree of Doctor in Sciences.

Concentration Area: Pharmaceutics and Cosmetics

Supervisor: Prof. Dra. Renata F.V. Lopez

Approved on:

Examiners

Prof. Dr. _____

Institution: _____ Signature:_____

Prof. Dr. _____

Institution: _____ Signature:_____

Prof. Dr. _____

Institution: _____ Signature:_____

Prof. Dr. _____

Institution: _____ Signature:_____

Prof. Dr. _____

Institution: _____ Signature:_____

DEDICATION

To everyone around the world displaced by bad leadership, religion and war

To everyone striving **genuinely** to make this world a better place

To my mother, Suzan Adunola Kehinde Ogunjimi

AKNOWLEDGEMENTS

I would like to thank my supervisor, Profa. Dra. Renata Fonseca Vianna Lopez for her supervision, dedication, advices, care and support all through this journey. Thank you so much for this opportunity to learn under you. I also appreciate her family who supports her and make her happy.

I also like to appreciate Profa. Dra. Monica Pupo, particular for making it possible to meet Profa. Renata and all her support during my PhD programme

I appreciate a host of FCFRP Professors: Prof. Dr. Freitas Osvaldo, Prof. Dr. Luis Alexandre, Prof. Dr. Flavio Emery, Prof. Dr. Wanderley, Profa. Dra. Lorena, Profa. Dra. Pryscila, Prof. Dr. Jonas and Prof. Dr. Eduardo Rocha. More than teaching and advising me, you were very accommodating and supportive.

I appreciate every single person in FCFRP maintenance unit, you were part of the first friends I made when I arrived. Thanks.

I appreciate Patricia Sper Simão, our laboratory technician for all her support and help during my research work.

I sincerely appreciate all my colleagues including those that have defended or completed their research works: Joel Goncalves, Daniela Bernardi, Karina Dias, Tatiana Pereira, Francieli Pereira, Raquel Petrilli, Danielle Ramos, Camila Lemos, Camila Cubayachi, Luciana Dalmolin, Bianca Martin, Gabriela Galvao, Hugo Favacho, Cynthia Nara, Paula Pereira, Iris Camilo, Yugo Martins, Talita Mota. You all made my stay in Brazil a wonderful and successful one. I will always remember you guys for your support and understanding me always.

This thesis will not be complete without appreciating everyone in the FCFRP postgraduate office Rosana, Eleni, Rose, Rafael and Henrique. Thank you so much for always helping out each time I come around.

I also appreciate the laboratory members of Prof. Osvaldo, Prof. Alexandre, Prof. Emery, Prof. Wanderley, Profa. Lorena, Profa. Pryscila for always being open and ready to help me during my Doctoral research.

I particularly appreciate Shaiani Gil of Prof. Emery's laboratory for always helping out when need arises.

My deepest appreciation goes to my Nigerian friends and their families - Michael Osungunna, Victor Bankole and Olakunle Jaiyesimi for making our friendship very worthwhile. It has always been a pleasure knowing you guys. I also appreciate the support of Dr. Joseph Adeyemi, Dr. Paul Arikawe and Dr. James Akindele.

I sincerely appreciate my parents Dr. Lawrence Ogunjimi and Mrs. Suzan Ogunjimi for their unending love and support. My love also goes to my brothers Fisayo Ogunjimi and Olakunle Ogunjimi and their families for their unrelenting support.

I really appreciate my wife's family Mr Adewale Adebayo and Mrs Selinah Adebayo for their support and love throughout this sojourn.

I sincerely appreciate my wife Adetola Ogunjimi for her undying love and support in all forms during this program. You are simply the best. I appreciate my son, Daniel-Oleg Ogunjimi for bringing joy into our lives - a joy that has sustained and strengthened me continuously to strive for success. I love you both so much.

I acknowledge Obafemi Awolowo University, Nigeria for granting me study leave to pursue a Doctorate degree.

I acknowledge the World Academy of Science (TWAS) and the Brazilian National Council for Scientific and Technological Development (CNPq) for availing me a fellowship to pursue a Doctorate degree with the TWAS-CNPq process number 190007/2013-3. I also acknowledge the São Paulo Research Foundation (FAPESP) from whom I benefited immensely in the thematic grant to my supervisor with process number 2014/22451-7.

Finally, I give praise to God for life, health and strength to complete this thesis.

Abstract

OGUNJIMI A.T. **Isotretinoin-loaded *Delonix* polymeric nanoparticles prospects as a delivery tool in the treatment of acne.** 2018. 163 p. Thesis (Doctorate). Faculdade de Ciências Farmacêuticas de Ribeirão Preto – Universidade de São Paulo, Ribeirão Preto, 2018

Oral isotretinoin (IST) has been effective in acne treatment; however, its use is associated with side effects such as skin dryness, epistaxis, immune disorder and psychiatric concerns while its topical gel application's effectiveness is hampered by irritancy. Protecting IST from direct skin contact and targeting its release to the hair follicles where the acne develops can reduce irritation and increase the effectiveness of treatment. Delonix (DLX) polymer is a natural galactomannan derived from *Delonix regia* seed that may be engineered to yield nanoparticles for IST skin targeting. Therefore, the aim of this study was to develop IST-loaded DLX (IST-DLX) polymeric nanoparticles and assess its skin targeting prospects for acne treatment. DLX was collected, purified and characterized by monosaccharide composition and molecular weight (Mw). Blank DLX nanoparticles, fluorescent DLX nanoparticles (BODIPY-loaded (BOD-DLX) nanoparticles) and IST-DLX nanoparticles were prepared and characterized by size, polydispersibility index (PdI), zeta potential (zp) and encapsulation efficiency (EE). *In vitro* release study of IST-DLX nanoparticles was performed using diffusion cells and synthetic membrane, while skin targeting of BOD-DLX and IST-DLX nanoparticles were assessed by confocal microscopy and differential tape stripping technique in dermatomed pig ear skin respectively. IST-DLX polymeric nanoparticles' IL-6, IL-10 and TNF-α modulation was assessed *in vitro* using lipopolysaccharide (LPS) stimulated AMJ-2 macrophage cells and antimicrobial activity was assessed in *Propionibacterium acnes* culture medium. IST-DLX nanoparticles' skin penetration and irritation were evaluated *in vivo* in Wistar rats (ethics committee approval protocol CEUA-FCFRP nº 17.5.213.60.3). DLX polymer Mw was ~177 kDa, containing predominantly mannose and galactose in ratio 6.3:1. IST-DLX nanoparticles' size determined by light scattering was between 215 to 232 nm, PdI < 0.2, zp < -30 mV, EE > 25 %. IST-DLX nanoparticles sustained IST release, with about 37% IST being released in 48 h. Confocal images showed that BOD-DLX nanoparticles accumulated in the epidermis and hair follicles as compared to free BODIPY solution which permeated into the dermis. Significantly higher and uncontrolled IST penetration into all layers of pig ear skin with IST-DLX polymer solution was observed as compared to lower, controlled but optimum IST accumulation into the pig ear skin when IST-DLX nanoparticles were used. IST-DLX nanoparticles targeted the hair follicle (26 %) as compared to IST solution (6.5 %) which permeated through all skin layers. IST-DLX polymeric nanoparticles significantly reduced IL-6 production in LPS stimulated macrophage cells at 48 h as compared to free IST solution which significantly reduced IL-6 production only at 24 h. Both IST-DLX nanoparticles and free IST solution did not inhibit *P. acnes* growth. No sign of inflammatory erythema was observed in IST-DLX nanoparticles treated Wistar rats with or without UVA irradiation as compared to free IST treated ones. Epidermal thickness of rats treated with IST-DLX nanoparticles was significantly smaller than those treated with free IST with or without UVA irradiation. It can be concluded that IST-DLX nanoparticles can target, deliver and sustain IST release to the skin at optimum concentrations, modulate IL-6 inflammatory responses and may prevent IST related inflammatory erythema *in vivo*. DLX polymer could be promising polymer for drug delivery.

Keywords: *Acne vulgaris*, Isotretinoin, Delonix nanoparticles, follicular targeting, topical delivery

Resumo

OGUNJIMI A.T. Potencial de nanopartículas poliméricas de Delonix contendo isotretinoína para o tratamento da acne**.** 2018. 163 f. Tese (Doutorado). Faculdade de Ciências Farmacêuticas de Ribeirão Preto – Universidade de São Paulo, Ribeirão Preto, 2018

A administração oral de isotretinoína (IST) é eficaz no tratamento da acne; no entanto, seu uso está associado a efeitos adversos, como ressecamento da pele, epistaxe, distúrbios imunológicos e psiquiátricos, enquanto a eficácia da aplicação tópica é prejudicada pela intensa irritação causada na pele. Proteger a IST do contato direto com a pele e direcionar sua liberação para os folículos pilosos, local onde a acne se desenvolve, pode reduzir a irritação e aumentar a eficácia do tratamento. O polímero Delonix (DLX), galactomanano natural derivado da semente de *Delonix regia*, pode ser manipulado para produzir nanopartículas para a liberação direcionada de IST na pele. Desta forma, o objetivo deste estudo foi desenvolver nanopartículas poliméricas de DLX (IST-DLX) contendo IST e avaliar seu potencial para o tratamento tópico da acne. O DLX foi coletado, purificado e caracterizado quanto a composição de monossacarídeos e massa molecular (MM). Nanopartículas DLX sem IST (branco), nanopartículas fluorescentes de DLX (nanopartículas contendo BODIPY (BOD-DLX)) e nanopartículas IST-DLX foram preparadas e caracterizadas por tamanho, índice de polidispersividade (PdI), potencial zeta (pz) e eficiência de encapsulação (EE). O estudo de liberação *in vitro* das nanopartículas IST-DLX foi realizado utilizando células de difusão e membrana sintética, enquanto a penetração cutânea das nanopartículas BOD-DLX e IST-DLX foi avaliada por microscopia confocal e *tape stripping* diferencial em pele de orelha de porco dermatomizada, respectivamente. A influência das nanopartículas IST-DLX na modulação de IL-6, IL-10 e TNF-α foi avaliada *in vitro* utilizando células de macrófagos AMJ-2 estimuladas com lipopolisacarídeos (LPS) e a atividade antimicrobiana foi avaliada em meio de cultura de *Propionibacterium acnes*. *In vivo*, as nanopartículas IST-DLX foram avaliadas quanto a penetração e irritação cutânea em ratos Wistar (protocolo de aprovação CEUA-FCFRP nº 17.5.213.60.3). A MM do polímero DLX foi de ~177 kDa, contendo predominantemente manose e galactose na proporção de 6,3:1. O tamanho das nanopartículas IST-DLX, determinado por dispersão de luz, foi entre 215 a 232 nm, PdI < 0,2, pz < -30 mV e EE > 25%. As nanopartículas IST-DLX sustentaram a liberação da IST, com cerca de 37% de IST sendo liberado em 48 h. As imagens de microscopia confocal mostraram que as nanopartículas BOD-DLX concentraram-se na epiderme e nos folículos pilosos em comparação com a solução de BODIPY livre, a qual permeou até a derme. Foi observada uma penetração de IST significativamente maior e descontrolada em todas as camadas da pele de orelha de porco quando a solução de polímero de IST-DLX foi usada em comparação com um acúmulo de IST menor e controlado quando as nanopartículas IST-DLX foram aplicadas. As nanopartículas IST-DLX direcionaram a IST para os folículos pilosos (26%) em comparação com a solução de IST (6,5%) que permeou por todas as camadas da pele. As nanopartículas IST-DLX reduziram significativamente a produção de IL-6 em células de macrófagos estimuladas por LPS, mesmo após 48 h, em comparação com a solução de IST livre, que reduziu significativamente a produção de IL-6 apenas até 24 h. Tanto as nanopartículas IST-DLX quanto a solução de IST livre não inibiram o crescimento de *P. acnes*. Não foi observado nenhum sinal de eritema nos ratos tratados com nanopartículas IST-DLX, com ou sem irradiação UVA, enquanto os tratados com solução de IST apresentaram eritema. A espessura da epiderme dos ratos tratados com as nanopartículas foi significativamente menor do que daqueles tratados com IST livre, com ou sem irradiação UVA. Conclui-se que as nanopartículas IST-DLX direcionam e sustentam a liberação de IST na pele em concentrações ótimas, modulam a resposta inflamatória da IL-6 e previnem o eritema inflamatório relacionado ao IST *in vivo*. Sendo assim, o polímero DLX pode ser considerado um polímero promissor para a liberação sustentada e direcionada de fármacos.

Palavras-chave: *Acne vulgaris*, isotretinoína, nanopartículas de Delonix, direcionamento folicular, liberação tópica

LIST OF FIGURES

LIST OF TABLES

LIST OF ABBREVIATIONS

AMJ-2	Macrophage (alveolar), infected with J2 virus
ARPE	Retina Pigment Epithelial cell
ATCC	American Type Culture Collection
DLX	Delonix
DMEM	Dulbecco's Modified Eagle Media
DMSO	Dimethyl sulfoxide
DoE	Design of Experiment
FBS	Fetal Bovine Serum
FDA	Food and Drug Administration
HEC	Human Epithelial Corneal cell
HEC gel	Hydroxy Ethyl Cellulose gel
HPLC	High Performance Liquid Chromatography
ICH	International Conference on Harmonization
IL-10	Interleukin 10
IL-6	Interleukin 6
IST	Isotretinoin
LoD	Limit of detection
LoQ	Limit of quantification
LPS	Lipopolysaccharide
MTT	Methyl thiazolyl diphenyl-tetrazolium bromide
NMR	Nuclear Magnetic Resonance spectroscopy
NRU	Neutral Red
PBS	Phosphate buffer solution
QbD	Quality by Design
SHEM	Supplemented Hormonal Epidermal Medium
TEM	Transmission Electron Microscopy
TNF-α	Tumor Necrosis Factor alpha

UFLC	Ultra-Fast Liquid Chromatography

TABLE OF CONTENTS

1 Introduction

Acne vulgaris is a common skin disease affecting probably every teenager at one stage during their lifetime (FDA; TAN & BHATE, 2015). The disease is distributed in the skin of the face, upper back, chest and shoulders where the pilosebaceous units has its highest density. It is not a life-threatening disease but can cause notable physical and mental scarring during adolescence, which is an important period of life needed for building confidence and self-esteem (WILLIAMS *et al.*, 2012; ZAENGLEIN *et al.*, 2016). Acne symptoms include soreness, pain, itching and notably, psychological concerns which negatively impart subject's quality of life.

The pathogenesis of acne which is multifactorial has made its treatment and management challenging. Retinoids, systemic antibiotics and other agents have been used in managing acne; however, Isotretinoin (IST), retinoic acid, clindamycin, tetracyclines, erythromycin, antiandrogens and benzoyl peroxide have been the mostly used either singly or in combination to ameliorate the symptoms of acne (JACOB *et al.*, 2001; OZOLINS *et al.*, 2004; THIBOUTOT *et al.*, 2009; WILLIAMS *et al.*, 2012).

Of these treatment approaches, oral IST has been the acne choice treatment which has demonstrated efficacious effects by targeting all pathogenetic factors of acne, directly or indirectly (KATSAMBAS & PAPAKONSTANTINOU, 2004). However, oral IST use is known to elicit diverse side effects including cheilitis, dry skin, epistaxis, calcification of attachment ligament areas, ocular opacity (FRAUNFELDER *et al.*, 2001; KATSAMBAS & PAPAKONSTANTINOU, 2004; RIGOPOULOS *et al.*, 2010), hepatotoxicity (SAIED & HAMZA, 2014), photo sensitivity, psychological disorders in addition to teratogenic concerns in women (WILLIAMS *et al.*, 2012). Topical IST products developed to locally manage acne show

seldom systemic absorption, skin dryness, significant skin irritation and photo-sensitivity (DUNN *et al.*, 2007; GOLMOHAMMADZADEH *et al.*, 2012; IOANNIDES *et al.*, 2002; QUEILLE-ROUSSEL *et al.*, 2001). Thus, increasing the desire for novel IST delivery approaches that can avoid systemic absorption and prevent side effects associated with topical IST use, in addition to effectively delivering a therapeutic dose of IST to the disease site.

Nanoparticles are acceptable drug delivery platforms due to their potentials of delivering drugs at optimum dose, target drugs to disease sites and improve therapeutic outcomes (ALEXIS *et al.*, 2008; KUMARI *et al.*, 2010b; WANG *et al.*, 2012). They are also beneficial when applied topically because they target and improve drug penetration into the skin, sustain drug release, protect against degradation and irritation (PROW *et al.*, 2011; ZHANG *et al.*, 2013). Biodegradable polymeric nanoparticles, specifically those derived from natural sources are attracting continuous interest due to their affordability, compatibility, non-irritancy, biodegradability and little or no toxicity (OGUNJIMI *et al.*, 2017; SARMAH *et al.*, 2011).

Natural polymers such as alginate (FRIEDMAN *et al.*, 2013), guar gum (GIRI *et al.*, 2013), chitosan (AGNIHOTRI *et al.*, 2004; HAFNER *et al.*, 2011; ÖZCAN *et al.*, 2013; TAN *et al.*, 2011) and others (BASAVARAJ *et al.*, 2010; DIAS *et al.*, 2016) have been used as topical nano-delivery polymers, with Chitosan being the most extensively studied (GELFUSO *et al.*, 2011; HAFNER *et al.*, 2011; ÖZCAN *et al.*, 2013). However, there exist other natural polymers with little or no information in literature about their use for topical delivery. One of such polymer is Delonix polymer (DLX), a galactomannan polysaccharide extracted from the endosperm of *Delonix regia* (Bojer ex Hook.) plant (KAPOOR, 1972; TAMAKI *et al.*, 2010).

Delonix regia, also known as Flamboyant, is a leguminous plant of the family Fabaceae, native to Madagascar but growing freely in other countries of the world including Brazil and Nigeria. The plant is used mostly ornamentals while its seed are sometimes used as beads. Biomedically, DLX polymer and its modified derivatives has been used as a sustained release (ADETOGUN & ALEBIOWU, 2009), mucoadhesive (DEVKAR *et al.*, 2014) and microencapsulating polymer (BETANCUR-ANCONA *et al.*, 2011); however, the versatility of the polymer as a topical nano-delivery tool has not been explored.

Thus, this current study aims at developing, optimizing, characterizing and exploring the prowess of DLX polymer as a polymeric nano-delivery platform for encapsulating and targeting IST to the skin in the treatment of acne. Additionally, the versatility of the DLX polymeric nanoparticles as a topical nano-delivery platform through the ocular route was also explored. The use of DLX polymer as a nano-delivery platform while being a green approach, will increase the database of plausible natural polymers for drug delivery and also benefit low income communities where this plant grows economically.

2 Literature Review

2.1 Skin

The skin is the largest organ in the body which accounts for approximately 15 % of the total adult body weight (KANITAKIS, 2002). It is a continuous organ which performs diverse vital functions such as prevention of excessive water loss from the body, thermoregulation and protection against hostile physical, biological and chemical substances. It could also serve as a route of delivering drugs for local and systemic disease prevention and treatment (ARCHER, 2010).

The skin is made up of three layers (Figure 1) which are the epidermis, dermis and the subcutaneous tissue or hypodermis, each serving distinct functions. The epidermis provides a waterproof barrier and dictates the tone of the skin; the dermis contains connective tissues, hair follicles, blood and lymph vessels, and sweat glands among others while the subcutaneous tissue is made up of fats and connective tissues (GRIFFITHS *et al.*, 2016; OPENSTAX, 2017 ; PROKSCH *et al.*, 2008).

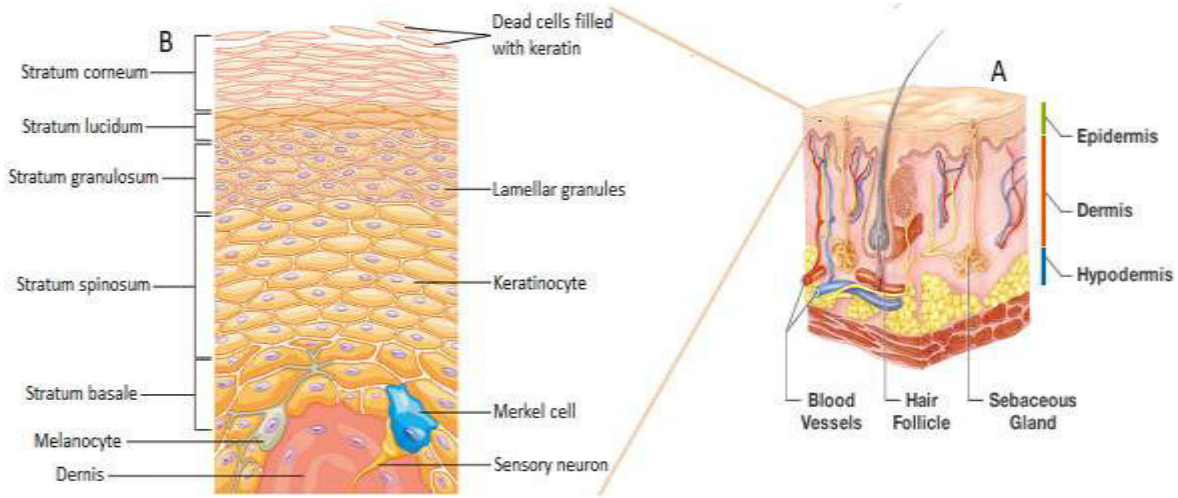

Figure 1: The skin illustration (A) and epidermal layers (B). Adapted from (OPENSTAX, 2017) and (WEBMDRESOURCES)

The epidermis is the stratified outermost skin layer, in constant renewal, that gives rise to other structures such as the pilosebaceous unit, sweat glands and nails. It is further subdivided into four layers according to keratinocytes morphology/age as they different from the deeper layers to the outermost hornified cells (Figure 1). From the deepest layer, the epidermis is divided into the basal cell layer (stratum basale/germinativum), squamous cell layer (stratum spinosum), granular cell layer (stratum granulosum) and cornified layer (stratum corneum). In some part of the body it consists of a fifth layer called stratum lucidum, lying between the stratum corneum and stratum granulosum (ARCHER, 2010; PROKSCH *et al.*, 2008).

The basal layer contains continuously dividing column-shaped basal cells that pushes older ones towards the cornified layer on the skin surface in a cycle of at least 14 days in humans. The squamous cell layer lies above the basal layer and is the thickest of the epidermis layer, being about 5 - 10 cells thick. They produce keratin, a tough, protective protein that makes up the skin, hair and nails involved in the transfer of some substances in and out of the body. The granular layer is composed of larger and flattened, living granular cells whose main function is to bind keratin filaments together. The outermost stratum corneum is made of several layers of continuously shedding dead keratinocytes (corneocytes) that provide mechanical support to the underlying epidermal layers, prevent water loss and foreign material invasion. The corneocytes are rich in protein but are surrounded by continuous lipid matrix (PROKSCH *et al.*, 2008; WEBMDRESOURCES).

Basically, the epidermis is composed of two cell types – keratinocytes and dendritic cells. The dendritic cells in the epidermis are the Langerhans cells, Merkel cells and melanocytes, each performing specific functions. The melanocytes are non-keratinocytes dendritic cells residing in

the basal layer that synthesize the pigment, melanin, which protects against UV rays. Merkel cells are oval-shaped dendritic cells domiciled within the basal layer, functioning as mechanoreceptors that are important for touch sensations. Langerhans cells are also dendritic by morphology and are more prominent in the stratum spinosum functioning as antigen presenting cells within the skin immune system (GRIFFITHS *et al.*, 2016; OPENSTAX, 2017).

The dermis is approximately 90 % of the skin thickness and functions mainly to regulate temperature and supply nourishment to the epidermis through the blood. It contains most of the body's water supply and the most specialized structures of the skin are domiciled within the dermis. These structures include the blood vessels that supply nourishment and oxygen to the skin and take away cell wastes; sweat glands that serve as thermo-regulators and excrete wastes; sebaceous glands that secret oil that keeps the skin smooth; nerve endings that transmit heat, pain and pressure sensations to the brain; lymph vessels that bathe the skin tissues with infection-fighting immune system cells; collagen, a tough insoluble protein that holds the dermis together; elastin that allows the skin to regain its initial structure when stretched and hair follicles (GRIFFITHS *et al.*, 2016; OPENSTAX, 2017). The subcutaneous layer which is made up of fats and connective tissues connects the skin to the bones and muscle; it functions as an insulator by conserving heat, a shock-absorber protecting inner organs and serves as a fat reservoir mostly used as energy reserve (GRIFFITHS *et al.*, 2016; OPENSTAX, 2017).

The topical treatment of skin diseases is attractive as it can reduce the systemic load and side effects of active pharmaceutical ingredients when compared to the oral or parenteral routes of administration; more importantly, when local skin diseases are being treated (PRAUSNITZ &

LANGER, 2008). The very efficient skin barrier, stratum corneum has however posed a major challenge to a drug reaches the viable layers of the skin where most skin diseases settle.

Current researches are therefore looking at approaches using nanotechnology, penetration enhancers, iontophoresis and sonophoresis in addition to leveraging on other penetration routes within the skin structure to improve drug penetration into or through the skin (NAIK *et al.*, 2000; PRAUSNITZ *et al.*, 2004; WILLIAMS, 2003).

In intact skin, active substances can enter into the deeper layers of the skin through three pathways (Figure 2); the transcellular route which involves the unidirectional movement of solutes through the horny cells and lipid matrix, intercellular route involving the diffusion of solutes around the corneocytes in a sinuous way but constantly remaining within the lipid matrix and the transappendageal route associated with the sweat ducts, follicles and sebaceous gland (BARRY, 2002).

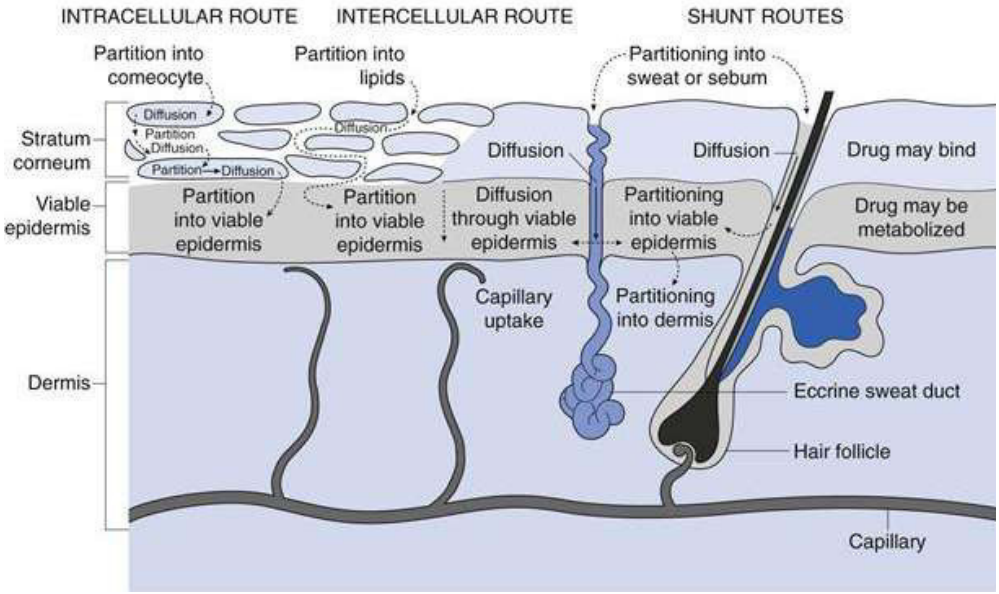

Figure 2: Transport routes within the mammalian skin (CLINICALGATEIKNOWLEDGE, 2015)

2.2 **Acne**

Acne vulgaris is a common but complex skin disease that affects probably every teenager at one point of their life, but can also extend as a chronic disease throughout adulthood. It is the eight most prevalent disease worldwide with lifetime prevalence approaching 90% (FDA; TAN & BHATE, 2015). It is a skin disorder with distribution corresponding to highest density of pilosebaceous units which are predominantly in the skin of the face, upper back, chest and shoulders. Acne is normally not a life-threatening disease, but could cause both visible and psychological scarring during the adolescent age, an important and vulnerable stage of life needed for building confidence and self-esteem. The symptoms of acne include soreness, pain and itching, but most importantly, its negative influence on the quality of life of subjects has precipitated diverse psychological concerns (KATSAMBAS & PAPAKONSTANTINOU, 2004; LEHMANN *et al.*, 2002; OBEREMOK & SHALITA, 2002; WILLIAMS *et al.*, 2012).

The grading of acne (Figure 3) has posed challenges as there is no real consensus on applicable parameters; as such, no scale can be called a ‘gold standard’. However, the Leeds revised acne grading system that grades acne based on photographic images comprising 12 facial, 8 chest and 8 back severity categories in addition to 3 facial grades for non-inflamed acne is one of the prominent grading system for acne while the global acne grading system (GAGS) uses a quantitative scoring system with total severity score based on the summation of six regional subscores (JACOB *et al.*, 2001; ZAENGLEIN *et al.*, 2016).

Figure 3: Clinical images of different types and degree of acne showing (A) macrocomedones (B-D) papules and pustules with presence of some scarring (E-F) nodules and cysts characteristic lesions with evidence of scarring (pictures adapted from www.google.com)

The pathogenesis of acne is multifactorial (Figure 4) and generally starts with an androgen controlled increase or altered sebaceous gland activity and sebaceous follicle obstruction, hypercornification of the pilosebaceous unit, microbial colonization of the pilosebaceous units by *Propionibacterium acnes* and inflammatory mediation when the body triggers the complement pathway against the bacterial colonization (BHAMBRI *et al.*, 2009; TOYODA & MOROHASHI, 2001; ZOUBOULIS *et al.*, 2005).

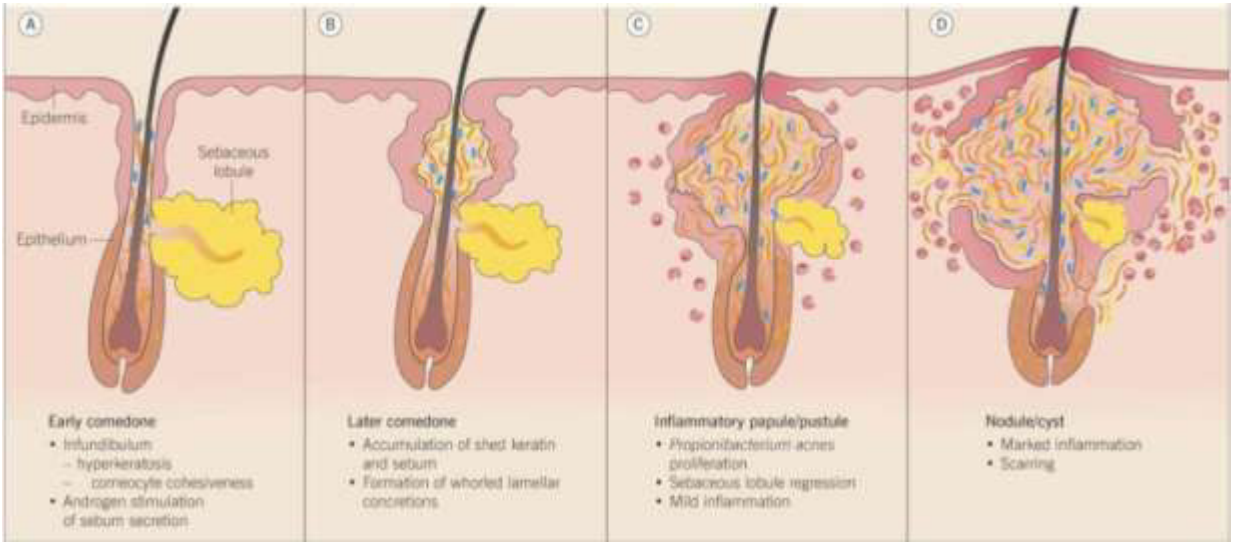

Figure 4: Pathogenetic pathway of acne (BOLOGNIA *et al.*, 2003)

The first factor observed in acne pathogenesis is the androgen-induced overproduction of sebum as the sebaceous glands are highly sensitive to androgens when compared to estrogens (CUNLIFFE, 1998). This significant increase generally concise with the puberty period, a period noted for the development of acne (TOYODA & MOROHASHI, 2001). This sebum is trapped in microcomedos, causing the follicle to be enlarged which furthers leads to the total destruction of normal follicular architecture and formation of thin-walled cystic lesions called comedo (TOYODA & MOROHASHI, 2001).

The second factor, hyperkeratinization has not been fully understood, but it has been shown to lead to sebaceous follicle obstruction. However, in acne-affected follicles, epithelium desquamation process is generally altered leading to thicker and more cohesive stratum corneum horny cells. These horny cells cohesiveness reduces their shedding in the normal process, eventually leading to follicular occlusion (TOYODA & MOROHASHI, 2001). The entrapment of sebum within the occluded follicles highly favors *P. acnes* colonization, being the third pathogenic factor.

P. acnes, an anaerobic gram-positive microbe survives optimally in anaerobic comedone sites filled with triglyceride substrates as nutrient source. Also, free fatty acids produced as metabolites of *P. acne* activity on trapped triglycerides can act as comedogenic and acnegenic factors in addition to irritating the follicular wall, leading to inflammatory responses (MARPLES *et al.*, 1971; TOYODA & MOROHASHI, 2001). The rupture of comedos and sipping of its contents into the dermis rather than the skin surface and *P. acnes* induced chemotactic factors sets the pace for inflammatory responses. This leads to various immunological processes including phagocytosis of *P. acnes* and release of inflammatory factors by the neutrophils (TOYODA & MOROHASHI, 2001; TUCKER *et al.*, 1980). Other factors such as emotional stress, psychological factors and genetic influences have been shown to exacerbate acne and comedone susceptibility (TOYODA & MOROHASHI, 2001).

The multifactorial pathogenicity of acne has made its treatment and management quite challenging. Acne, being a human disease and due to its multifactorial pathogenicity lacks fitting animal models, making research into the development of new acne treatment and management strategies challenging. Several *in vivo* and other *in vitro* approaches to studying acne using sebocytes, keratinocytes or monocytes in association with *Propionibacterium acnes* has yielded few successes as results do not accurately fit with real acne scenarios (MIRSHAHPANAH & MAIBACH, 2007; ZOUBOULIS *et al.*, 1998).

2.2.1 **Acne treatment and management**

The combination of personal hygiene, counseling, retinoids and systemic antibiotics have been used in the treatment and management of acne. Isotretinoin (IST), retinoic acid, clindamycin, tetracyclines, erythromycin, antiandrogens, benzoyl peroxide, among others have

been used to treat acne and have been shown to have very strong effects to moderate, to no effect on the different pathogenetic factors implicated in acne (JACOB *et al.*, 2001; WILLIAMS *et al.*, 2012). These drugs generally target one or more factors in the pathogenic pathway of the disease. Other complementary and alternative treatment approaches in acne includes the use of *Aloe vera*, fruit derived acids, pyridoxine and ayurvedic herbal treatments whose mechanism of potential benefits were biological plausible; however, their use have been relegated due to poor data quality and inconclusiveness of study (MAGIN *et al.*, 2006).

Of these treatment options, oral IST has been shown to have superior efficacy in treating acne; however, its use comes with several side effects (ERTURAN *et al.*, 2012; FRAUNFELDER *et al.*, 2001; LIU *et al.*, 2007; STRAHAN & RAIMER, 2006). Because it is the drug of interest in this work, its beneficial and harmful effects will be specified in the next section.

Other oral medications that have been successfully used in the treatment of acne include oral antibiotics and contraceptives. Oral antibiotics are used for severe acne and have only been shown to reduce lesions and not clear off the acne, a major need of patients. The preferred antibiotics include benzoyl peroxide, oral tetracyclines and erythromycin. No specific benefit of one antibiotic over the other has been seen, nor oral antibiotics being better over topical antibiotic preparations; therefore, antibiotic choice depends on the preference and tolerability of a patient (OZOLINS *et al.*, 2004). However, several concerns over antibiotic resistance have been raised as acne treatment with antibiotics is generally for longer periods (EADY *et al.*, 2003). Combined oral contraceptives containing oestrogen (ethinylestradiol) and a progestogen have also been prescribed for use to treat acne in women as oestrogen suppresses sebaceous

gland activity, decreases ovarian and adrenal androgens while progesterone binds to both progesterone and androgen receptors to effect its androgenic effects. (AROWOJOLU *et al.*, 2012). This treatment option is however used only in women and it is associated with known oral contraceptive side effects such as headaches and breast tenderness while its use has to be balanced with a woman's desire for pregnancy

The use of topical treatment alone or in combination has also shown efficacy in effectively treating mild acne, with each treatment option offering different modes of action and acting within the application site (WILLIAMS *et al.*, 2012). Different topical preparations have also been employed. Topical antibiotics improve acne in a yet to be understood mechanism which probably might be due to direct actions on *P. acnes*. Topical benzoyl peroxide has been shown to be a safe and effective treatment option for mild to moderate acne, exerting its effect through different mechanisms (FAKHOURI *et al.*, 2009; HUGHES *et al.*, 1992; LYONS, 1978). Topical retinoids (tretinoin, adapalene and IST) generally require medical prescriptions and they tend to locally target all pathogenic stages of acne, however, only IST have been shown to successfully reduce sebum secretion (WILLIAMS *et al.*, 2012). Skin irritation is however a major concern in the use of these topical retinoids, thus prompting the need for novel approaches to deliver IST topically.

Table 1 shows therapeutic options that has been used in the treatment of acne, their targets in the pathogenic pathway of acne and the degree of their effectiveness (WILLIAMS *et al.*, 2012).

Table 1: Targets in acne management (WILLIAMS *et al.*, 2012)

	Sebum secretion	Keratinization	Follicular *P. acnes*	Inflammation
Benzoyl peroxide	-	(+)	+++	(+)
Retinoids	-	++	(+)	+
Clindamycin	-	(+)	++	-
Antiandrogens	++	+	-	-
Azelaic acid	-	++	++	+
Tetracyclines	-	-	++	+
Erythromycin	-	-	++	-
Isotretinoin (IST)	+++	++	(++)	++

+++ = very strong effect, ++ = strong effect, + = moderate effect, (+) = indirect/weak effect, –= no effect

Other approaches that have been used in the treatment of acne are the use of lasers, light sources and photodynamic therapy. Studies suggests that photodynamic therapy, infrared lasers, broad-spectrum light sources, pulsed dye lasers, intense pulsed light and potassium titanyl phosphate laser are the major sources of light used in optically mediated acne treatment. All studies suggests short term improvement in inflammatory acne using optical treatment approaches; however, pain, redness, increased pigmentation and swelling are known adverse effects and the long term benefits and comparativeness of these optical treatments with conventional acne therapies requiring further studies (SAKAMOTO *et al.*, 2010).

2.2.2 **Isotretinoin**

Isotretinoin (IST), also known as *13-cis-retinoic acid* is a retinoic acid derivative that has been used orally in the treatment of severe acne and also tried in aging and certain cancer therapy. Its mechanisms of action in acne therapy have not been completely elucidated, but it has been shown to mediate in all pathogenetic pathways of acne.

IST is a yellow to orange colored powder with molecular weight of about 300.44 Da. Its chemical structure is shown in Figure 5.

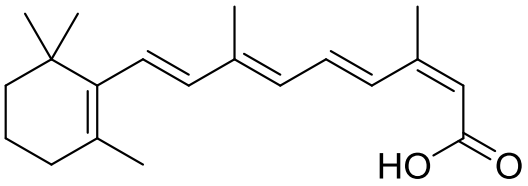

Figure 5: Isotretinoin chemical structure

Oral IST has shown better efficacy in the treatment of mild to severe acne, but its use is associated with diverse side effects (ERTURAN *et al.*, 2012; FRAUNFELDER *et al.*, 2001; MCLANE, 2001; STRAHAN & RAIMER, 2006). For instance, oral IST causes dry skin and lips, cheilitis, epistaxis, photosensitivity, secondary infections and can lead to temporary worsening of acne lesions while its teratogenicity mandates that its use in women of child bearing age should be accompanied with necessary contraceptives. In two large clinical trials sponsored by Roche on IST, mucocutaneous side effects involving the eyes, mouth, lips and other epidermal surfaces were reported (BRELSFORD & BEUTE, 2008). Other side effects that have been reported include psychiatric disorders, inflammatory bowel disease, hepatotoxicity and hypertriglyceridemia, which have necessitated liver function tests and lipid level monitoring in patients using oral IST (CHARAKIDA *et al.*, 2004; MCLANE, 2001). Psychiatric concerns on oral IST use in patient has been controversial; however, data related to depression, suicidal ideation, suicide attempts and suicide has been well documented (NG *et al.*, 2002; STRAHAN & RAIMER, 2006). These side effects have thus led to the search of safer alternatives routes for IST.

Topical IST, commercially available in gel form has been shown to have clinical efficacy directly or indirectly on all four pathogenic pathways of acne. Randomized controlled clinical

trials show that higher strength IST formulations are more efficacious than lower strength ones but at the expense of local irritations including erythema, peeling, scaling, dryness and redness. IST, like other topical retinoids induces local effects like skin sensitivity which are further worsened by exposure to UV light (WILLIAMS *et al.*, 2012; YENTZER *et al.*, 2009).

Novel approaches using vesicular carriers such as liposomes and nanoparticles have been exploited in the targeted delivery of IST to the skin, with an extra bid to reduce known local side effects associated with the commercial gel. Raza (RAZA, SINGH, SINGAL*, et al.*, 2013) systemically optimized IST solid lipid nanoparticles (SLN), studied the skin retention and *in vivo* skin compliance of IST in SLN and commercial gel. Their results showed that optimized SLNs delivered substantial amount of IST to the skin and demonstrated better skin compliance as compared to commercial gel. They however did not quantify the amount of IST in different layers of the skin. In another study, they demonstrated higher skin retention and accumulation of IST from loaded-nanocolloidal carriers (SLN and nanolipid carrier (NLC)) into the dermis using an *in vitro* Laca mice model as compared to commercial gel. The study also showed that loaded SLN and NLC significantly reduced the minimum inhibitory concentration (MIC) as compared to free IST when incubated with *P. acnes* (RAZA, SINGH, SINGLA*, et al.*, 2013) suggesting a probable direct antimicrobial action of IST on *P. acnes*.. Another study assessed the *in vitro* skin permeation and accumulation of IST from different IST-loaded SLNs in comparison to IST tincture. They concluded that loaded SLNs produced optimum IST accumulation in skins and prevented the systemic uptake of IST (LIU *et al.*, 2007). In another related study, microemulsions loaded with IST were assessed in terms of skin accumulation using pig skin model in comparison to commercial Isotrexin® gel containing IST and erythromycin (GÜRBÜZ *et al.*, 2015). They also observed significant accumulation of IST from loaded microemulsions

into skin layers as compared to commercial gels, with higher IST amounts recovered from the stratum corneum as compared to the rest of the skin (GÜRBÜZ *et al.*, 2015). There is however no study that has explored polymeric platform for the delivery of IST in the treatment of acne. Polymeric nanoparticles do not penetrate into the skin but studies have shown that they can preferentially target and accumulate in hair follicles and release their encapsulated contents (ALVAREZ-ROMÁN *et al.*, 2004; MITTAL *et al.*, 2013); these polymeric nanoparticles platforms could be beneficial in acne treatment.

2.3 **Polymeric nanoparticles**

Interest in biodegradable polymeric nanoparticles has surged over the past few decades as they have been proven to be effective drug delivery platforms. They can effectively deliver small molecules, peptides, proteins and genes to target sites, minimize non-specific toxicity and increase therapeutic benefits, increase bioavailability and control the release of these molecules. Their surfaces can also be adequately functionalized or modified to target specific biological ligands associated with diseases, for diagnosis and therapeutic purposes. These polymeric nanoparticulate systems can also protect drug molecules from degradation, thus increasing their stability (KUMARI *et al.*, 2010b; OGUNJIMI *et al.*, 2017; SOPPIMATH *et al.*, 2001). Biodegradable polymeric nanoparticles, which are generally within the size range of 100 to 1000 nm are prepared by scalable methods that have been shown to significantly improve encapsulation efficiency of drug molecules when compared to other nanoparticulate carriers such as liposomes and SLNs; they have been used to deliver molecules successfully through the oral, ocular, intravenous and transdermal routes (KUMARI *et al.*, 2010a; WIN & FENG, 2005).

Biodegradable polymers used in the synthesis of polymeric nanoparticles can be divided into synthetic, semi-synthetic and natural polymers. Synthetic polymers such as poly lactic acid (PLA), poly glycolic acid (PGA), poly lactic acid-co-glycolic acid (PLGA) among others and semi-synthetic polymers such as ethyl cellulose and hydroxypropyl methyl cellulose have been studied as delivery platforms for drug molecules through different routes and for diverse diseases (ANDERSON & SHIVE, 2012; ELZOGHBY *et al.*, 2011; KUMARI *et al.*, 2010b). However, natural polymers are attracting more interest nowadays as nano-delivery platforms because of their biocompatibility, biodegradability, affordability, little or no toxicity, non-irritancy and availability (HUANG & FU, 2010). They also possess mucoadhesive properties and generally swell to form a gel-like layer on their surfaces which can retard fluid ingression into their polymer core, thereby sustaining drug release (OGUNJIMI *et al.*, 2017; SARMAH *et al.*, 2011). Like synthetic polymers, their surfaces can also be modified or functionalized for targeted delivery (LIN *et al.*, 2008; WANG *et al.*, 2011).

Natural polymers including guar gum, alginate, gelatin and chitosan have been studied as nano-delivery platforms for different diseases through the ocular (BHOWMIK *et al.*, 2013; GRATIERI *et al.*, 2010; NAGARWAL *et al.*, 2009), pulmonary (GRENHA *et al.*, 2008; SHAM *et al.*, 2004; ZAHOOR *et al.*, 2005) and transdermal (AHMED & KHALID, 2014; FRIEDMAN *et al.*, 2013; NITTA & NUMATA, 2013) routes, in addition to their use in cancer (GUO *et al.*, 2013; KIM *et al.*, 2008; LEE *et al.*, 2011) and antiretroviral therapies (JAIN *et al.*, 2008; MENG *et al.*, 2011). Chitosan, a cationic polysaccharide and its derivatives has been the most extensively studied polymer for biological applications (AHMED & KHALID, 2014; GELFUSO *et al.*, 2011; GRATIERI *et al.*, 2010; HAFNER *et al.*, 2011; KIM *et al.*, 2008; LEE *et al.*, 2011; LOH *et al.*, 2012); however, there are other natural polymers of interest that are currently

underutilized, but which could have potentials for drug delivery. One example of these polymers is Delonix (DLX) polymer.

2.3.1 **Delonix polymer**

Delonix (DLX) polymer is a galactomannan polysaccharide extracted from the endosperm of *Delonix regia* (*Bojer ex Hook.) fam. Fabaceae,* seed. Delonix plant, also called Flamboyant (Figure 6) is a leguminous plant native to Madagascar but growing freely in diverse countries around the world including Brazil and Nigeria. The plant is widely used as an ornamental while its seeds, highly rich in a polymeric galactomannan are used as beads when dried. Delonix galactomannan has been shown to be composed of galactose and mannose repeating units (KAPOOR, 1972; NWOKOCHA *et al.*, 2017; TAMAKI *et al.*, 2010).

Figure 6: *Delonix regia* (flamboyant) tree (source: google.com)

Delonix and its modified derivatives have currently been characterized (NWOKOCHA *et al.*, 2017) as an excipient for sustained release oral tablets (ADETOGUN & ALEBIOWU, 2007; ADETOGUN & ALEBIOWU, 2009; TEKADE & GATTANI, 2009, 2010), mucoadhesive (DEVKAR *et al.*, 2014) and microencapsulation agent (BETANCUR-ANCONA *et al.*, 2011). We are currently aiming at assessing Delonix polymeric nanoparticles prospects as a topical delivery platform in the treatment of acne.

3 Objectives

The general objective of this dissertation was to evaluate the prospect of IST-loaded DLX polymeric nanoparticles in the treatment of acne and the versatility of DLX polymer as a drug delivery platform. In order to achieve this objective, the sub-objectives of this study were;

- Extract, purify and characterize DLX polymer
- Prepare, optimize and characterize DLX polymeric nanoparticles
- Prepare and characterize IST-loaded DLX polymeric nanoparticles
- Develop and validate a HPLC method for the quantification of IST
- Evaluate the prospect of IST-loaded DLX polymeric nanoparticles for skin targeting *in vitro*
- Assess how IST-loaded DLX polymeric nanoparticles can mediate in the pathogenic pathways of acne *in vitro*
- Investigate IST-loaded DLX polymeric nanoparticles photo-protection and skin penetration *in vivo*
- Evaluate the versatility and prospect of DLX polymeric nanoparticles in ocular delivery

4 Materials and Methods

4.1 **Raw materials, solvent and reagents**

- Acetone (Synth, Brazil)
- Amphotericin B (Sigmaaldrich, USA)
- Brain Heart Infusion (BHI) medium (Oxoid Microbiology Products, UK)
- Cholera Toxin (Sigmaaldrich, USA)
- Dimethyl sulfoxide (DMSO) (Synth, Brazil)
- DLX polymer (Extracted and processed from *Delonix regia* trees in the Ribeirao Preto campus of University of São Paulo)
- Dulbecco's Modified Eagle's Medium (DMEM) (Life Technologies)
- Epidermal growth factor (EGF) (Sigmaaldrich, USA)
- Ethanol (Merck, Germany)
- Fetal Bovine Serum (FBS) (Life Technologies, USA)
- Gentamycin (Life Technologies)
- HPLC grade Acetonitrile (J.T. Baker, USA)
- Hydrocortisone (Sigmaaldrich, USA)
- Hydroxy Ethyl Cellulose (Embra Farma, Brazil)
- IST (Glsyntech, USA)
- ITS liquid media supplement (ITS) (Sigmaaldrich, USA)
- Methanol, HPLC grade (J.T. Baker, USA)
- MilliQ water (Millipore, USA)
- Neutral Red dye (Merck, Germany)
- Olive oil (Vineves, Portugal)
- Poloxamer 407 (BASF, Germany)
- Polyethylene glycol sorbitan monolaurate *(Tween 20)* (Synth, Brazil)
- Polyethylene glycol sorbitan monooleate (*Tween 80*) (Synth, Brazil)
- Resazurin (Sigmaaldrich, USA)
- Sodium Chloride (Vetec, Germany)

- Sodium phosphate (mono and di-basic) (Synth, Brazil)
- Sorbitan monooleate (Span 80) (Synth, Brazil)
- Trifluroacetic acid (Tedia, USA)
- Trypsin (Life Technologies, USA)

4.2 **Equipments and accessories**

- Analytical balance (Shimadzu, Kyoto, Japans
- Arbitrary Waveform generator (Agilent Technologies, California, USA)
- Ball mill (Retsch, Germany)
- Bath sonicator (QUIMIS, Brazil)
- Cell incubator (Thermo Scientific, USA)
- Centrifuge (Thermo Scientific Heraeus Megafuge 16R, ThermoFisher Scientific, USA)
- Confocal microscope (Leica TCS SP8 Confocal microscope, Leica, Germany).
- Dermatome 75 mm (NOUVAG AG, Switzerland)
- Differential Refractometer (Waters, USA)
- Flow cytometer (BD FACSCanto I, USA)
- Gas-Liquid Chromatography/Mass spectrometer (GCMS) (Shimadzu, Kyoto, Japan)
- High Performance Liquid Chromatography (HPLC) (Shimadzu, Kyoto, Japan)
- Laminar flow hood (VECO, Brazil)
- Magnetic agitator (TECNAL, Brazil)
- Magnetic agitator, 15-point (Marte, Brazil)
- Micro hair clipper (WAHL, USA)
- Microplate reader (Cary 50 MPR, VARIAN Inc., USA)
- Microplate Reader (Cary 50 MPR, VARIAN Inc., USA)
- Nuclear Magnetic Resonance (NMR) Spectroscopy (Bruker, USA)
- Perylstatic pump, PumpPro (Watson-Marlow Bredel, UK)

- Philips UVA Actinic BL/10 lamp (Eindhoven, Netherlands)
- Probe Ultrasound (VCX 500, Sonic & Materials, USA)
- Semi-micro osmometer (K-7400, KNAUER).
- Super micro hair clipper (WAHL, USA)
- UFLC Prominence system (Shimadzu®, Kyoto, Japan)
- Ultra Turrax homogenizer (IKA, Germany)
- Ultrafreezer -80^{o}C (Thermo Scientific, USA)
- UV Spectrophotometer (UV-1800, Shimadzu, Japan)
- VLX-3W Vilber Lourmat Radiant Power Meter (Marne-la-Vallee, France)
- Vortex Genius 3 (IKA, Germany)
- Zetasizer Nano ZS (Malvern, United Kingdom)

4.3 **Cell lines and culture mediums**

The cell lines used in this study are 3T3 Balbc Fibroblast cells (Cell Bank, Rio de Janeiro, Brazil), Retinal Pigment Epithelial (ARPE-19, Cell Bank, Rio de Janeiro, Brazil), Immortalized Human Corneal Epithelial (HCE) cells**,** AMJ–2 macrophage cells (ATCC, USA) and *Propionibacterium acnes* (CCT) purchased from the Fundação Tropical de Pesquisas e Tecnologia André Tosello, Campinas, SP, Brazil. The culture medium for 3T3 Balbc fibroblast and AMJ-2 macrophage cells was DMEM completed with 10 % FBS and antibiotics, that of ARPE-19 was DMEM:F12 (1:1) completed with 10 % FBS and antibiotics while that of HCE was Supplemented Hormonal Epidermal Medium (SHEM). The SHEM is composed of DMEM:F12 (1:1) and supplemented with 5% FBS, amphotericin B, ITS, dimethyl sulfoxide (DMSO), hydrocortisone, epidermal growth factor (EGF), cholera toxin and gentamycin. The cells were generally maintained under cryopreservation in liquid nitrogen using their respective

complete growth mediums and 10 % DMSO. The culture medium for *P. acnes* was BHI and cells were cultured under anaerobic conditions.

4.3.1 **Neutral Red stock solution**

Neutral red stock solution was prepared by dissolving 0.4 g of Neutral Red powder in 100 mL of MilliQ water. The stock solution was prepared freshly and stored in the dark at room temperature for not more than 2 months.

4.3.1.1 **Neutral Red medium**

The Neutral Red medium was prepared by mixing 1 mL of Neutral Red stock solution with 79 mL of complete DMEM. The Neutral Red medium was generally incubated overnight at 37^{o}C and centrifuged (600 g, 10 min) before use.

4.3.1.2 **Neutral Red Desorb solution**

The Neutral Red desorb solution comprising of ethanol, distilled water and glacial acetic acid was always prepared freshly by mixing the three components in percentages of 50, 49 and 1 % respectively throughout this study.

4.4 **Collection and purification of Delonix polymer**

Delonix (DLX) polymer was collected manually (after identification by a Botanist) from mature and ripe pods (fruit) of *Delonix regia* plant within the vicinity of the University of Sao Paulo, Ribeirao Preto campus. Seeds from the pods were split open and the polymeric endosperm was removed, dried (50ºC) in oven and pulverized. The milled unpurified DLX polymeric mass was redispersed in sufficient distilled water (to a maximum of 2 % dispersion) for 48 h, filtered

under negative pressure with a Buchner funnel to remove all undissolved materials and then precipitated with excess absolute ethanol (Figure 7). The precipitate was filtered and washed twice with acetone, oven dried at 50ºC, pulverized, sieved (250 µm sieve-size) and stored until needed. The DLX polymer obtained from this process was named DLXp.

Figure 7: DLX polymer purification process

4.5 **Preparation of DLX polymer solution**

The DLX polymer solution throughout this study was prepared by dispersing required amounts of DLXp polymer in 0.5 M NaOH for 24 h to obtain a homogeneous dispersion. The solubilized polymer was centrifuged and filtered (15000 x g, 20 min; 0.8 µm pore filter) to remove undissolved matter. The mildly viscous polymer filtrate was sonicated (20 Hz, 40 % amplitude; VCX 500, Sonic & Materials, Inc, USA) for 30 min and the solution stored in refrigerator for at least 24 h before use. This polymer solution was named DLXs while the polymer solution described above but without sonication process was termed DLXu.

4.6 **Characterization of DLX polymer**

4.6.1 **General analysis**

The total carbohydrate content of DLX polymer was determined by the phenol-sulfuric acid assay method (DUBOIS *et al.*, 1956) while protein content was determined by Bradford assay (BRADFORD & WILLIAMS, 1977) method using Coomassie Brilliant Blue G 250.

4.6.2 **Monosaccharide composition**

The process of preparing DLX polymeric nanoparticles (described in subsequent sections of this work) involves sonication of the polymer dispersion. Thus, monosaccharide composition was determined for the sonicated (DLXs), unsonicated (DLXu) and purified (DLXp) DLX polymer dispersion.

The DLXp, DLXs and DLXu were completely hydrolyzed with 2 mol/L trifluoroacetic acid (TFA, 5h, 100ºC). The hydrolyzed polymers were reduced with sodium borohydride for 2 h and the alditols were acetylated with pyridine:acetic anhydride (1:1 v/v, 18 h) at room temperature. The resulting alditol acetates were analyzed by GCMS using ZB-5MS (30m x 0.25mm x 0.25um) Zebron-Phenomenex column (OGUNJIMI *et al.*, 2017).

4.6.3 **Methylation analysis: DLXs and DLXu**

The polysaccharides (5 mg) were methylated according to established methods (CIUCANU & KEREK, 1984). Each per-O-methylated polysaccharide was pre-treated with 72% v/v H_2SO_4 (1 h, 4ºC) and water was added to a final acid concentration of 8% (18 h) at room temperature. The hydrolyzed polymer were reduced with acetylated borohydride and analyzed by CGMS as described in 4.4.2 (OGUNJIMI *et al.*, 2017).

4.6.4 ^{13}C and ^{1}H Spectroscopy

The DLXs and DLXu polymers were subjected to NMR analysis. All NMR spectra were obtained using a Bruker 400 MHz Avance III 14.1 T spectrometer equipped with an inverse 5-mm pentanuclear resonance probe head (QXI) at 303K. Chemical shifts were expressed in δ (ppm) relative to the resonance of DSS (sodium 4,4-dimethyl-4-silapentane-l-sulphonate) and methanol used as an internal standard (~ = 0) for ^{1}H and for ^{13}C respectively (OGUNJIMI *et al.*, 2017)

4.6.5 Determination of Molecular weight (Mw)

The average Mw of DLXs and DLXu polysaccharides were determined by size exclusion chromatography (Waters Gel Permeation Chromatography, Model 510), using a Sepharose CL-4B chromatographic column (43 x 1.8 cm, Mw range of $3x10^4 – 5x10^6$) and water as the mobile phase at a flow rate of 0.6 mL/min. Eluted samples were monitored with a differential refractometer (Model R401, Waters, USA). Sugars were identified by comparing the retention times shown in the peaks of DLXs and DLXu samples with those of dextran standard samples (OGUNJIMI *et al.*, 2017).

4.7 DLX Polymeric Nanoparticles - Design and Development

4.7.1 Design of Experiment (DoE)

To adequately control critical parameters that could influence the DLX polymeric nanoparticles properties, a Quality-by-Design (QbD), modified nanoprecipitation approach was employed. The potential factors that could influence the desired quality of the DLX polymeric nanoparticles were assessed by deploying a Fishbone diagram (Figure 8).

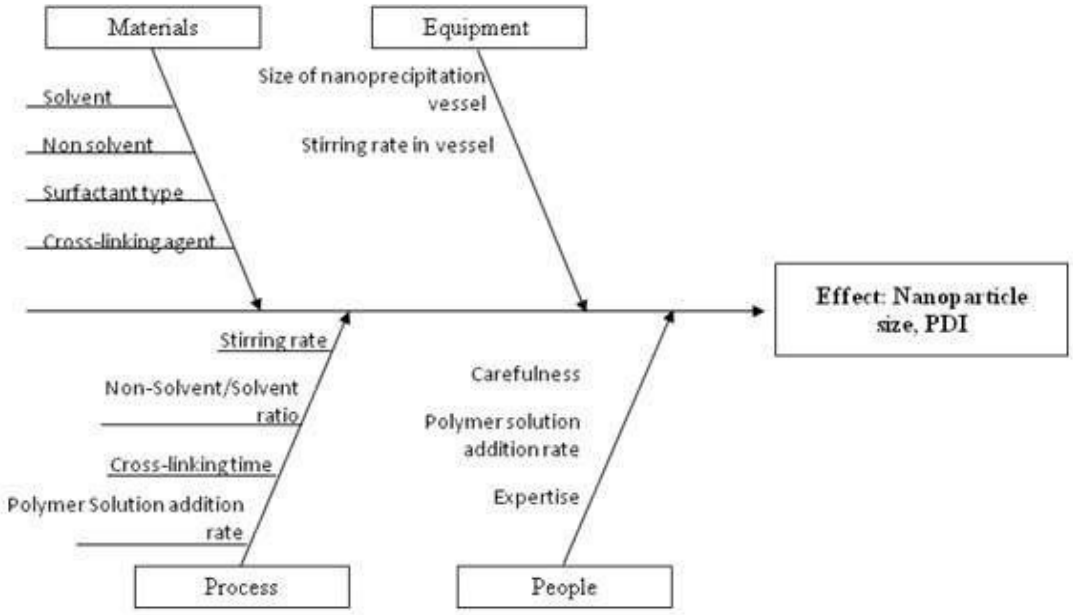

Figure 8: Fishbone diagram of probable factors that could influence the properties of Delonix polymeric nanoparticles

Selection of non-solvent was done with attention to the perceived toxicity of non-solvent; therefore, non-solvents such as methanol and acetone were avoided. Thus, 1 % DLX polymer solution was added drop-wise to isopropyl alcohol (IA), ethanol or IA/ethanol mixture (1:1 and 1:3) containing Tween 80 as surfactant. DLX polymeric nanoparticles produced were characterized by hydrodynamic diameter and polydispersibility index (PdI).

After selection of ethanol as the optimum non-solvent medium, different surfactants were tested to select an optimum surfactant that could stabilize the DLX polymeric nanoparticles. For this, 1 % DLX polymer solution was added drop-wise to ethanol containing 5% of Poloxamer 407, Span 80, Tween 80 or Tween 20. The DLX polymeric nanoparticles thus produced were characterized by hydrodynamic diameter and PdI. Decision on the surfactant selection and surfactant concentration for the final DLX polymeric nanoparticles preparation method was made based on results from these experiments.

Based on carefully researched knowledge space and experiments described above, three factors that could influence the desired DLX polymeric nanoparticles properties were selected - *polymer concentration, surfactant mix ratio and non-solvent/solvent ratio*.

These factors were thereafter tested at three levels using a completely randomized 15-experiment Box Behnken statistical design shown in Table 2. The influence of these process variables on selected DLX polymeric nanoparticles hydrodynamic diameter, PdI and zeta potential (zP) was evaluated. Analysis of Variance (ANOVA) was performed to identify statistically significant factors while general linear modeling was used for parameter estimate.

Table 2: Box Behnken design for DLX polymeric nanoparticles

	Coded variable		
Formulation	X_1	X_2	X_3
F1	-1	0	1
F2	1	1	0
F3	1	0	1
F4	-1	1	0
F5	1	-1	0
F6	0	0	0
F7	-1	0	-1
F8	0	1	1
F9	0	0	0
F10	-1	-1	0
F11	1	0	-1
F12	0	-1	-1
F13	0	0	0
F14	0	-1	1
F15	0	1	-1

Coded variables	Uncoded variables	-1	0	1
X_1	Polymer concentration (%)	1.0	1.5	2.0
X_2	Surfactant mix ratio (Tween 80:Span 80)	3:2	4:1	1:0
X_3	Non-solvent : solvent ratio	10	15	20

4.7.2 **Preparation of blank DLX polymeric nanoparticles**

The DLX polymeric nanoparticles were prepared by a modified nanoprecipitation process (Figure 9) using absolute ethanol as the non-solvent. The non-solvent solution was first prepared by adding necessary volume of 5 % surfactant mix (Tween 80 and/or Span 80) to absolute ethanol (non-solvent) based on the Box Behnken design in Table 2 and mixing for 10 minutes under moderate magnetic stirring. Exactly 1 mL of DLX polymer solution was added to the non-solvent solution under magnetic stirring (1000 rpm) at a polymer flow rate of approximately 1 mL/min. The mildly turbid DLX polymeric nanoparticles dispersion was allowed to stand briefly under reduced magnetic stirring speed. The mixture was then centrifuged at 15,000 g for 10 min, the supernatant was decanted, and the surface of the nanoparticles washed twice with distilled water. The nanoparticles were redispersed in 5 mL PBS and passed through a 0.45 µm syringe filter before evaluation. The nanoparticles were evaluated by hydrodynamic diameter, PdI and zP.

Figure 9: Set up for the preparation of DLX polymeric nanoparticles

4.7.3 **Characterization of blank DLX polymeric nanoparticles**

4.7.3.1 **Size distribution and zeta potential**

The DLX polymeric nanoparticles size and distribution were evaluated using 1 mL of syringe-filtered (0.45 µm Millipore syringe filter) nanoparticles dispersion by dynamic light scattering (DLS) utilizing a Nano ZS at 25ºC and a scattering angle of 90º. Zeta potential was determined by laser doppler micro-electrophoresis technique with the same instrument (Malvern Zetasizer nano ZS90 series). Results reported are average of triplicate determinations.

4.7.3.2 **Statistical analysis**

Results obtained were subjected to appropriate statistical analysis including Response Surface Regression and General Linear Modeling using Statistica 10 software (StatSoft, USA), One-Way and Two-Way ANOVA using GraphPad Prism 5.0 software (GraphPad, USA).

4.7.4 **Surfactant mix influence on DLX polymeric nanoparticles size**

Based on results obtained from Box Behnken experimental design and statistical analysis, three separate DLX polymeric nanoparticles were prepared using 1% DLX polymer solution, non-solvent/solvent ratio of 10, but varying surfactant mix ratio (Tween 80:Span 80 of 1:0, 4:1, 3:2). This was done to specifically confirm the influence of surfactant mix ratio on DLX polymeric nanoparticles characteristics. DLX polymeric nanoparticles size, PdI and zeta potential were evaluated, average of quadruplicate experiments was reported, and the results were analyzed by ANOVA using GraphPad Prism 5.0 (GraphPad, USA)

4.7.5 **Surfactant mix influence on DLX polymeric nanoparticles swelling/stability**

To further confirm the influence of surfactant mix ratio on DLX polymeric nanoparticles characteristics, the formulations described in section above were subjected to swelling/stability analysis by measuring the size, PdI and zP of the DLX polymeric nanoparticles daily for six days. Results were recorded as percent size increase; experiments were performed in quadruplicates and analyzed by ANOVA using GraphPad Prism 5.0 (GraphPad, USA).

4.8 **Quantification of Isotretinoin: Method Development and Validation**

4.8.1 **Chromatographic conditions**

IST in methanol was analyzed by a simple and rapid HPLC method using a UFLC Prominence system (Shimadzu®, Kyoto, Japan) comprising of a binary pump LC – 20AD, a degasser DGU –20A3, an autosampler SIL – 20AHT and PDA detector SPD – M20A. Data acquisition and analysis was performed using a Shimadzu® Controller Module (CBM - 20A Prominience) coupled to a computer on which Shimadzu® LC Solution software has been installed. Reverse phase chromatographic separation was carried out in a ShimPack VP-ODS C_{18} column (150 mm × 2.0 mm i.d., 5µm; Shimadzu Corporation, Kyoto, Japan) fixed with a C_{18} column guard Shim-pack GVP-ODS (Shimadzu Corporation, Kyoto, Japan, 2.0 mm × 5 mm), placed in a thermostat (CTO–20A) controlled oven compartment with temperature of 30°C. The mobile phase consists of 0.1 %v/v trifluoroacetic acid (TFA) and acetonitrile (30:70). The mobile phase was selected based on several tests using different proportions of TFA and acetonitrile until a fine separation and resolution of IST and pig skin extracts were achieved. The injection volume was 10 µL, flow rate was 0.6 mL/min while the elution time was fixed at 10 min and PDA detection was at 358 nm.

4.8.2 **Determination of absorption wavelength of Isotretinoin**

Based on chromatographic conditions described above, 10 µL of a 5 µg/mL solution of IST in methanol was injected into the UFLC system and the chromatogram produced were analyzed by varying the absorption wavelength between 330 and 370 nm. The wavelength that produced the highest area under the curve was selected as absorption wavelength of IST solution. The highest area was achieved at wavelength 358 nm.

4.8.3 **Validation of analytical method**

The ICH guideline (Q2 (R1) for method validation was used and it was assessed by selectivity, linearity, accuracy, precision and sensitivity (ICH, 2005). Recovery of IST from pig skin, rat skin, DLX polymer solution spiked with IST and commercial IST capsule was also evaluated. Recovery from commercial IST capsule was done to ascertain the authenticity and concentration equivalence of the commercial IST capsule and purchased generic IST powder used in this study.

4.8.4 **Selectivity**

The major 'impurities' that are expected during our studies are rat skin, pig skin and polymer extracts. Thus, the selectivity of the chromatographic conditions for the quantification of IST was ascertained. Full thickness skin from pig ear (1 cm^2) was soaked in 5 mL of methanol containing IST (5 µg/mL) for 1 h protected from lights. The skin was thereafter removed, cut in tiny pieces into 5 mL of methanol in a falcon tube and homogenized using the Ultra Turrax (IKA, Germany). The IST-skin-methanol dispersion was centrifuged (15,000 g, 10 min), filtered with 0.45 µm syringe filter, diluted with methanol and analyzed using HPLC chromatographic

condition. The same process was applied to Wistar rat skin; however, the rat was shaved before removal of skin portion.

IST (1 mg) was solubilized in 3 mL of DLX polymer solution under bath sonication for 30 min protected from light, filtered and analyzed using the HPLC chromatographic conditions. IST was also analyzed in PBS/ethanol (7:3, receiver medium for IST) mixture to ascertain the methods adequacy in quantifying IST.

4.8.5 **Linearity**

Linearity was determined from IST solutions (in methanol) at concentrations of 0.3, 1.5, 3, 6, 12 and 15 µg/mL. Each batch concentration was prepared by diluting separate stock solutions and evaluated using the HPLC chromatographic conditions. Analytical curves of integrated area (Shimadzu® LC Solution software) to IST concentrations were plotted. Curves were subjected to linear regression based on the equation y = mx + c; where y is area, x is IST concentration, m is the slope of the curve and c is the intercept. Linearity was ascertained by values of $R^2 \geq 0.99$. Determinations were done in quadruplicate, protected from light, while calculations were done using Microsoft Excel software (Microsoft, USA).

4.8.6 **Accuracy**

The accuracy of the method was determined using three concentrations of 2.0, 10.0 and 14.0 µg/mL representing low, medium and high IST concentrations respectively. The results were expressed in percent ± relative error according to Equation 1.

$$P = \frac{C_{exp}}{C_{theo}} \times 100 \qquad \text{Equation 1}$$

where P is accuracy, C_{exp} is experimental concentration and C_{theo} is theoretical concentration. Five different replicates were used in determining the accuracy and all experiments were performed protected from light.

4.8.7 **Precision**

Intra-day and inter-day precision was determined using the same concentrations (2.0, 10.0 and 14.0 µg/mL) in the accuracy section. Five different replicates were used in the determination of precision.

Intra-day precision was determined within a single day by back-calculating the concentration of IST using the linearity equation. Results were calculated as relative standard deviation using Microsoft Excel software (Microsoft, USA).

Inter-day precision was determined and carried out over three different days using the same concentrations by back-calculating the concentration of IST using the linearity equation. Results were calculated as relative standard deviation using Microsoft Excel software (Microsoft, USA).

4.8.8 **Sensitivity**

The limit of detection (LoD) and limit of quantitation (LoQ) were determined based on standard deviation of response and slope according to equations 2 and 3. The LoD is the lowest analyte concentration of a substance that can be distinguished from a blank solution while LoQ is the lowest analyte concentration that can be reliably detected and quantified.

$$LoD = \frac{3.3\,\sigma}{s} \qquad \text{Equation 2}$$

$$LoQ = \frac{10\,\sigma}{s} \qquad \text{Equation 3}$$

where σ is standard deviation of areas under the curves and s is the slope of the calibration curve

4.8.9 **Isotretinoin recovery**

IST recovery from dermatomed pig ear skin was evaluated using three different IST concentrations. IST was dissolved in methanol at concentrations of 2.5, 6.25 and 12.5 µg/mL. Exactly 1 mL each of these solutions was added to 1 cm^2 of pig ear skin in a falcon tube. The skin was allowed to absorb the IST solution by gently blowing dry air into the falcon tube until dryness in a light protected environment. The skin was thereafter cut into small pieces, extracted by 4 mL of methanol and homogenized using the Ultra Turrax, centrifuged (15,000 g, 10 min), filtered with 0.45 µm syringe filter, diluted with methanol and analyzed using the validated HPLC chromatographic conditions. The same process above was performed using Wistar rat skin. IST solubilized in DLX polymer solution at concentrations of 2.5, 6.25 and 12.5 µg/mL was also quantified to ascertain that no detrimental interaction exist between IST and DLX polymer solution.

IST was also recovered from commercial IST capsule (Roacutane(). This was done in two ways. First, the gelatin capsule containing alleged 20 mg of IST was cut using a scissors into a 50 mL falcon tube and 20 mL of methanol was added. The mixture was homogenized using the Ultra Turrax, centrifuged (15,000 g, 10 min), supernatant filtered with 0.45 µm syringe filter and analyzed using the validated HPLC chromatographic condition. Secondly, gelatin capsule containing alleged 20 mg of IST was broken into a 50 mL falcon tube, and 20 mL olive oil (Vineves, Portugal) was added, homogenized using the Ultra Turrax, centrifuged (15,000 g, 10 min) and the amount of IST in the supernatant olive oil was analyzed using HPLC by dissolving

an aliquot of the supernatant in methanol. All experiments were performed protected from light and results reported are average of three separate determinations.

4.9 **Fluorescent dye loading into DLX polymeric nanoparticles**

Two florescent BODIPY dyes - hydrophilic and lipophilic - synthesized by our collaborators (Prof. Flávio da Silva Emery group, at FCFRP-USP) were used in this study. The characteristics of these dyes are described below.

4.9.1 **Properties of BODIPY dyes**

The BODIPY dye structures and characteristics are as illustrated in Figure 10 and 11 respectively, while their Log $P_{octanol/water}$ was determined by utilizing the MarvinSketch software.

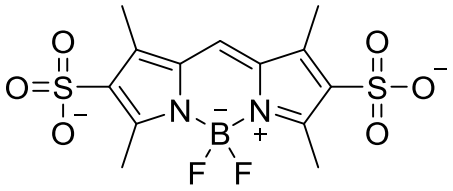

Figure 10: Hydrophilic BODIPY: 5,5-difluoro-1,3,7,9-tetramethyl-*5H*-4λ^4,5λ^4-dipyrrolo[1,2-*c*:2',1'-*f*][1,3,2]diazaborinine-2,8-disulfonate (λ_{max} abs 491 nm λ_{max} emiss 510 nm) (LI *et al.*, 2008), Log $P_{octanol/water}$ = - 4.93

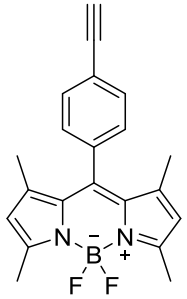

Figure 11: Lipophilic BODIPY: 10-(4-ethynylphenyl)-5,5-difluoro-1,3,7,9-tetramethyl-5H-4λ^4,5λ^4-dipyrrolo[1,2-*c*:2',1'-*f*][1,3,2]diazaborinine (λ_{max} abs 491 nm, λ_{max} emiss 510 nm)(HU *et al.*, 2012), Log $P_{octanol/water}$ = - 0.19

4.9.2 **Preparation and characterization of BODIPY-DLX polymeric nanoparticles**

In order to demonstrate the encapsulation capacity of DLX polymeric nanoparticles and its applicability, DLX polymeric nanoparticles were loaded with test hydrophilic or lipophilic BODIPY dyes. 10 mg of lipophilic or hydrophilic BODIPY were initially dissolved in the non-solvent (ethanol) or DLX polymer solution respectively before nanoparticles preparation as previously described. The preparation was based on the selected optimal DLX polymeric nanoparticles formulation determined from the Box Behnken statistical analysis. Briefly, 1 mL of DLX polymer solution was pumped into 10 mL of ethanol (non-solvent) containing 5 % surfactant mix, Tween 80:Span 80 in ratio 3:2. The nanoparticles were evaluated by hydrodynamic diameter, PdI, zP and entrapment efficiency. All experiments were performed protected from light and results reported are average of triplicate determinations.

The entrapment efficiency (*EE*) of the BODIPY-DLX polymeric nanoparticles was determined by ultracentrifugation (15,000 g, 10 min) and the amount of free BODIPY in the supernatant was measured using a validated UV spectrophotometric method (UV-1800, Shimadzu, Japan) at an absorbance of 495 nm. The *EE* was calculated indirectly as described in Equation 4.

$$EE\ (\%) = \left(\frac{Theoretical\ BODIPY\ amount - BODIPY\ in\ supernatant}{Theoretical\ BODIPY\ amount}\right) \times 100 \quad \text{Equation 4}$$

4.9.3 **Dispersion of lipophilic BODIPY-DLX polymeric nanoparticles**

Exactly 1 g of DLX polymeric nanoparticles loaded with lipophilic BODIPY was dispersed in distilled water and was visually assessed for homogeneity in comparison to free lipophilic BODIPY in distilled water or methanol.

4.10 Isotretinoin loading into DLX polymeric nanoparticles

4.10.1 Solubility of IST in DLX polymer solution

The amount of IST that can be effectively solubilized in DLX polymer solution was determined. Excess of IST was added to 5 mL of DLX polymer solution and dispersed with vortex before bath sonication (QUIMIS, Brazil) for 30 min. The dispersion was thereafter centrifuged (15,000 g, 10 min) and the supernatant was filtered with 0.45 µm syringe filter. The amount of IST solubilized in the DLX polymer solution was then quantified using the validated HPLC method.

4.10.2 Preparation and characterization of IST- DLX polymeric nanoparticles

Two approaches were used in loading IST into DLX polymeric nanoparticles. The first approach involved dissolving IST in the non-solvent (ethanol) medium while the second approach leveraged on the solubilizing properties of the natural DLX polymer. In the first method, 10 mg of IST was dissolved in 10 mL ethanol containing 5 % of Tween 80:Span 80 (3:2) and 1 mL of DLX polymer solution was added drop-wise as previously described to produce IST-DLX polymeric nanoparticles. In the second method, 1 or 3 mg/mL of IST was solubilized in 1 % DLX polymer solution. 1 mL of this IST-DLX polymer solution was added drop-wise as previously described to produce IST-DLX polymeric nanoparticles. The IST-DLX polymeric nanoparticles were evaluated by hydrodynamic diameter, PdI, zP and *EE*. Experiments were performed protected from light and results reported are average of three separate determinations.

IST-DLX polymeric nanoparticles were also characterized by transmission electron microscopy (TEM) using a JEM-100CXII transmission electron microscope (JEOL, Japan) with an accelerating voltage ranging from 100 kV to 200 kV. Fiji software (ImageJ, NIH, USA) was

used to determine the size of the nanoparticles. Result reported is an average of 50 different nanoparticles.

4.11 *In vitro* release studies

4.11.1 Determination of IST sink condition

Due to the lipophilicity of IST, all dissolution and release studies were performed in PBS/ethanol (7:3) solution. Thus, the amount of IST that can successfully dissolve in this condition was determined. Excess of IST was added to 5 mL PBS/ethanol (7:3) solution and gently stirred overnight, protected from light. The mixture was centrifuged (15,000 g, 10 min), the supernatant filtered with 0.45 µm syringe filter and IST amount dissolved in the supernatant was quantified using the previously validated HPLC method. Sink condition was calculated as one-tenth of the amount of IST dissolved in PBS/ethanol (7:3) solution. Experiments were done in quadruplicate.

4.11.2 IST-DLX polymeric nanoparticles *in vitro* release

A Franz diffusion cell model was used in evaluating the *in vitro* release of IST from IST-DLX polymeric nanoparticles. Before the experiment, each model Franz diffusion cell was calibrated to know the exact volume of receiver medium (PBS/ethanol 7:3) it can take. A dialysis membrane (12 - 14 kDa, Fisherbrand, Fisher Scientific, USA) was mounted between the donor and receiver compartment of the Franz diffusion cell (surface area of 1.085 cm^2). PBS/ethanol (7:3) was added to the receiver compartment with continuous magnetic agitation. To comply with sink conditions, 1 mL of IST-DLX polymeric nanoparticles (50 µg/mL) or IST-DLX polymer solution (50 µg/mL) was added to the donor compartment. At predetermined time intervals, 1 mL of the receiver medium was removed and immediately replaced with 1 mL fresh receiver medium. The collected samples were syringe filtered (0.45 µmL) and the amount of IST

released was quantified by the previously validated HPLC method. Results were reported as an average of three separate determinations. All experiments were performed protected from light. A curve of released IST concentration vs time was thereafter plotted. Kinetic modeling was performed using the DDsolver software (ZHANG *et al.*, 2010) and the models were assessed by release rate parameters and correlation coefficient R^2 in order to select the best fitting models.

4.12 *In vitro* skin penetration studies

4.12.1 Preparation of pig ear skin

Fresh pig ears from the abattoir (Olho d'agua, Ipua, SP, Brazil) were delivered to the laboratory protected in ice and immediately processed. Full thickness skins, free of fat and muscle were removed from the outer surface of the pig's ear with the aid of a scalpel and were immediately stored at -80 ^{o}C until needed for use.

Just prior to use, the processed pig ear skins were defrosted, washed with distilled water and thereafter dermatomed. All pig ear skins were dermatomed to a thickness of approximately 700 µm before use in all experiments.

4.12.2 Skin resistance/integrity test

Before use, dermatomed skin were cut into adequate sizes (approximately 3.5 x 3.5 cm) and evaluated for stratum corneum resistance/integrity. Skin pieces were mounted on Franz diffusion cells with an approximate diameter of 1 cm and were filled with PBS in the donor and receiver medium. The AC current *I*, passing through the Franz diffusion system was measured using a multimeter in a setup (Figure 12) consisting of a 20 MHz Arbitrary Waveform generator (Agilent Technologies, California, USA) set to a frequency of 10 Hz and RMS voltage of 100 mV.

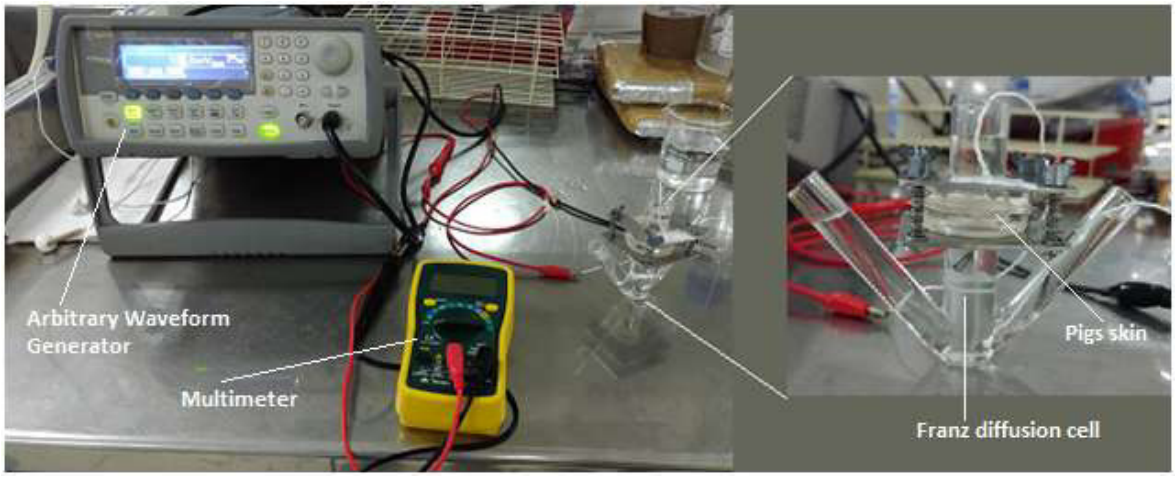

Figure 12: Setup for the determination of stratum corneum resistivity

The resistance in the system was determined by Ohms law as shown in Equation 5

$$V = IR \qquad \text{Equation 5}$$

where V is potential difference, I is the current and R is the resistance. The resistivity of the dermatomed skin were thereafter determined as previously described (TANG *et al.*, 2001). Only skins with resistivity higher than 35 kΩ.cm^2 were utilized in all skin penetration studies.

4.12.3 **Influence of PBS/ethanol (7:3) on Pigs' ear skin resistance/integrity**

Ethanol is a known skin permeation enhancer (WILLIAMS & BARRY, 2012). To ascertain that the receiver medium PBS/ethanol (7:3) will not negatively affect the integrity of pigs' ear skin during studies, the skins were subjected to integrity test. Dermatomed pig ear skins were mounted on Franz diffusion cells containing PBS/ethanol (7:3) in the receiver compartment and PBS in the donor compartment. The AC current I, passing through the model Franz diffusion system over a specified time interval was measured using a multimeter in a setup (Figure 12) consisting of a 20 MHz Arbitrary Waveform generator set to a frequency of 10 Hz and RMS voltage of 100 mV. The resistance in the system was determined by the Ohms law (Equation 5)

and resistivity calculated as previously described (TANG *et al.*, 2001). Experiments were performed in triplicate.

4.12.4 *In vitro* BODIPY-DLX polymeric nanoparticles skin penetration/distribution

In vitro penetration/distribution of lipophilic BODIPY-DLX polymeric nanoparticles into dermatomed pig ear skin was evaluated using a Franz diffusion cell model. Dermatomed (700 µm) pig ear skin was mounted in between the donor and receiver compartment of a model Franz diffusion cell. Exactly 1 mL of lipophilic BODIPY-DLX polymeric nanoparticles or lipophilic BODIPY-DLX polymer solution (550 µg/mL BODIPY) was added to the donor compartment of the Franz diffusion cell and allowed to stand for 1 or 6 hours protected from light. After each experimental time, the skins were retrieved and the stratum corneum surface was cleaned with isopropanol-soaked gauze. The skin was cut into small rectangular pieces, embedded into Tissue-Tek (Sakura Finetek, Netherlands) with stratum corneum facing up and stored at -20 ^{o}C before cryo-sectioning. The embedded skin was cryo-sectioned transversely (Leica CM1860 Cryostat, Leica, Germany) and 10 µm cryo-sections were visualized in a Confocal microscope (Leica TCS SP8 Confocal microscope, Leica, Germany).

4.12.5 *In vitro* IST-DLX polymeric nanoparticles skin penetration

In vitro skin release and penetration of IST from IST-DLX polymeric nanoparticles was evaluated using a dermatomed pig ear skin mounted on a model Franz diffusion cell. Dermatomed pig ear skin (≈ 700 µm) was mounted in between the donor and receiver compartment of a model Franz diffusion cell. The receiver compartment was filled with PBS/ethanol (7:3) and assessed for stratum corneum integrity as previously described. Only skins with resistivity higher than 35 kΩ.cm^2 were used for the experiment. Exactly 1 mL of IST-

DLX polymeric nanoparticles or IST-DLX polymer solution (≈ 400 µg/mL of IST) was added to the donor compartment and allowed to stand under gentle magnetic agitation of the receiver compartment for 1, 3, 6 and 12 h respectively. Additionally, at 6 h, the formulation in the donor compartments of some specific Franz diffusion cells were removed but allowed to further stand till 12 h. After each specified experimental time interval, skin resistivity was re-determined to ascertain the integrity of the skin, 1 mL of the receiver medium was removed, filtered and the amount of IST was quantified using the validated HPLC method. The skin pieces were thereafter unmounted and processed for differential tape stripping. An extra experiment was performed following this same procedure but with a double dose of IST-DLX polymeric nanoparticles (≈ 800 µg/mL of IST). All experiments were done in triplicate, protected from light and results obtained were subjected to ANOVA analysis (Prism GraphPad, USA).

4.12.5.1 **Differential tape stripping process**

Upon removal of the permeated skin, they were placed on a flat surface with the stratum corneum facing upwards and gently cleaned with isopropanol-soaked gauze and allowed to dry. Stratum corneum and follicular IST penetration was evaluated by a modified differential technique comprising of tape stripping followed by cyanoacrylate skin surface biopsies. Exactly 15 scotch heavy duty tape strips (3M, St. Paul, Minnesota, USA) were applied to the surface of the stratum corneum and were gently pulled to remove stratum corneum biopsies (DE ROSA *et al.*, 2003; GELFUSO *et al.*, 2013). Complete removal of the stratum corneum was confirmed by the appearance of a glittering surface. The tape strips were carefully placed in a 50 mL falcon tube and extracted under vortex followed by sonication with 5 mL methanol. Subsequently, a single drop of cyanoacrylate glue was placed on the shinning surface and a single tape was applied with a gentle pressure and allowed to stand for 5 min for complete dryness

(LADEMANN *et al.*, 2006; TEICHMANN *et al.*, 2005). The tape strip was thereafter removed with visible skin surface biopsy showing follicular casts. The biopsy cast was placed in a 50 mL falcon tube, extracted under vortex and sonication with 5 mL methanol.

In order to quantify IST in the viable epidermis and dermis, the remaining skin piece was separated. The skin piece was inserted into a clean and transparent polythene bag and placed in hot water (60 ^{o}C) for exactly 1 min (ABD *et al.*, 2016; KLIGMAN & CHRISTOPHERS, 1963). The viable epidermis was separated from the dermis by gentle scrapping with the aid of blunt spatula and forceps. The viable epidermis was collected, and dermis cut to small pieces into a 50 mL falcon tube, methanol was added and the skin pieces homogenized with the Ultra Turrax for complete extraction. All methanol extracts were centrifuged (15,000 g, 10 min), filtered with 0.45 µm syringe filter and the amount of IST in the extracted tape strip biopsies, viable epidermis and dermis were quantified by the validated HPLC method. All experiments were performed in triplicate protected from light.

4.13 *In vitro* photo-irritation study

4.13.1 Cell culture and photo-irritation

The 3T3 neutral red uptake phototoxicity test according to INVITTOX Protocol No. 78 (LIEBSCH & SPIELMANN, 2002b) and OECD TG 432 (OECD, 2004) was employed in the photo-irritation study. Exactly 100 µL of 3T3 Balbc fibroblasts (1 x 10^5cells/mL) in complete DMEM were seeded into 96-well plates and incubated (37^{o}C, 5% CO_2, 24 h) for adherence. Two plates were used for each test substance; one was to determine cytotoxicity (no UV irradiation) and the other was used to determine phototoxicity (UV irradiated). After 24 h, the growth media was removed; the cells were washed with 150 µL of PBS and treated with different

concentrations of free IST and IST-DLX polymeric nanoparticles dispersed in DMEM respectively. The concentration of IST in the IST-DLX polymeric nanoparticles was equivalent to that of free IST tested. The IST concentration range tested was between 100 µg/mL and 6.8 µg/mL with a dilution factor of 1.47 as described in the protocol. Free IST stock was prepared by dissolving 10 mg of IST in 1 mL DMSO and dilutions were made with DMEM. After incubation for 1 h, one plate labeled +UV was irradiated with 5 J cm^{-2} of UVA radiation from a Philips UVA Actinic BL/10 lamp (Eindhoven, Netherlands) while the other plate labeled –UV was kept in the dark. The UVA radiation was calculated with a VLX-3W Vilber Lourmat Radiant Power Meter (Marne-la-Vallee, France) equipped with UVA (365 nm) sensor. After irradiation, the test solutions were removed, the cells were washed twice with 150 µL PBS, replaced with complete culture medium and incubated overnight. Thereafter, the medium was removed and 100 µL of Neutral Red medium was added to each well and incubated for 3 h. After incubation, the Neutral Red medium was removed, the cells washed once with PBS, blotted dry and 150 µL of freshly prepared desorbing solution (ethanol/water/acetic acid; 50:49:1) was added to each well to extract Neutral Red from viable cells. The two plates were agitated for 10 min and analyzed using a microplate reader (Cary 50 MPR, VARIAN Inc., USA) at 540 nm. Each test material was added in sextuplicates.

The result was analyzed based on two prediction models; the Photo-Irritancy Factor (PIF) based on comparison of one concentration curve and the Mean Photo Effect (MPE) based on the comparison of two concentration curves.

The PIF is calculated based on the EC_{50} values of cytotoxic substance in the presence or absence of UVA irradiation according to Equation 9, with PIF value > 5 indicating potential phototoxicity.

$$PIF = \frac{EC_{50}(-UV)}{EC_{50}(+UV)} \qquad \text{Equation 9}$$

However, in situations where EC_{50} could not be determined, a different approach is utilized. If the EC_{50} (+UV) is achieved while the test is performed up to the maximum concentration (100 µg/mL) of the test substance, the C_{max} is used instead of the EC_{50} (-UV); PIF values > 1 thus predicts phototoxic. In situations where both EC_{50} cannot be achieved, no phototoxic potential is predicted, with a PIF = 1 being indicative of non-phototoxic potential; however, this is a limitation of the PIF model which thus necessitated the MPE model to compliment the results of PIF (LIEBSCH & SPIELMANN, 2002a; OECD, 2004).

The MPE model, developed in 1997 (HOLZHÜTTER, 1997) is based on the comparison of a series of responses from related concentration ranges in the presence and absence of UVA and calculated based on an algorithm that was fitted into a software called "Phototox" (version 2.0, ZEBET, Germany) (OECD, 2004). An MPE value < 0.1 predicts non-phototoxic potential while values > 0.1 predicts phototoxic potential of a substance.

4.13.2 *In vitro* inflammatory response

Inflammatory response study was performed using AMJ–2 macrophage cells (ATCC, USA). Cells were seeded into 24-well plates at a density of 2 x 10^5 cells per well using complete DMEM as culture medium. After 24 h of cell adherence, each well was treated with 500 µL complete DMEM containing 87.5 µg of free IST or IST-DLX polymeric

nanoparticles equivalent to 87.5 µg of IST and 1 ng of lipopolysaccharide (LPS). Cells treated with only 500 µL complete DMEM and 1 ng of lipopolysaccharide (LPS) were used as controls. Cells were incubated for 24 h and 48 h respectively. After the respective incubation times, the supernatant of each well was collected and the concentration of inflammatory cytokines, IL-6, IL-10 and TNF-α were analyzed using an ELISA kit (R&D Systems Corporation, USA). Experiments were performed in duplicate and the result analyzed by ANOVA using GraphPad 5.0 (Prism GraphPad, USA).

4.14 *In vitro* antimicrobial activity against *Propionibacterium acnes*

P. acnes was incubated and cultured in Brain Heart Infusion (BHI) for 48 h under anaerobic conditions and the bacterial suspension was adjusted to approximately 1 x 10^8 CFU/mL. Before culture, the cells were activated according to the method stipulated by the source. The cells were treated with different concentrations of free IST, IST-DLX polymeric nanoparticles and blank DLX polymeric nanoparticles based on a double dilution method using a stock solution (20 % DMSO) of 1000 µg/mL equivalent of IST. Dispersions of blank DLX or IST-DLX polymeric nanoparticles were adjusted with same volume of DMSO. First, 100 µL of BHI was added to each well of a 96-well culture plate, after which 100 µL of stock solution of free IST, IST-DLX polymeric nanoparticles or blank DLX polymeric nanoparticles were added to the first well and diluted accordingly. Then, 10 µL of a 1 x 10^8 CFU/mL *P. acnes* suspension was added to each well and the plates were incubated for 24 and 48 h respectively. A line of 8 wells were not inoculated with *P. acnes* to ascertain non-contamination of the BHI medium while another line of 8 wells were inoculated with 10 µL of 1 x 10^8 CFU/mL *P. acnes* but without the addition of IST. All treatment concentrations were done in triplicate. After each treatment time, the plates were treated with resazurin and incubated for 30 min.

4.15 *In vivo* topical IST administration studies

4.15.1 Animals

Male Wistar Hannover rats (*Rattus novergicus albinus*), aged 6 to 8 weeks (220 - 260 g body mass) were purchased from the central animal house of the University of Sao Paulo (USP) in Ribeirao Preto. The animals were kept in the animal house of the Faculty of Pharmaceutical Sciences in Ribeirao Preto (FCFRP-USP) in cages with beddings that are changed 3 times a week. The animal room was equipped with an air extractor with 20 air changes per hour, natural humidity, temperature maintained between 20 to 24ºC, and animals were subjected to a 12 h light-12 h dark condition. Three animals were housed in a cage (40x33x16 cm) with unrestricted access to filtered water and feed. All experimental protocols were approved by the Ethical committee of the Faculty of Pharmaceutical Sciences in Ribeirao Preto, University of Sao Paulo (approval inserted in the Annex).

One day before the commencement of topical studies, the hair at the back of the rats was shaved using a super micro hair clipper (WAHL, USA). An area approximately 9.08 cm^2 (Figure 13) was marked out for formulation treatment throughout the studies.

4.15.2 Preparation of 2% HEC gel and incorporation of free IST, DLX and IST-DLX polymeric nanoparticles

A 4 % HEC gel was prepared by weighing 4 g of HEC and dispersing it in 100 mL MilliQ water under gentle magnetic agitation. The pH was adjusted to 7.2 just before the gel formation.

In order to prepare 20 g of blank 2 % HEC gel, 10 g of MilliQ water and 10 g of 4 % HEC gel were added together in a beaker and stirred slowly with the aid of a glass rod until a homogenous 2 % HEC gel was produced.

IST is a lipophilic drug, thus in order to prepare 20 g of 2 % HEC gel containing free IST; first, 10 mg of IST was dissolved in 300 µL of Ethanol and the mixture was made up to 10 g with MilliQ water, vortexed in a 15 mL falcon tube, and then mixed slowly with 10 g of 4 % HEC gel in a beaker with a glass rod. The final product was a 2 % HEC gel containing 500 µg IST per gram of 2 % HEC gel.

In order to prepare 20 g of 2 % HEC gel containing IST-DLX polymeric nanoparticles, IST-DLX polymeric nanoparticles containing an equivalent of 10 mg IST was dispersed in MilliQ water to a final weight of 10 g. This dispersion was gently mixed with 10 g of 4 % HEC gel in a beaker with a glass rod until homogeneity was ascertained. The final product was a 2 % HEC gel containing IST-DLX polymeric nanoparticles equivalent to 500 µg IST per gram of 2 % HEC gel.

In order to prepare 20 g of 2 % HEC gel containing DLX polymeric nanoparticles, 1 g DLX polymeric nanoparticles was dispersed in MilliQ water to a final weight of 10 g. This dispersion was gently mixed with 10 g of 4 % HEC gel in a beaker with a glass rod until homogeneity was ascertained.

4.15.3 **Cutaneous irritation**

Twenty-four animals were divided into 4 groups (CN, CP, N-DLX, DLX-IST) of 6 animals each. The sample size was calculated based on the Resource Equation method

(FESTING AND ALTMAN, 2002, FESTING, 2006, CHARAN AND KANTHARIA, 2013). The marked area in each animal was treated topically daily for 2 weeks with 5 mg/cm^2 of test formulation (SCCS/1358/10) using a blunt spatula (Figure 13).

Figure 13: Application of gels to the marked animal trunk

The CN group received only 2 % hydroxyethyl cellulose (HEC) gel, CP group received 2 % HEC gel containing IST, N-DLX group received 2 % HEC gel containing DLX polymeric nanoparticles and DLX-IST group received 2 % HEC gel containing IST-DLX polymeric nanoparticles (Figure 14). Approximately 50 mg of the respective 2 % HEC gel was applied to the 9.08 cm^2 marked area; this amount was such that CP and IST-DLX group received equivalently a total of 25 µg IST each.

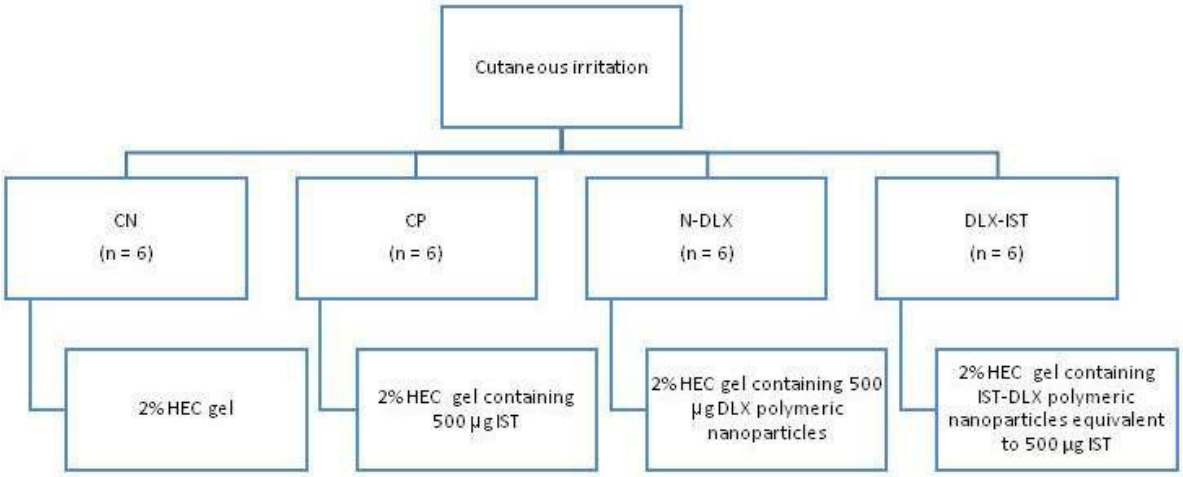

Figure 14: Animal groups for cutaneous irritation

A day after the last application, the treated area was cleaned with a cotton swab moistened with water, photographed after 30 minutes with a digital camera and visualized macroscopically. The animals were thereafter sacrificed by decapitation; before decapitation, the animals were anesthetized with 10 % ketamine and 2 % xylazine (1:1) solution at 0.1 mL per 100 g of animal weight intraperitoneally. Anesthesia was confirmed by the absence of reflex when the rat toe was pinched. The animals were decapitated with a single cut and death was confirmed by the absence of breathing movements and heart rate. The treated skin area was thereafter removed by dissection, processed for histology, stained with hematoxylin and eosin before microscopic evaluation.

4.15.4 **Cutaneous Photo-irritation**

This experiment was carried out with the same formulations used in the cutaneous irritation study described above. The difference between these experiments is the exposure of the treated skin to UV light. Thus, 24 animals were divided into 4 groups (CN, CP, N-DLX, DLX-IST) of 6 animals each (Figure 14). Animals were treated as described under cutaneous irritation but for only 5 days.

About 15 min after each day application, the animals were held for 3 min as shown in Figure 15 and exposed to UVA irradiation totaling a dose of approximately 0.67 J cm^{-2}, determined using Coherent Fieldmax II radiometer (Top radiometer, Portland, USA) (BENEVENUTO *et al.*, 2015). Immediately after the last UVA treatment, the treated skin area was wiped with a cotton swab moistened with water and photographed after 30 minutes with a digital camera for further macroscopic analysis. The animals were thereafter sacrificed by decapitation; before decapitation, the animals were anesthetized with 10 % ketamine and 2 %

xylazine (1:1) solution at 0.1 mL per 100 g of animal weight intraperitoneally. Anesthesia was confirmed by the absence of reflex when the rat toe was pinched. The animals were decapitated with a single cut and death was confirmed by the absence of breathing movements and heart rate. The treated skin area was thereafter removed by dissection, processed for histology and stained with hematoxylin and eosin before microscopic evaluation.

Figure 15: Set up for the irradiation of animals

4.15.5 **IST quantification in Wistar rat skin**

18 animals were divided into 3 groups (CN, CP and DLX-IST) of 6 animals each (Figure 16). The marked area was exposed to 5 mg/cm^2 of formulation using a spatula for 12 h. After 12 h, the formulation was removed, and the treated skin area was cleaned with a cotton swab moistened with water. The animals were thereafter sacrificed by decapitation as described before.

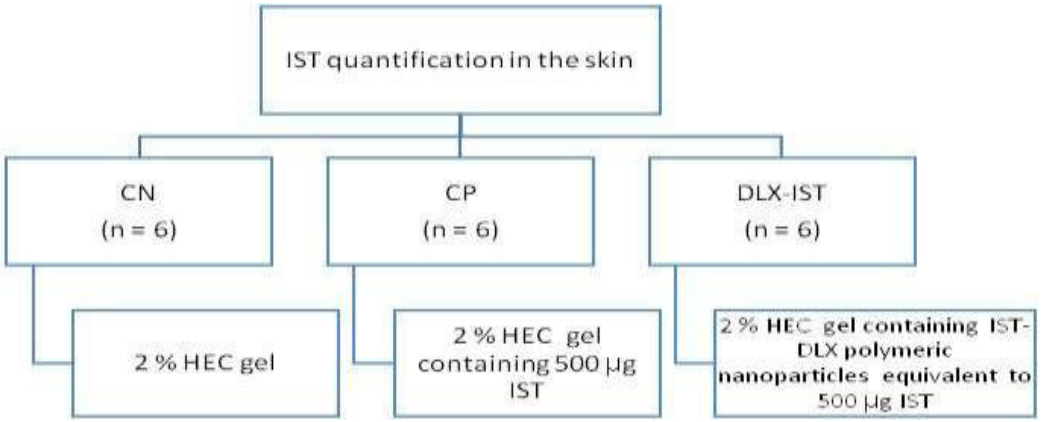

Figure 16: Animal groups for IST quantification in Wistar rat skin

A tape stripping process (Figure 17) was immediately performed on the treated skin area to separate the stratum corneum from the rest of the skin layers. The tape strip biopsies were placed in a 50 mL falcon tube and extracted with methanol by vortex and bath sonication (QUIMIS, Brazil). Complete removal of stratum corneum was confirmed by a shining viable epidermis surface (Figure 17). The remaining skin area was removed by dissection and cut in pieces into a 50 mL falcon tubes, extracted with 5 mL methanol and homogenized with the Ultra Turrax (IKA, Germany). The methanol extract was centrifuged (15,000 g, 10 min), filtered with 0.45 µm syringe filter and the amount of IST was quantified using the validated HPLC method. Results were analyzed by student t test using GraphPad software (GraphPad Prism 5.0, USA)

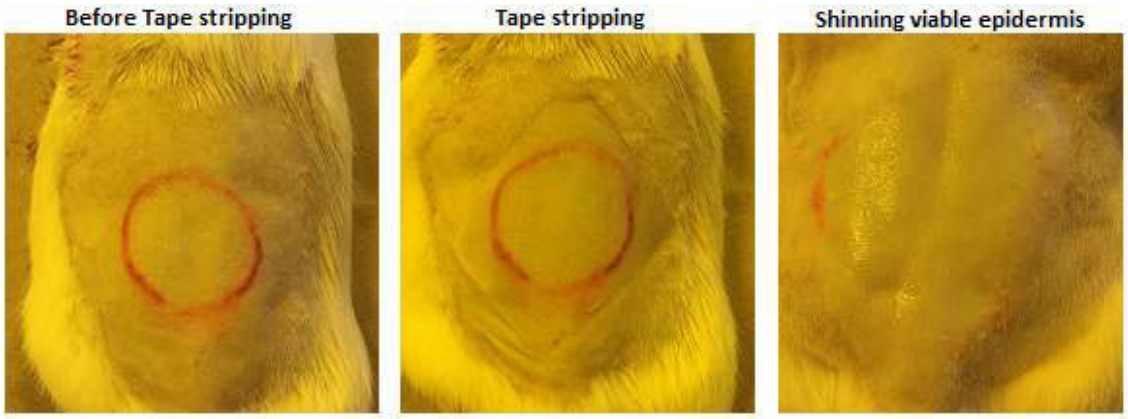

Figure 17: Tape stripping process on Wistar rats (slightly yellow appearance was due to working conditions under yellow light

4.16 DLX polymer Versatility

The versatility of DLX polymer as a drug delivery polymer in diverse diseases and routes of administration was defined as one of the objectives of this study. Thus, the versatility of DLX polymeric nanoparticles as an ocular delivery polymer was assessed in diverse ways.

4.16.1 *In vitro* DLX polymeric nanoparticles stability in simulated ocular fluids

The stability of DLX polymeric nanoparticles was assessed in simulated ocular fluid components to ascertain its usability as an ocular delivery system.

4.16.1.1 Incubation with Lysozyme

The stability of optimized DLX polymeric nanoparticles was analyzed according to established methods (DE CAMPOS *et al.*, 2005) by incubation at 37ºC in lysozyme solution. Exactly 1 mL of DLX polymeric nanoparticles was added to lysozyme in purified water (9 mL) such that the final concentration of lysozyme is 1 mg/ml and was placed under gentle agitation. The mean particle size, PdI and zeta potential were measured at time 0 and every hour for 6 h. Results were recorded as average of quadruplicate determinations.

4.16.1.2 Incubation in simulated lachrymal fluid (SLF)

The stability of DLX polymeric nanoparticles was assessed in SLF containing 0.67% $^{w}/_{v}$ NaCl, 0.2% $^{w}/_{v}$ $NaHCO_3$ and 0.008% $^{w}/_{v}$ $CaCl_2$ $2H_2O$ (MIYAZAKI *et al.*, 2001). Exactly 1 mL of DLX polymeric nanoparticles was added to STF solution under gentle agitation and incubation at 35^{o}C. The mean particle size, PdI and zeta potential were measured during the incubation process for up to 6 h. Results recorded were average of quadruplicate determinations.

4.16.1.3 Incubation with mucin

The zeta potential of DLX polymeric nanoparticles was determined in mucin (0.4 mg/mL) dispersion. Mucin, like lysozyme is a major component of the precorneal fluid. The zeta potential of mucin dispersion with and without DLX polymeric nanoparticles at 35ºC was evaluated. Zeta potential values reported are average of quadruplicate determinations.

4.16.1.4 Osmolality determination

The osmolarity of DLX polymeric nanoparticles dispersion was determined using a semi-micro osmometer (K-7400, KNAUER).

4.16.2 *In vitro* cell toxicity studies

In vitro cytotoxicity assay was carried out using two ocular cell lines namely Retinal Pigment Epithelial (ARPE-19) and Human Corneal Epithelial (HCE) cells. The ARPE-19 cells were routinely cultured in DMEM/F12 medium (1:1) supplemented with 10% FBS and antibiotics while the HCE cells were cultured in SHEM. The cells were incubated in standard culture conditions (incubation at 37ºC in 5% CO_2 atmosphere) and the medium was change every 2 - 3 days while cell growth was monitored daily by phase-contrast microscopy. Cells were allowed to reach at least 80% confluence before each trypsinization process.

4.16.2.1 Cytotoxicity assay

Cytotoxicity was carried by MTT and Neutral Red (NRU) assay techniques. The ARPE-19 and HCE cells were seeded at a density of 1.5 x 10^5 cells per well in 100 µL of their respective complete growth medium into 96-well plates and incubated (37ºC in a 5% CO_2 atmosphere) for 24 h for adherence. The growth medium was thereafter removed and replaced with 100 µL blank DLX polymeric nanoparticles dispersed in their respective incomplete medium supplemented with 1 % FBS and were incubated for 24, 48 and 72 h. The DLX polymeric nanoparticles were

tested at concentration range of 100 - 1483.3 µg/mL. After the specified hours of incubation, the test nanoparticles dispersion was removed; cells were washed with 150 µL of PBS and incubated with 100 µL of NRU (final concentration of 0.05 mg/mL) or 100 µL of MTT (final concentration of 5 µg/mL) in incomplete medium respectively for 3 h. The cells were thereafter washed with 150 µL of PBS and completely drained before addition of 100 µL DMSO, for MTT assay or 150 µL of neutral red desorb solution (1:50:49 v/v of glacial acetic acid/ethanol/water) for NRU assay. The plates were agitated for 10 min before absorbance was read at 570 nm (MTT) and 540 nm (NRU) in a microplate reader (Cary 50 MPR, VARIAN Inc., USA). Cell viability (%) was calculated as described in equation 6

$$Cell\ viability\ (\%) = \frac{Abs_{sample}}{Abs_{control}} \times 100\ \%$$ Equation 6

where Abs_{sample} represent measurements from wells treated with DLX polymeric nanoparticles and $Abs_{control}$ measurement from untreated wells. Result reported as mean ± SD were from quadruplicate determinations.

4.16.3 ***In vitro*** **cellular uptake studies**

Cellular uptake studies of BODIPY-DLX polymeric nanoparticles were performed in ARPE-19 and HCE cell lines. The BODIPY employed in these experiments was the hydrophilic BODIPY. Flow Cytometry, a laser based microfluidic cell analysis technology for cell counting and biomarker detection was deployed to evaluate/quantify the cellular uptake of the labeled BODIPY-DLX polymeric nanoparticles by the ARPE-19 and HCE cells while confocal microscopy technique was further used to affirm the results obtained from the flow cytometry.

4.16.4 **Flow Cytometry**

The ARPE-19 and HCE cells were seeded into 6-well plates at a density of 3 x 10^5 cells/well and 4 x 10^5 cells/well in their respective complete medium and incubated (37°C in a

5% CO_2 atmosphere) for 24 h for cells adherence. The cells were thereafter washed with PBS and incubated with 1 mL BODIPY-DLX polymeric nanoparticles (5 mg/mL of BODIPY) or BODIPY solution (5 mg/mL) dispersed in respective incomplete medium. Control wells were treated with blank DLX polymeric nanoparticles dispersion. After 24 h, the cells were washed twice with PBS, trypsinized with 300 µL of trypsin (0.25%), neutralized with respective complete medium, centrifuged and resuspended in PBS. Prior to analysis in the flow cytometer (BD FACSCanto I, USA), 5 µL of propidium iodide was added to the samples. Analysis was performed at excitation wavelengths of 495 nm and 488 nm with emission wavelengths at 525 nm and 670 nm respectively for BODIPY and propidium iodide. Percent uptake was calculated based on the dot plots (BD-FACSDiva Software) obtained from the flow cytometry result. Results reported were average of quadruplicate determinations.

4.16.5 **Confocal microscopy**

The ARPE-19 and HCE cells were seeded into 6-well plates containing sterilized glass cover slips (22 mm x 22 mm) at a density of 3 x 10^5 cells/well and 4 x 10^5 cells/well in respective complete medium and incubated (37ºC in a 5% CO_2 atmosphere) for 24 h for adherence. The cells were washed with PBS and incubated for 24 h with 1 mL BODIPY-DLX polymeric nanoparticles (5 mg/mL of BODIPY) or BODIPY solution (5 mg/mL) dispersed in respective incomplete medium. Control wells were treated with blank DLX polymeric nanoparticles dispersion. After treatment, the cells were washed twice with PBS, fixed with 2 mL paraformaldehyde (1%) per well and stored at 4 ºC overnight protected from light. The cells were washed again with PBS and the glass cover slips were carefully lifted and placed inverted on glass microscope slides containing a drop of DAPi dye. The slides were kept for 24 h protected from light before visualization in confocal microscope (Leica TCS SP8 Confocal

microscope, Leica, Germany). It should be noted that the HCE cells were also incubated with BODIPY-DLX polymeric nanoparticles and BODIPY solution for further 48 h.

5 Results and Discussions

Some results and discussions in relation to the collection, purification and characterization of Delonix polymer, in addition to the processes involved in the development and optimization of DLX polymeric nanoparticles and its potential for ocular drug delivery has already been published in Carbohydrate Polymers (OGUNJIMI *et al.*, 2017).

5.1 **Collection and purification of Delonix polymer**

Delonix polymer was extracted from the seeds of *Delonix regia* plant collected between February and April of 2014 when the pods were ripe and wet as previously described (OGUNJIMI *et al.*, 2017). Exactly 1,243 g raw and dry Delonix endosperm was collected and after the purification process, there was a yield of about 87.5 % with loss mostly due to the milling method. The Delonix endosperm was purified to a fine, light brown powder (Figure 18) and was stored for use.

Figure 18: Delonix polymer in pod, seed and powder

5.2 **Characterization of Delonix polymer**

It is important to have substantial information about the general content of DLX polymer. Delonix polymer has been previously characterized and shown to be composed of galactomannans made up of mannose and galactose units (TAMAKI *et al.*, 2010). Our result shows that the DLX polymer (DLXp) produced by the purification process has a 54 % total carbohydrate content composed of mannose (Man), galactose (Gal) and trace amounts of protein, while the nature of the remaining contents were outside the scope of our analysis. However, the sonicated and unsonicated DLX polymer solution, DLXs and DLXu, contain predominantly 99 and 98 % carbohydrate made of mannose and galactose (Table 3).

The Man:Gal ratio of DLXp, DLXs and DLXu are as shown in Table 3. This pattern has also been previously reported in other study involving DLX polymer characterization (BENTO *et al.*, 2013). There was however, a difference in the galactose content of DLXp, DLXs and DLXu; this difference between DLXp and DXLs or DLXu may be attributed to a beta elimination process in the presence of alkali (NaOH), a known phenomenon associated with alkali treatment of galactomannans (BENTO *et al.*, 2013).

Table 3: DLX polymer mannose:galactose ratio

Fraction	**Total sugar (%)**	**Protein (%)**	**Man:Gal* ratio**
DLXp	54	Trace	4.6:1
DLXu	98	-	5.3:1
DLXs	99	-	6.3:1

Also, the difference in the Man:Gal ratio between DLXu and DLXs could be due to the influence of sonication which has been previously documented (PRAJAPAT & GOGATE,

2015). However, this difference did not significantly influence the basic properties of the DLXs used in preparing DLX polymeric nanoparticles. In fact, the fractions of DLXs and DLXu analyzed by GPC showed a polydispersed polymer system with very close molecular weight of ~170 kDa and 185 kDa in addition to a close similarity between the chromatographic elution profile of DLXu and DLXs samples as monitored by refractive index (Figure 19). The result also shows that the process of making DLX polymer solution further purified the DLX polymer, making it contain only galactomannans.

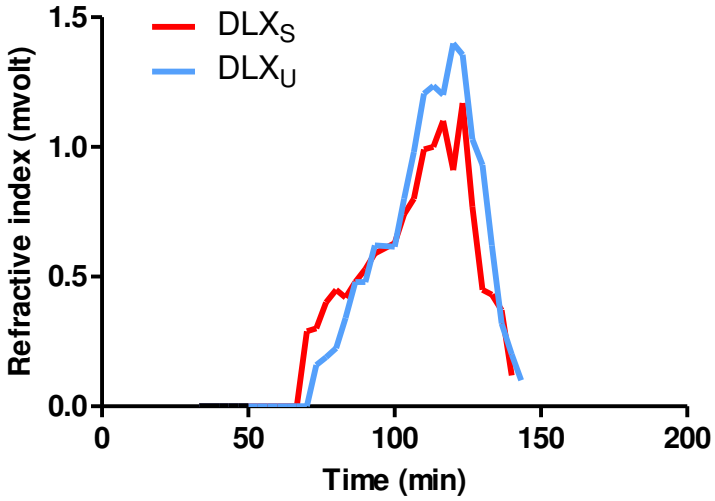

Figure 19: Chromatographic elution profile of sample monitored by refraction index (RI).

The methylation analysis of DLXs and DLXu galactomannans were performed by a sequence of procedures in order to obtain fully O-methylated derivatives (SASSAKI *et al.*, 2005). Hydrolysis of per-O-methylated derivatives produced mixtures of partially methylated monosaccharides: 2,3,4,6-Me,-Man, 2,3,4,6-Me,-Gal, 2,3,6-Me3-Man and 2,3-Me2-Man (Figure 20).

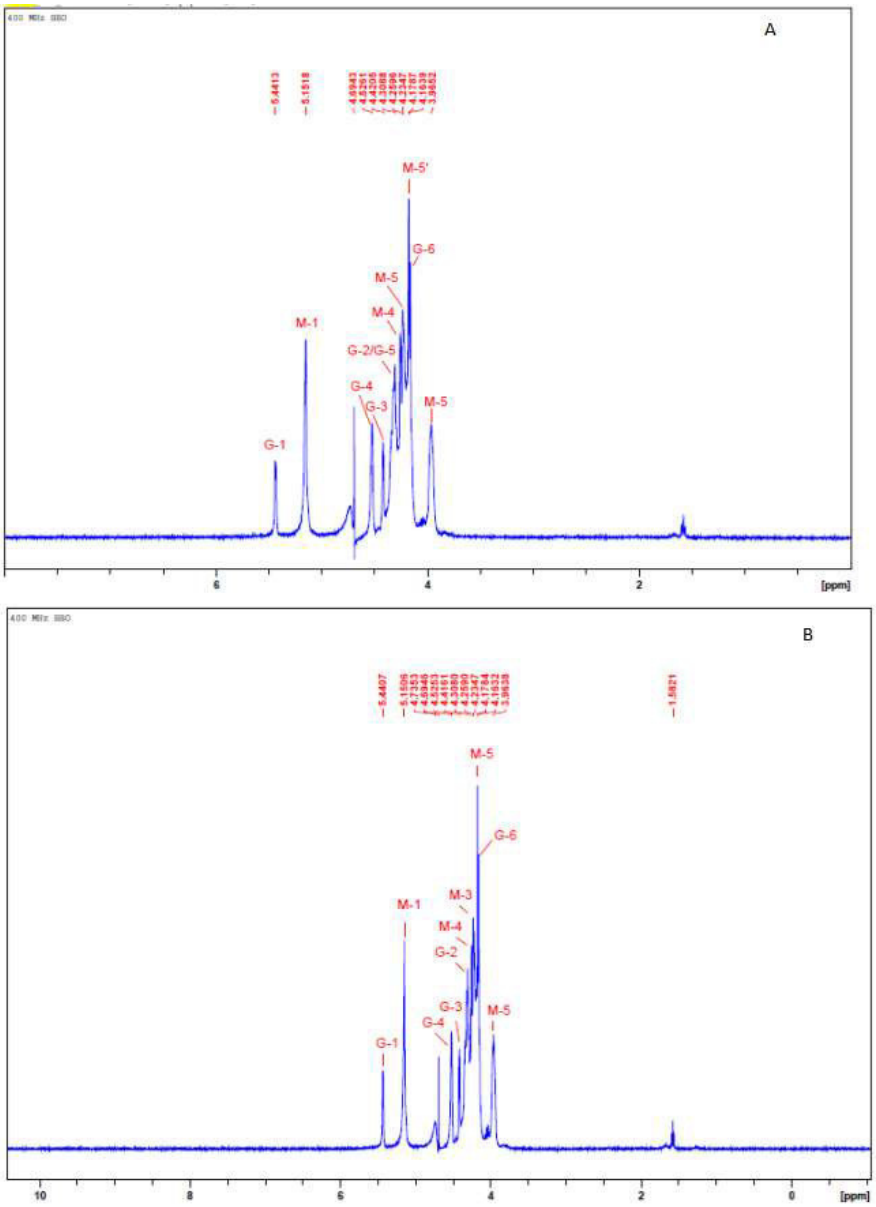

Figure 20: ^{1}H NMR spectra of (A) DLXu (B) DLXs. M, mannose and G, galactose sugar signals

The galactomannans ^{1}H-NMR (Figure 20) and ^{13}C-NMR (Figure 21) spectroscopy analysis showed that resonances in the ^{13}C-NMR spectra are in close agreement with those reported for other galactomannans (BENTO *et al.*, 2013). The ^{1}H- and ^{13}C-NMR spectral demonstrated a close relationship in the DLXs and DLXu structures, signifying minimal

alteration due to sonication. The signals at the anomeric region of ^{13}C- NMR (Figure 21) indicates that the mannopyranosyl residues are β-linked while the galactopyranosyl residues are α-linked.

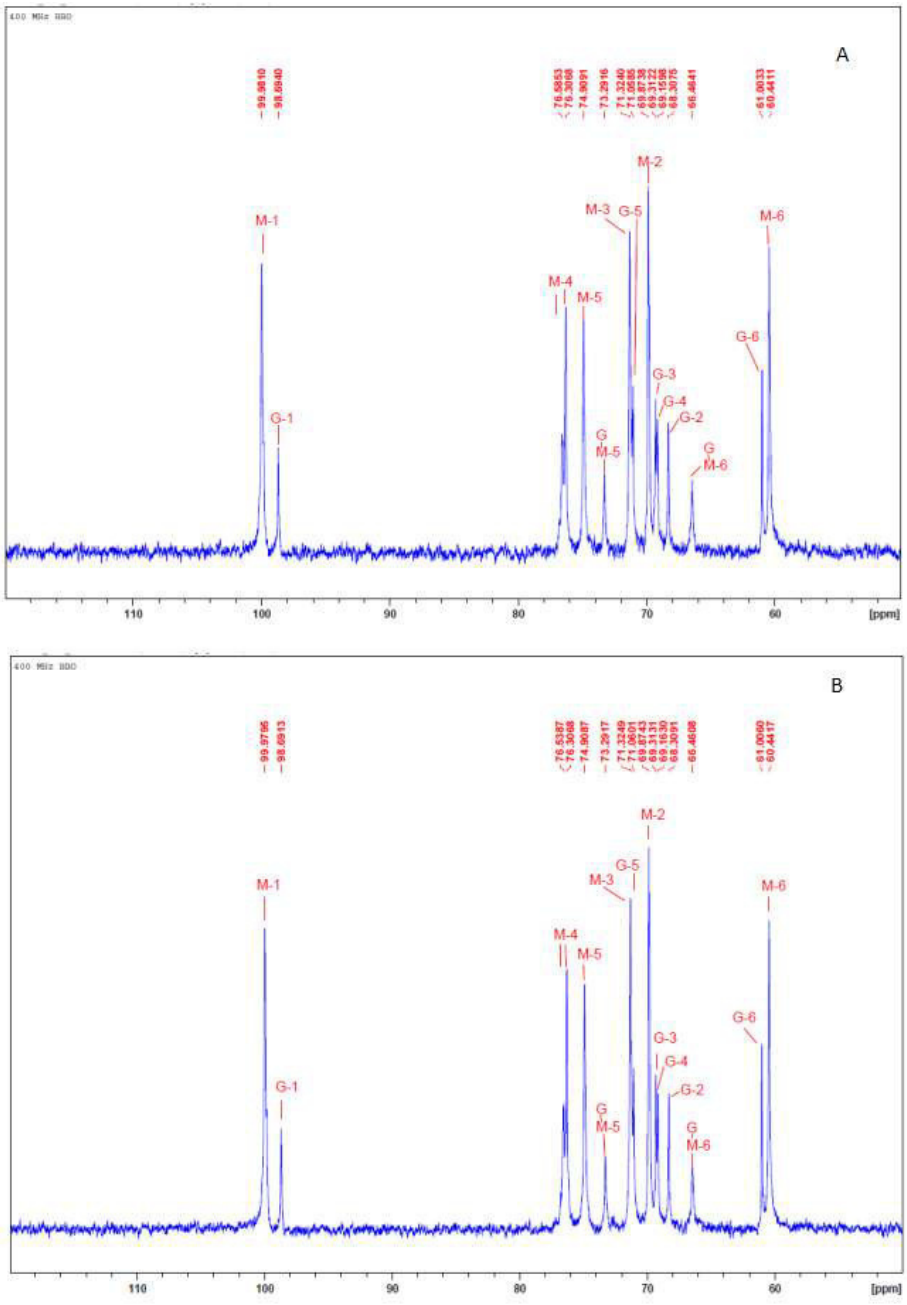

Figure 21: ^{13}C NMR spectra of (A) DLXu (B) DLXs, M, mannose and G, galactose sugar signals

The DLXu O-substituted resonances at C4 showed two clear peaks. The more abundant peak at 76.3 can be attributed of two contiguous unsubstituted O-mannopyranosyl residues while the peak at 77.59 may be ascribed to the superimposition of signals from diads, where only one of the two mannose residues is substituted. The same results were observed for DLXs, indicating an irregular distribution of *Gal* in the side chain of DLX galactomannan (Figure 22) and also showing no major effect of sonication on the galactomannans.

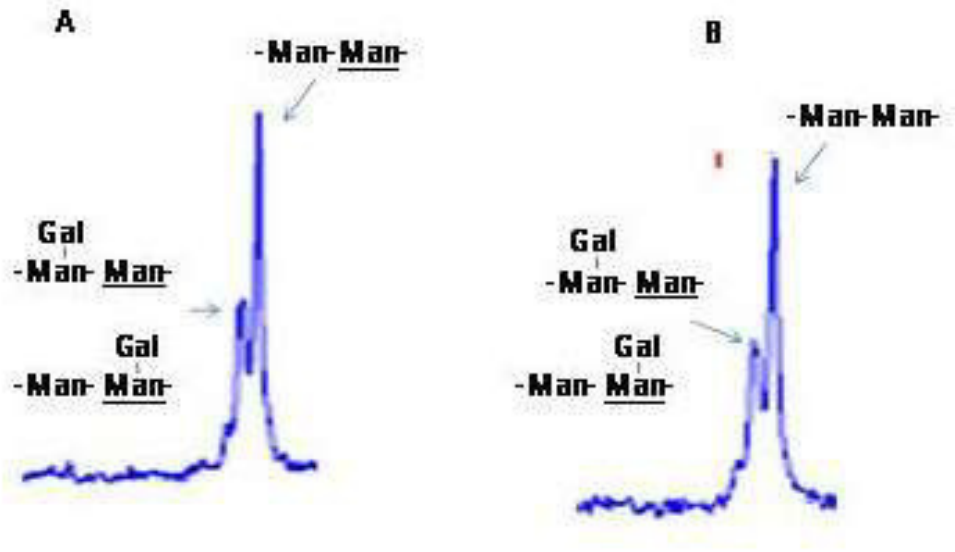

Figure 22: ^{13}C NMR spectra region of C4 for D-mannosyl units in *Delonix regia* galactomannan showing chemical shift for the underlined Man (A) DLXs (B) DLXu

5.3 **Design of Experiment: selection of parameters**

From the perspective of formulation design, diverse processes and formulation variables can individually or interact to influence a product's desired outcome. Equipment, materials, process and people have been noted to generally influence the characteristics of designed nanoparticles (Figure 8). People and process factors could have a great influence on

nanoparticles outcome even if the materials are controlled. In this way, all the parameters described in the Fishbone diagram represented in Figure 8 were evaluated and some of them were controlled to avoid their influence in the process of obtaining the nanoparticles. For example, to circumvent probable non-uniformity from processes involving people such as dropping of polymer solution into non-solvent, an automated PumpPro perylstatic pump was used.

Delonix polymer is hydrophilic and as such needs an organic non-solvent to produce nanoparticles with the nanoprecipitation technique. Toxicity and size was a major factor considered in choosing the right non-solvent in producing DLX polymeric nanoparticles. Non-solvent such as methanol, acetone and isopropyl alcohol (IA) were considered more toxic when compared to ethanol. However, IA was tested as a probable non-solvent as it is considered as less toxic than methanol and acetone. Table 4 shows DLX polymeric nanoparticles size when ethanol or ethanol-IA mixture was used as non-solvent and 5 % Tween 80 was used as surfactant.

Table 4: Preliminary study: influence of non-solvent and magnetic agitation speed on DLX polymeric nanoparticles

Non-solvent	Magnetic agitation speed (rpm)	Hydrodynamic diameter (nm)
Isopropyl Alcohol (IA)	600	[a]602.0 ± 47.2
IA:Ethanol (1:1)	600	533.3 ± 29.5
IA:Ethanol (1:3)	600	[a]484.4 ± 4.8
Ethanol	600	[b]466.2 ± 13.4
Ethanol	1000	[b]330.6 ± 8.8

One Way ANOVA [a]$p < 0.001$; [b]$p < 0.0001$

Result shows that increase in the amount of ethanol in the ethanol:IA mix led to a decrease in DLX polymeric nanoparticles size. It is known that nanoprecipitation failure can occur or larger nanoparticles sizes are formed when the differences in the dielectric constant between the solvent and non-solvent is high (BILATI *et al.*, 2005). Water has a dielectric constant of about 80.1, ethanol has 24.6 while IA has 19.9 (BILATI *et al.*, 2005); this could be responsible for the observed difference in size.

The magnetic agitation speed of the non-solvent at the time of addition of the DLX polymeric solution was also preliminary evaluated (Table 4). An increase in the magnetic agitation speed from 600 to 1000 rpm led to a significant reduction in DLX polymeric nanoparticles size. Thus, ethanol and 1000 rpm was chosen as the non-solvent and agitation speed respectively for all DLX polymeric nanoparticles preparation in this study.

Different surfactants and surfactant concentrations were tried to choose a suitable surfactant and surfactant concentration for DLX polymeric nanoparticles preparation (some results are not shown in this thesis). Table 5 shows results of size, PdI and zeta potential of DLX polymeric nanoparticles prepared using different surfactants at different concentrations.

Table 5: Preliminary study: influence of surfactant and surfactant concentration on DLX polymeric nanoparticles

Non-solvent	Hydrodynamic diameter (nm)	Zeta Potential
Poloxamer 407 (3%)	229.0 ± 11.2	[a,b]-7.84 ± 0.82
Span 80 (5%)	[a]623.8 ± 70.0	[a]-18.64 ± 2.08
Tween 80 (5%)	[a]309.4 ± 9.9	[b]-23.69 ± 4.95

One Way ANOVA [a]$p < 0.001$; [b]$p < 0.0001$

The DLX polymeric nanoparticles prepared using Poloxamer 407 (P407) had considerable small size, PdI and zeta potential but it was difficult to completely dissolve P407 in absolute ethanol. Nanoparticles were difficult to produce using Tween 20 as the non-solvent medium thickens as the DLX polymer solution was added drop-wise making it difficult to manipulate. DLX polymeric nanoparticles made with Tween 80 had adequate sizes, zeta potential but high PdI while those made from Span 80 had considerably large sizes but low PdI.

Thus, through carefully researched knowledge space and based on results above, three factors were chosen - *polymer concentration, surfactant mix ratio and non-solvent/solvent ratio* - as factors that could influence the properties of the DLX polymeric nanoparticles. In brief, polymer concentration was chosen based on the knowledge space available as increase in polymer concentration generally leads to increase in viscosity, which consequently produces nanoparticles with larger sizes (BILATI *et al.*, 2005). Surfactant mix ratio was selected based on results which showed that Span 80, when used alone produced large DLX polymeric nanoparticles with PdI < 0.2 while using Tween 80 alone produced DLX polymeric nanoparticles with higher PdI. We hypothesized that including Span 80, a lipophilic surfactant in the preparation could have some control on the swelling of the hydrophilic DLX polymer, thereby controlling its size. Non-solvent/solvent ratio was selected due to solvent economics and the hydrophilic nature of DLX polymer.

5.4 **Characterization of DLX polymeric nanoparticles**

Process and formulation variables can affect product outcome in a nanoprecipitation process to different extents, depending particularly on the interaction of the variables. Table 6

shows the nanoparticles size, PdI and zeta potential of the DLX polymeric nanoparticles based on the combination of factors tested at different levels in the DoE described in Table 2.

Table 6: Hydrodynamic diameter, PdI and zeta potential of DLX polymeric nanoparticles. Data shown are mean ± SD of 3 replicates.

Formulation	Hydrodynamic diameter (nm)	PdI	Zeta potential (mV)
F1	215.4 ± 3.8	0.192 ± 0.022	-38.5 ± 6.1
F2	315.2 ± 9.6	0.189 ± 0.004	-40.3 ± 8.1
F3	321.9 ± 11.2	0.215 ± 0.026	-62.5 ± 4.1
F4	252.7 ± 8.8	0.150 ± 0.031	-37.9 ± 4.3
F5	357.7 ± 8.5	0.214 ± 0.006	-65.2 ± 5.0
F6	276.3 ± 13.1	0.185 ± 0.008	-67.7 ± 6.4
F7	231.3 ± 5.8	0.140 ± 0.006	-39.9 ± 4.1
F8	266.7 ± 4.4	0.149 ± 0.020	-37.2 ± 5.9
F9	276.3 ± 13.1	0.185 ± 0.008	-67.7 ± 6.4
F10	225.7 ± 3.9	0.162 ± 0.009	-59.7 ± 8.5
F11	318.8 ± 10.6	0.175 ± 0.007	-68.8 ± 8.2
F12	260.1 ± 10.0	0.157 ± 0.016	-31.8 ± 3.1
F13	276.3 ± 13.1	0.185 ± 0.008	-67.7 ± 6.4
F14	261.1 ± 15.2	0.225 ± 0.021	-39.8 ± 2.4
F15	270.3 ± 12.5	0.176 ± 0.006	-49.1 ± 8.0

The DLX polymeric nanoparticles have mean particle sizes ranging between 215 to 360 nm (Table 6). Particle size distribution was observed to be narrow with PdI values less than 0.230, indicating a system that is not very polydispersed. The zeta potential of the DLX

polymeric nanoparticles was negative with values smaller than -30 mV. This suggests the presence of adequate electrical stability due to repulsive forces existing between particles (VERONOVSKI *et al.*, 2010). Neutral galactomannans like DLX polymer in solution normally tends to have slightly negative zeta potentials confirming their neutrality (Carneiro-da-Cunha et al, 2011). However, the high negative zeta potential observed in the DLX polymeric nanoparticles dispersion may be due to the dispersion of the DLX polymer in 0.5 M NaOH. Increase in the pH of a solution has been shown to have a significant influence on the zeta potential of nanoparticles (CARNEIRO-DA-CUNHA *et al.*, 2011). Thus, we successfully prepared stable hydrophilic Delonix polymeric nanoparticles using a simple and innovative nanoprecipitation process by using surfactant mix to control nanoparticles properties without the use of toxic cross-linking agents such as glutaraldehyde. This simple method could also be deployed in the preparation of other useful hydrophilic polymers of natural origin including chitosan.

In order to understand the influence of the selected variables on DLX polymeric naoparticles characteristics, the result obtained in Table 6 was subjected to regression analysis and general linear modeling. Using the 15-experiment Box Behnken design, individual variable effects and their two-way interactions on DLX polymeric nanoparticles characteristics are estimable while the three-way interaction is used to estimate the error. Thus, the statistical model in Equation 7 was deployed to understand this interaction.

$$y = \beta_o + \beta_1 X_1 + \beta_2 X_2 + \beta_3 X_3 + \beta_4 X_1 X_2 + \beta_5 X_1 X_3 + \beta_5 X_2 X_3 + \varepsilon \qquad \text{Equation 7}$$

where y is the response, X_1, X_2 and X_3 (predictors) are polymer concentration, Tween-Span ratio and Non-Solvent/Solvent ratio respectively, β_o is the mean response when all variables are zero and $\beta_{1\text{-}5}$ represent change in mean response per unit change in predictors respectively. From results in Table 6, PdI and zeta potential were adequate for polydispersibility and stability requirements, thus only the hydrodynamic diameters were subjected to regression analysis. Table 7 is the result of regression analysis showing the individual and interacting effect of the predictors on the hydrodynamic diameter of DLX polymeric nanoparticles. From the result, a general linear model for predicting the DLX polymeric nanoparticles size was derived from significant predictors as shown in Equation 8;

$$y = 275.0533 + 48.5625X_1 - 17.3750X_1X_2 \qquad \text{Equation 8}$$

It can be observed from Table 7 that polymer concentration significantly influenced the DLX polymeric nanoparticles size. The positive estimated β1 parameter further suggests that the influence of polymer concentration is such that an increase in polymer concentration will lead to increase in DLX polymeric nanoparticles size. This is expected as several studies have shown that increase in polymer concentration generally leads to an increase in viscosity that hampers diffusion of solvent towards the non-solvent in a nanoprecipitation process (BILATI et al., 2005; DONG et al., 2015) which normally involves diffusion of a solvent into the non-solvent; water being the solvent and ethanol being the non-solvent.

Table 7: Regression analysis: estimated effect of nanoprecipitation predictors on DLX polymeric nanoparticle size

	Hydrodynamic diameter (nm)	Hydrodynamic diameter (nm)	Hydrodynamic diameter (nm)	Hydrodynamic diameter (nm)	-95.00%	+95.00%	Hydrodynamic diameter (nm)	Hydrodynamic diameter (nm)	-95.00%	+95.00%
	Param.	Std.Err	t	p	CnfLmt	CnfLmt	Beta (ß)	St.Err.ß	CnfLmt	CnfLmt
Intercept	275.0533	3.259534	84.38425	0.000000	267.5368	282.5698				
Polymer concentration (%w/v)	48.5625	4.463301	10.88040	0.000005	38.2701	58.8549	0.937318	0.086147	0.738662	1.135975
Tween-Span Ratio	0.0375	4.463301	0.00840	0.993502	-10.2549	10.3299	0.000724	0.086147	-0.197932	0.199380
Non solvent-solvent Ratio	-1.9250	4.463301	-0.43130	0.677640	-12.2174	8.3674	-0.037155	0.086147	-0.235811	0.161501
Polymer concentration (%w/v)*Tween-Span Ratio	-17.3750	6.312060	-2.75267	0.024956	-31.9306	-2.8194	-0.237135	0.086147	-0.435791	-0.038479
Polymer concentration (%w/v)*Non solvent-solvent Ratio	4.7500	6.312060	0.75253	0.473293	-9.8056	19.3056	0.064828	0.086147	-0.133828	0.263485
Tween-Span Ratio*Non solvent-solvent Ratio	-1.1500	6.312060	-0.18219	0.859965	-15.7056	13.4056	-0.015695	0.086147	-0.214352	0.182961

There was no individual influence of surfactant mix ratio or non-solvent/solvent ratio on DLX polymeric nanoparticles size. This kind of result has been reported by other studies employing nanoprecipitation in the production of nanoparticles (ALI & LAMPRECHT, 2013; BILATI *et al.*, 2005), as non-solvent/solvent proportions in nanoprecipitation processes has its importance in solvent/non-solvent volume control (economics) (BILATI *et al.*, 2005). However, the interaction of polymer concentration and surfactant mix ratio produced a significant effect on DLX polymeric nanoparticles.

Response surface plot of DLX polymeric nanoparticles hydrodynamic diameter, polymer concentration and surfactant mix ratio is as shown in Figures 23. The plot shows that DLX polymeric nanoparticles with smaller sizes are achieved at lower level of polymer concentration and surfactant mix ratio (highest Span 80 proportion). This result could be attributed partly to the low viscosity of polymer solution at lower concentration and additionally to the orientation and proportions of the Tween 80 and Span 80 in the nanoparticles dispersion. This prompted further studies and analysis to really understand the role of surfactant mix ratio in the size of DLX polymeric nanoparticles.

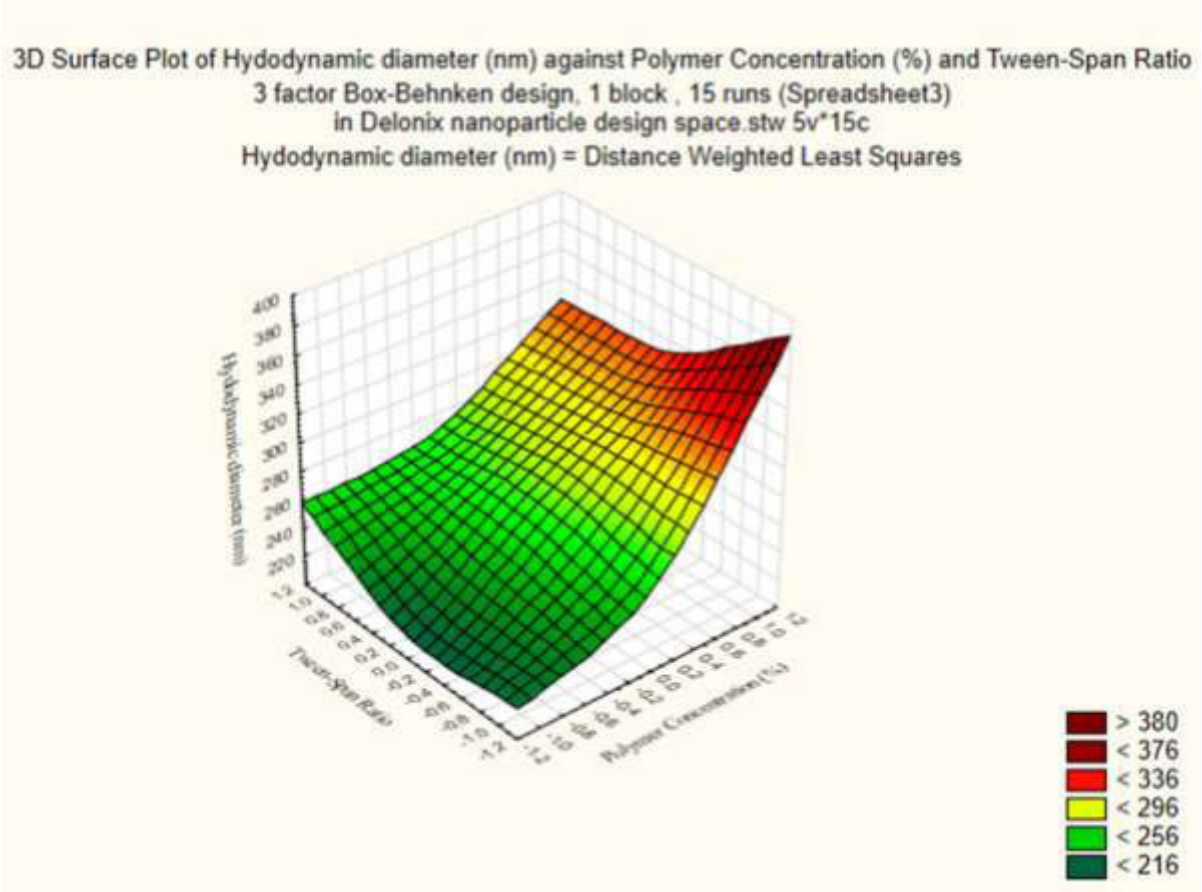

Figure 23: Response surface plot of DLX polymeric nanoparticles hydrodynamic diameter vs polymer concentration and surfactant mix ratio

The hypothesis that, probably, the orientation of Tween 80 and Span 80 in the DLX polymeric nanoparticles dispersion could have a significant influence on the swelling of DLX polymer and consequently its size as hydrophilic polymers such as DLX polymer have the tendency to swell when in contact with aqueous medium was considered. Thus, in the presence of only or higher amounts of Tween 80 (hydrophilic-lipophilic balance (HLB) = 15), DLX polymeric nanoparticles could have had direct contact with the aqueous medium, leading to 'minute' swellings which led to the size increase; however, with increase in Span 80 (HLB = 4.3) ratio, the orientation of Span 80 might have reduced or prevented DLX polymeric nanoparticles

from having contact with the aqueous medium, leading to reduced swelling and consequently smaller sizes of DLX polymeric nanoparticles. In fact, studies have proposed that changes in nanocapsule diameter with respect to Tween and Span concentration could be dependent on surfactant packing parameters (KHOEE & YAGHOOBIAN, 2009; MITCHELL & NINHAM, 1981). The probable schematic depicting DLX polymeric nanoparticles in dispersion prepared with a mixture of Tween80 and Span80 is as shown in Figure 24.

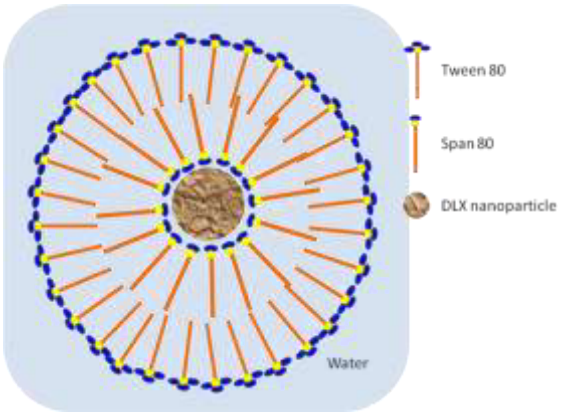

Figure 24: Proposed schematic of DLX polymeric nanoparticles in dispersion

The result of hydrodynamic diameter of three DLX polymeric nanoparticles prepared by varying only the surfactant mix ratio and keeping DLX polymer concentration at 1 % and non-solvent/solvent ratio of 10 is as shown in Table 8.

Table 8: Surfactant mix influence on DLX polymeric nanoparticles size. Data shown are the mean ± SD of 4 replicates.

Tween 80:Span 80	Hydrodynamic diameter (nm)	PdI	Zeta Potential
1:0[a,b]	232.8 ± 3.6	0.185 ± 0.005	-64.6 ± 8.7
4:1[b,c]	215.4 ± 3.6	0.193 ± 0.003	-66.5 ± 3.9
3:2[a,c]	203.6 ± 6.1	0.156 ± 0.006	-58.9 ± 4.4

One-Way ANOVA with Tukey's posttest: [a]$p < 0.001$; [b]$p < 0.01$; [c]$p < 0.05$

ANOVA analysis indicates a significant difference in DLX polymeric nanoparticles size between the three preparations, with the DLX polymeric nanoparticles containing higher proportion of Span 80 having smaller nanoparticles size, thus supporting our initial hypothesis.

The DLX polymeric nanoparticles described above were further subjected to a six-day swelling analysis by measuring nanoparticles size over this period. Figure 25 shows the DLX polymeric nanoparticles size increase as a function of time.

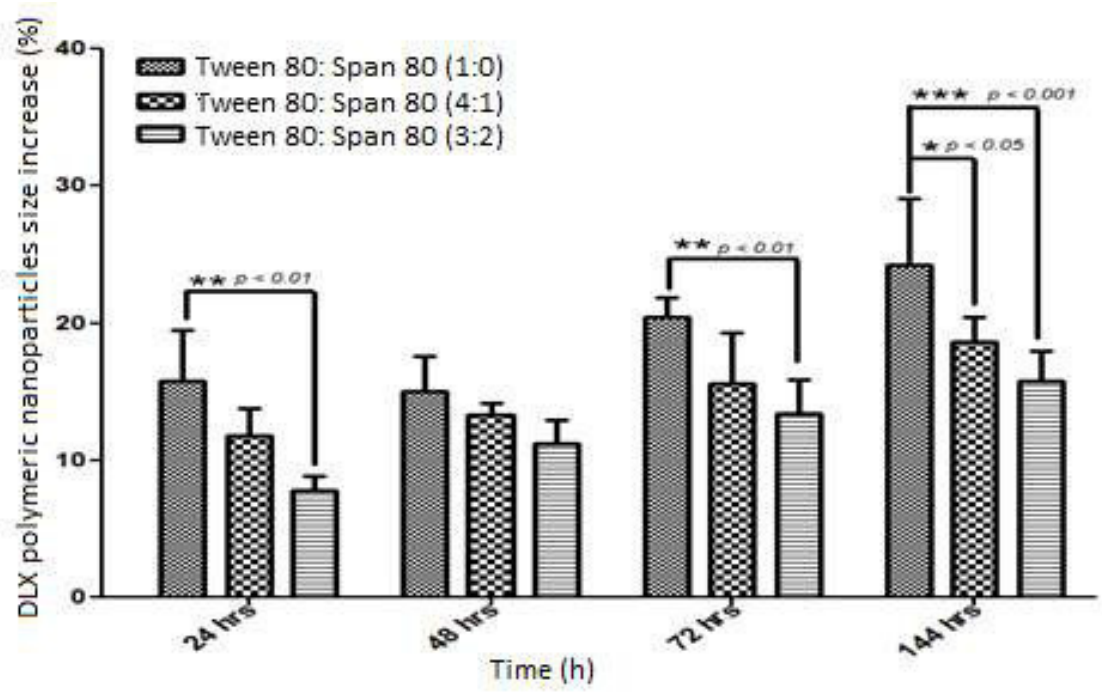

Figure 25: Surfactant mix ratio influence on DLX polymeric nanoparticles % size increase

It was observed that DLX polymeric nanoparticles prepared with surfactant mix containing highest amount of Span 80 (Tween-Span ratio, 3:2) has a lower percent size increase as compared to the other DLX polymeric nanoparticles suggesting that Span 80 has an influence in controlling the swelling and consequently the size of DLX polymeric nanoparticles. A 2-Way ANOVA analysis further shows a significant difference in the percent size increase of DLX

polymeric nanoparticles, with nanoparticles containing Tween-Span ratio of 3:2 having the lowest percent size increase after 6 days. Also, using Equation 8 to predict, the theoretical DLX polymeric nanoparticles size prepared using DLX polymer concentration level -1 (1 %w/v) and surfactant mix ratio -1 (Tween80:Span80 ratio 3:2) was 209 nm showed acceptable closeness to the experimental DLX polymeric nanoparticles size of 203.6 ± 6.1 nm prepared using the same parameters.

Based on these affirmations, DLX polymeric nanoparticles prepared using surfactant mix containing Tween 80 and Span 80 in ratio 3 to 2 was chosen and continuously used to prepare DLX polymeric nanoparticles for all subsequent studies.

Figure 26 shows the TEM photomicrograph of DLX polymeric nanoparticles prepared using Tween-Span surfactant mix ratio of 3:2. The photo was analyzed using *Fiji* software (ImageJ, USA) and DLX polymeric nanoparticles sizes were determined to be in the range of 28 to 38 nm. The difference in the DLS (about 204 nm, Table 8) and TEM sizes could be due partly to the fact that DLS determination is based on intensity determination of hydrodynamic diameter while TEM is based on number. Also, the hydrophilic and swelling nature of the DLX polymer might have influenced the size difference observed as the TEM photomicrograph is a dry size determination.

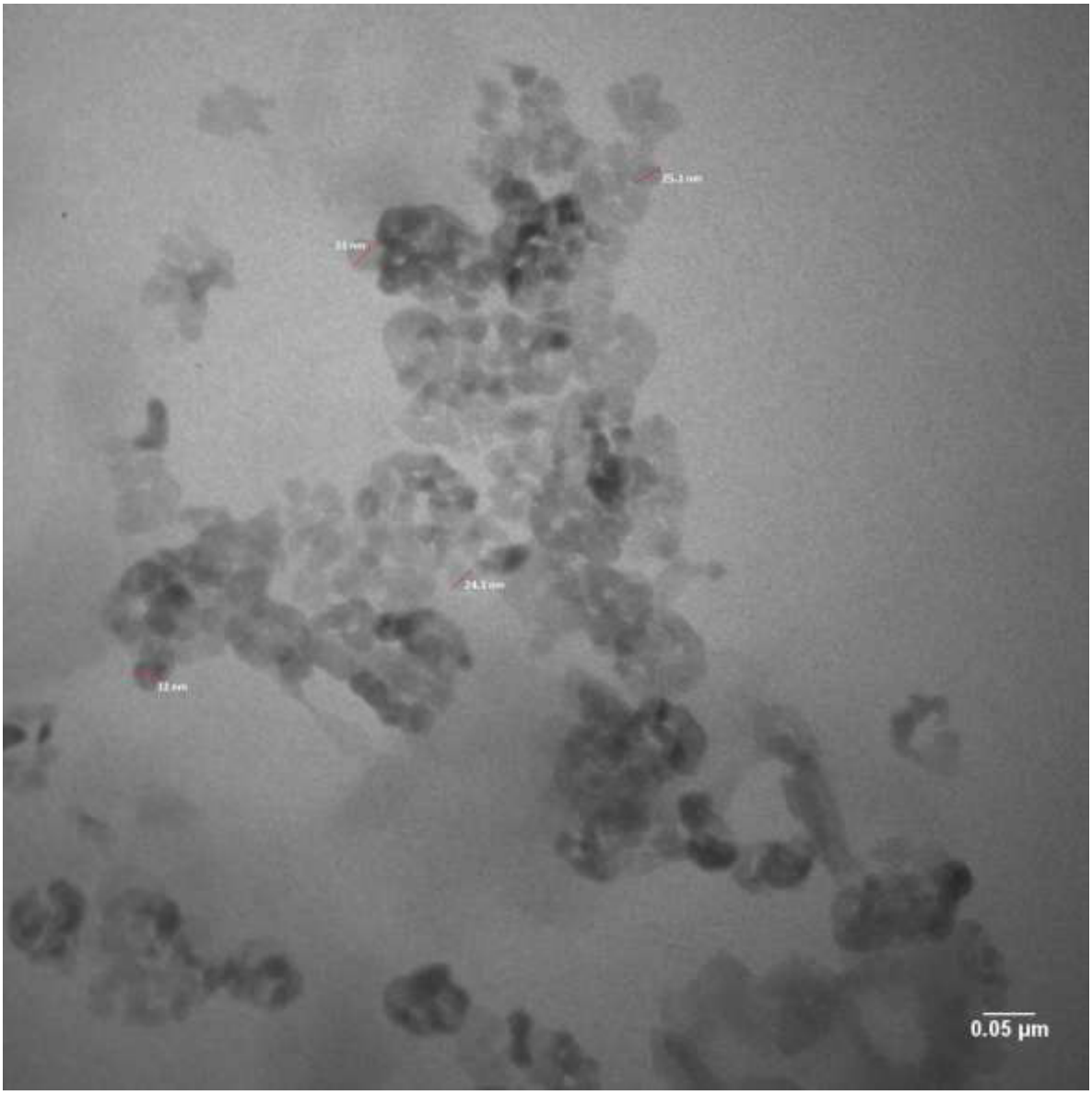

Figure 26: TEM photomicrograph of blank DLX polymeric nanoparticles

5.5 **Quantification of Isotretinoin: Method Development and Validation**

A method was developed and validated for the quantification of IST as previously described in the method section. Figure 27 shows the chromatograph of IST in methanol under the conditions described with retention time of 7.6 min.

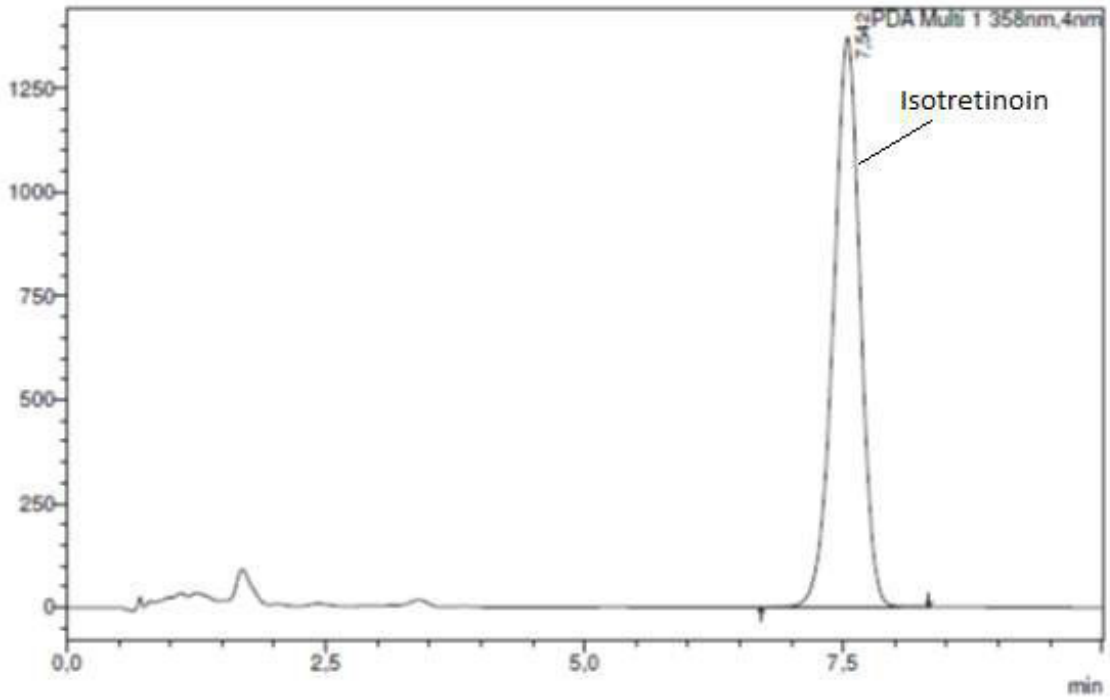

Figure 27: Chromatogram of IST in methanol determined by the parameters of the proposed method: C18 column, acetonitrile (70%) and 0.1 %v/v Trifluoroacetic acid (30%) as mobile phase, flow rate of 0.6 mL/min, injection volume of 10 µL, oven temperature of 30^{o}C and wavelength of 358 nm

5.5.1 **Selectivity of method for Isotretinoin quantification**

It is important to ascertain that no other substance interfere with the quantification of IST based on the developed method. In this study, homogenized pig ear skin extract, Wistar rat skin, PBS-ethanol (7:3) as receiver medium and excipients in Roacutan® commercial capsule are probable substances that could interfere with IST. Figure 28 shows the chromatogram of the perceived 'impurities' with and without IST. The figures show no interference with the retention time of IST as they did not present the same retention times with that of IST, confirming the selectivity of this method for the quantification of IST. Likewise, the analysis of Wistar rat skin extract in PBS-ethanol (7:3) and methanol did not interfere with the IST peak, with retention times before 2.5 min.

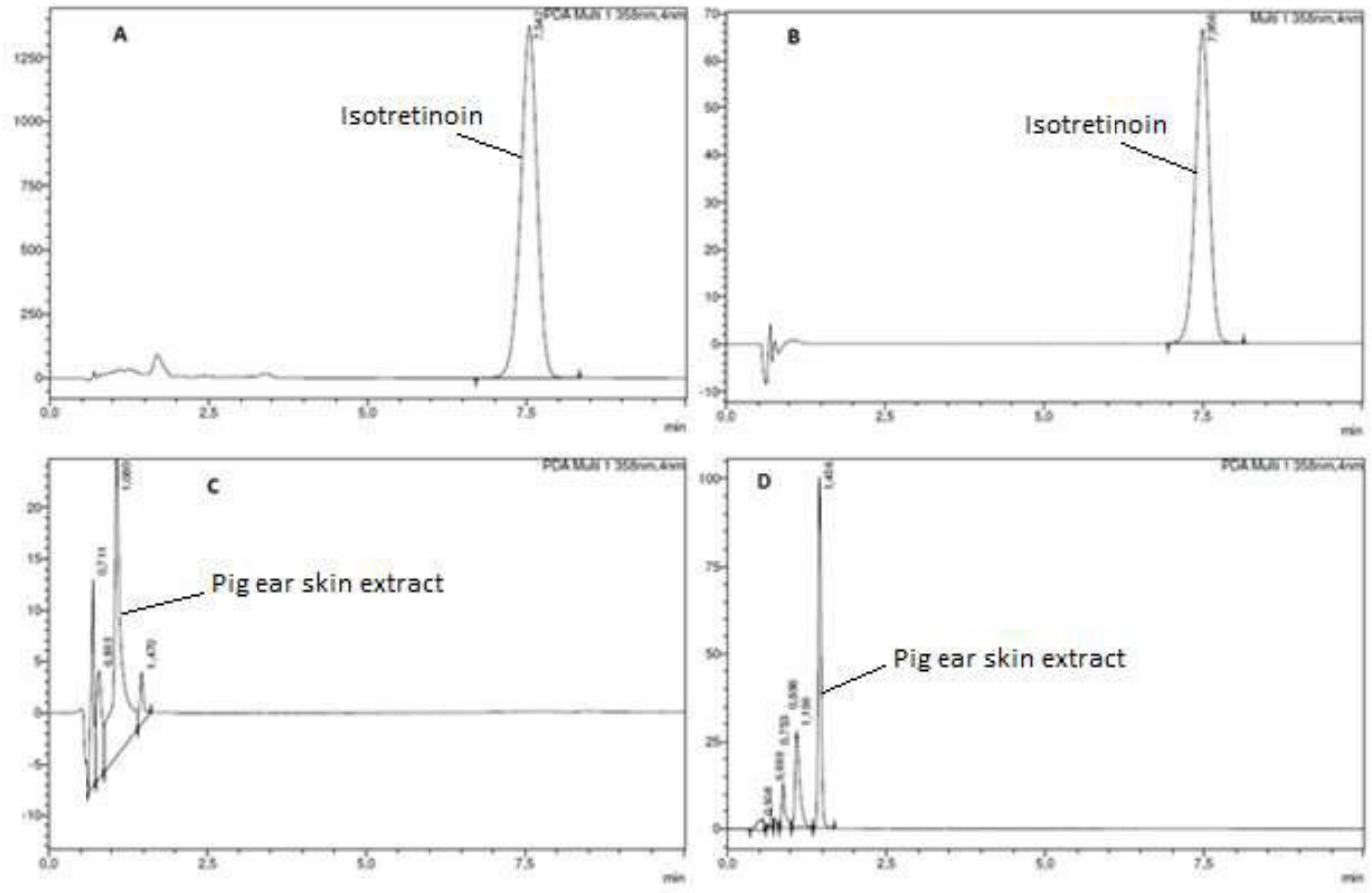

Figure 28: Chromatogram of (A) IST in methanol (B) IST from Roacutan capsule (C) homogenized pig ear skin in methanol (D) homogenized pig ear skin in PBS/ethanol (7:3)

5.5.2 **Linearity**

The proposed method was selective and linear within the IST concentration range of 0.3 and 15 µg/mL with adequate regression coefficient R^2 = 0.993. Figure 29 shows the plot of peak chromatogram areas versus IST concentration. The regression equation for the analytical curve was y = 77966x – 14136; where y is the peak area corresponding to IST concentration, x.

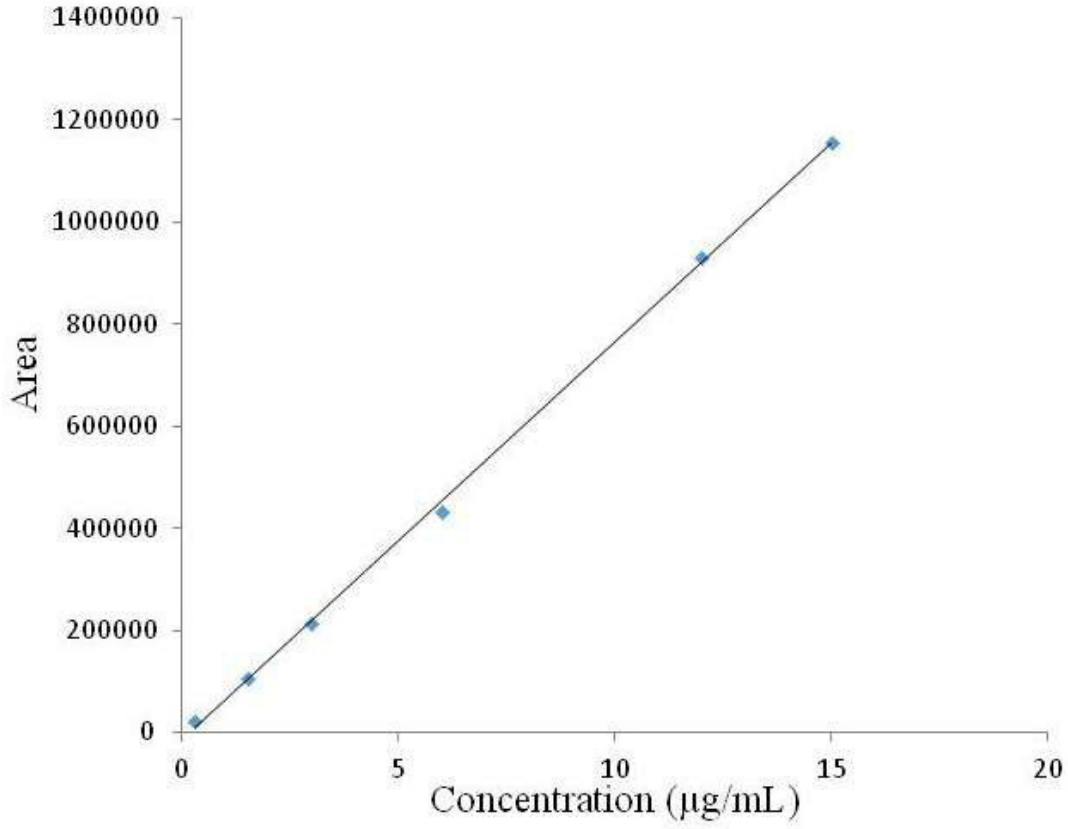

Figure 29: Plot of chromatogram area against IST concentration

5.5.3 **Detection and Quantification Limits**

The detection limit (LoD) of an analytical method is the lowest amount of an analyte that can be conveniently detected but not necessarily quantifiable while quantification limit (LoQ) is the lowest amount of an analyte that can be detected and quantitatively determined to a degree of accuracy and precision (ICH, 2005). The LoD and LoQ for this validated method, calculated using Equations 2 and 3, respectively, were 0.056 and 0.169 µg/mL respectively. The LoD and LoQ determined experiment were adequate to quantify IST throughout all experiments.

5.5.4 **Accuracy and Precision**

The accuracy of an analytical procedure expresses the closeness or agreement between a theoretical concentration of a test material and the experimental value (ICH, 2005), generally

expressed as relative error. Table 9 shows the accuracy of the proposed method with respect to percent recovery and relative error. The result shows acceptable values of percent recovery and relative error which was lower than 5 %.

Table 9: Accuracy parameters for validated Isotretinoin method

Accuracy Parameters	**Isotretinoin Concentration (µg/mL)**		
	2.0	**10.0**	**14.0**
Mean recovery (µg/mL)	1.99	9.85	14.07
Percent recovery (%)	99.6	98.49	100.5
Relative error	0.40	1.51	0.50

Precision evaluates the closeness of measurements of a single analyte to the repeated aliquot measurements of the same homogenous sample and it is generally expressed as variance, standard deviation or coefficient of variation. It could be precision measured over a short interval of time called intra-day precision or repeatability, or that measured over different days called inter-day or intermediate precision (ICH, 2005). Table 10 shows the precision of intra-day and inter-day analysis of IST using the proposed method. Result shows acceptable values of precision which were generally lower than 5 %.

Table 10: Precision parameters for validated Isotretinoin method

Isotretinoin concentration (µg/mL)		**2.0**	**10.0**	**14.0**
% RSD	**Day 1**	2.95	2.35	1.13
	Day 2	1.70	1.82	2.36
	Day 3	0.93	2.63	2.98

5.5.5 IST Recovery from pig ear skin, Wistar rat skin, DLX polymer solution and Roacutan® capsule

Recovery from pig ear skin, Wistar rat skin and DLX polymer solution was performed to verify that no detrimental interaction exists between IST, pig ear and Wistar rat skin or DLX polymer and ascertain that IST can be adequately and accurately extracted from these samples. Table 11 shows that, within the scope of extraction process, recovery of IST from pig ear and Wistar rat skin matrix, and DLX polymer solution were adequate, with recovery values at different spike concentrations higher than 98 %.

Table 11: Isotretinoin recovery from pig ear skin, Wistar rat skin and DLX polymer solution

	Theoretical IST concentration (µg/mL)		
	2.5	**6.25**	**12.5**
Pig Ear Skin			
Experimental concentration (µg/mL)	2.55	6.24	12.28
% Recovered	101.96	99.86	98.28
% RSD	2.58	1.54	2.13
Wistar rat skin			
Experimental concentration (µg/mL)	2.48	6.17	12.3
% Recovered	99.2	98.72	98.4
% RSD	1.88	2.96	2.04
DLX polymer solution			
Experimental concentration (µg/mL)	2.56	6.37	12.84
% Recovered	102.47	101.92	102.72
% RSD	2.57	1.65	0.63

The recovery of IST concentrations of 2.5, 6.5 and 12.5 µg/mL from pig ear skin, Wistar rat skin and DLX polymer solution was between 98.2 and 102.72 respectively with % RSD values lower than 5 %. This result clearly demonstrates the adequacy and reproducibility of the

extraction method employed in this study and non-detrimental interaction between IST, pig ear skin, Wistar rat skin or DLX polymer solution.

Table 12 shows the recovery amount and percentage of IST from commercial Roacutan® capsule. The recovery using methanol to extract IST directly from Roacutan and olive oil was adequate with percent recoveries of 95.28 and 94.68 %. This result is important as its shows that the validated method for the quantification of IST is adequate to quantify IST in commercial capsules.

Table 12: Recovery of IST from Roacutan® 20 mg capsule

Theoretical IST amount (20 mg)	**Methanol**	**Olive Oil**
Experimental IST amount (mg)	19.06	18.94
% Recovered	95.28	94.68
% RSD	1.27	0.97

5.6 **Preparation and characterization of BODIPY-DLX polymeric nanoparticles**

The characteristics of BODIPY-loaded DLX polymeric nanoparticles are as shown in Table 13, demonstrating the possibility of DLX polymeric nanoparticles to encapsulate hydrophilic and lipophilic molecules.

Table 13: Characteristics of BODIPY-DLX polymeric nanoparticles

DLX polymeric nanoparticles	Hydrodynamic diameter (nm)	PdI	Zeta Potential (mV)	Encapsulation efficiency (%)
Loaded with hydrophilic BODIPY	232.8 ± 11.1	0.185 ± 0.009	-69.7 ± 7.5	68.6 ± 5.7
Loaded with lipophilic BODIPY	222.8 ± 9.1	0.132 ± 0.013	-65.6 ± 3.2	6.0 ± 1.6

BODIPY-DLX polymeric nanoparticles sizes were < 235 nm, PdI was < 0.2 while zeta potential values was < -30 mV affirming stability. Encapsulation efficiency of lipophilic BODIPY into DLX polymeric nanoparticles was significantly low, ≈ 6% as compared to the hydrophilic BODIPY which was ≈ 69%. The encapsulation efficiency can be explained by the partition coefficient (Log $P_{octanol/water}$) of the hydrophilic (-4.93) and lipophilic (-0.19) BODIPY dyes. The $LogP_{octanol/water}$ in this study was calculated using free MarvinSketch software (ChemAxon, Hungary). Although, the MarvinSketch software used in determining the $LogP_{ocatanol/water}$ do have some limitations, particularly in relation to the structure of the BODIPYs, as it did not take into account the core of the structure, thereby, making the values calculated only relative and 'illustrative'; however, the insolubility of lipophilic BODIPY in water was demonstrated (Figure 30B). In comparison to free lipophilic BODIPY which is obviously insoluble in aqueous medium, lipophilic BODIPY-DLX polymeric nanoparticles homogeneously dispersed in aqueous medium (Figure 30C). Thus, despite the low encapsulation efficiency of lipophilic BODIPY in DLX polymeric nanoparticles, the loaded DLX polymeric nanoparticles homogenously dispersed in aqueous medium.

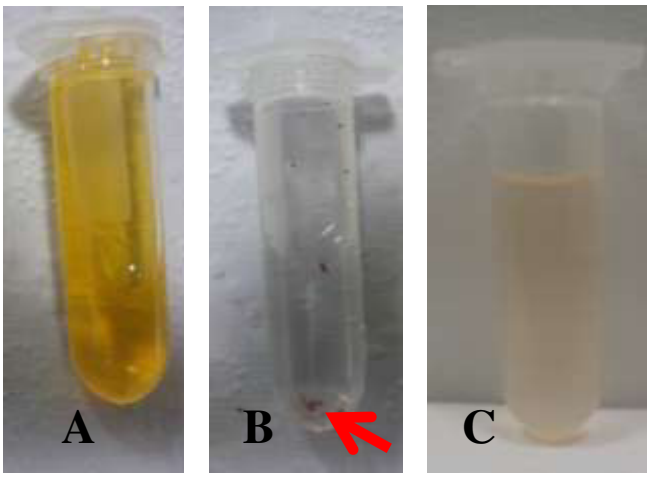

Figure 30: Dispersion of lipophilic BODIPY (A) in methanol (B) in water (C) loaded in DLX polymeric nanoparticles

5.7 **Preparation and characterization of IST-loaded DLX polymeric nanoparticles**

The maximum amount of IST that can be conveniently solubilized in 1% DLX polymer solution was determined to be 3.14 ± 0.09 µg/mL. IST-DLX polymeric nanoparticles were prepared using 1 mL of respective IST-DLX polymer solution, 10 mL of ethanol and Tween 80:Span 80 ratio of 3:2. Table 14 shows the size, polydispersibility, zeta potential and encapsulation efficiency of IST-DLX polymeric nanoparticles prepared by using different concentrations of IST in ethanol or DLX polymer solution.

Table 14: Characteristics of IST-DLX polymeric nanoparticles prepared by adding IST in different amounts in solvent or non-solvent

Amount of IST and solvent of its dispersion	**Hydrodynamic diameter (nm)**	**PdI**	**zP (meV)**	**Encapsulation Efficiency (%)**
Blank DLX polymeric nanoparticles	203.6 ± 6.1	0.156 ± 0.006	-58.9 ± 4.4	-
10 mg IST in ethanol	222.6 ± 2.9	0.128 ± 0.021	-57.1 ± 6.6	[a]5.2 ± 0.8
1 mg/mL IST-DLX polymer solution	231.8 ± 9.9	0.174 ± 0.015	-69.4 ± 0.8	[a,b]33.9 ±1.6
3 mg/mL IST-DLX polymer solution	229.7 ± 9.6	0.181 ± 0.004	-67.1 ± 2.8	[a,b]26.9 ± 1.8

One Way ANOVA [a]$p < 0.0001$; [b]$p < 0.001$

Nanoparticles sizes determined using DLS technique were comparable and lower than 232 nm, PdI was lower than 0.2 showing a not very dispersed system and the zeta potential was higher than -30 mV, demonstrating adequate stability within the dispersion. These sizes were significantly higher than blank DLX polymeric nanoparticles size (203 ± 6.1). This increase may be due to corresponding viscosity increase in drug-polymer dispersion. This viscosity increase may lead to production of larger droplets, consequently producing larger nanoparticles (BHARDWAJ *et al.*, 1995). TEM microscopic evaluation of IST-DLX polymeric nanoparticles

also suggest similar sizes to blank DLX polymeric nanoparticles with average size of 29.5 nm ± 5.3 (Figure 31).

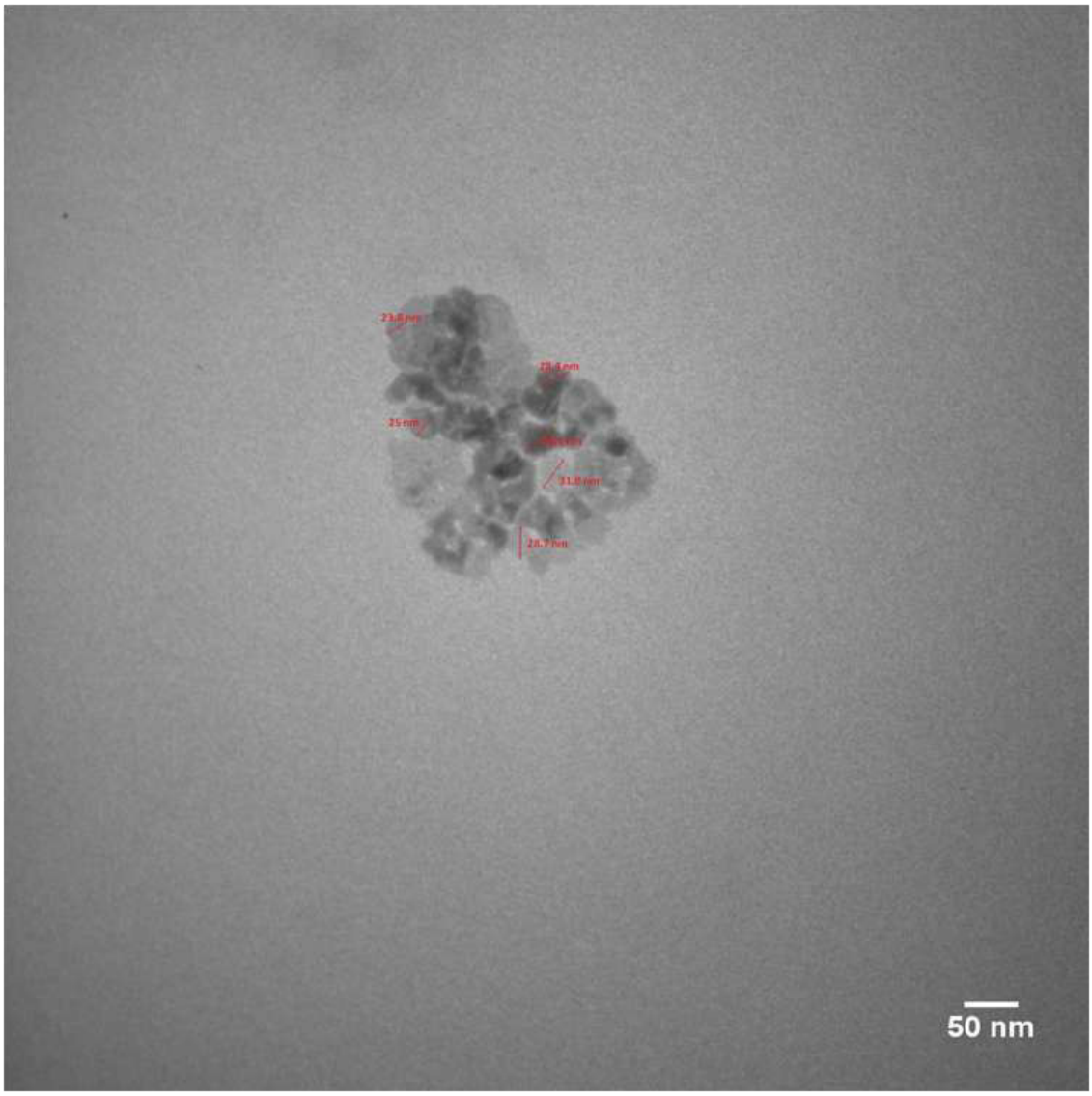

Figure 31: TEM photomicrograph of IST-DLX polymeric nanoparticles

The encapsulation efficiency when 10 mg of IST was dissolved in non-solvent ethanol was 5.2 ± 0.8 % (Table 14). This low amount encapsulated could be attributed to the lipophilicity of IST, reducing its ability to partition into the DLX polymer as compared to the non-solvent ethanol. About 34 and 27 % of IST was encapsulated when 1 and 3 mg/mL of IST-DLX polymer

solution was used respectively with IST encapsulation efficiency decreasing with an increase in IST concentration. DLX polymeric nanoparticles encapsulated approximately 520 µg of IST when 10 mg IST was dissolved in ethanol, 340 µg IST when 1 mg IST was solubilized in DLX polymer solution and 810 µg when 3 mg IST was solubilized in DLX polymer solution. Thus, based on IST quantity encapsulated in DLX polymeric nanoparticles, the method in which 3 mg IST was solubilized in DLX polymer solution was chosen as the IST-DLX polymeric nanoparticles preparation method throughout this study.

5.8 *In vitro* studies

5.8.1 Sink condition

Dissolution study of poorly soluble drugs is always a challenge as there is a small gap between complete solubilization and saturation of a drug in a dissolution medium. Sink condition describes the excess solubilizing power of a dissolution medium and has been recommended to be 5 and preferably 10 times the volume that will completely solubilize a drug (ROHRS, 2001). IST is a lipophilic drug, thus PBS/ethanol (7:3) was used as a receiver medium in all experiments. It is therefore important to quantify the amount of IST that will conveniently dissolve in PBS/ethanol (7:3). The amount of IST that dissolved in PBS/ethanol (7:3) was determined to be 41.8 ± 1.8 µg/mL; thus, the sink condition for IST in PBS/ethanol was calculated to be approximately 4.2 µg/mL and this value was considered in choosing the donor concentration in the release study.

5.8.2 *In vitro* IST release

The release profile of IST from IST-DLX polymeric nanoparticles and IST-DLX polymer solution was as shown in Figure 32.

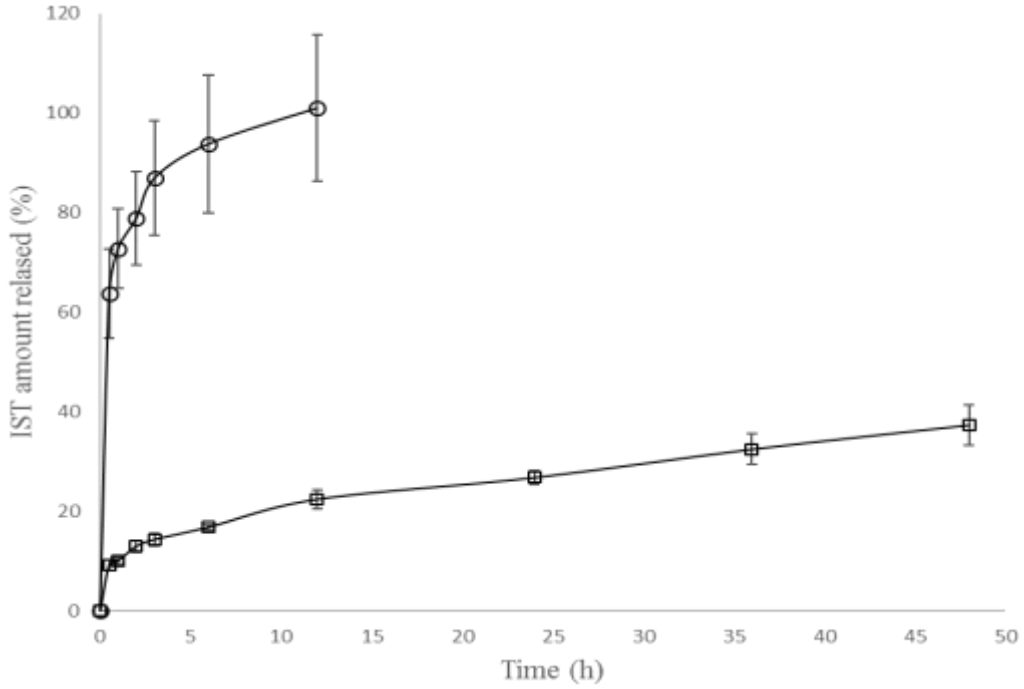

Figure 32: IST release: IST-DLX polymeric nanoparticles □ and IST-DLX polymer solution ○

Figure 32 shows that 100 % of IST was released from IST-DLX polymer solution within 12 h while IST release from IST-DLX polymeric nanoparticles was sustained over 48 h with about 37.31 % released.

The IST-DLX polymeric nanoparticles release curve shows a two-phase release profile; the first phase probably due to a burst release from drugs on the surface of the IST-DLX polymeric nanoparticles and the latter showing a quasi-linear release of IST. To better understand the release of IST from IST-DLX polymeric nanoparticles, the dissolution data was

subjected to kinetic modeling. The DDsolver software was employed in the modeling because it employs a nonlinear curve-fitting approach in estimating kinetic parameters by fitting non-transformed dissolution data. Other methods of kinetics modeling which employs manual calculation often involve transformation of non-linear data to a linear form before linear regression analysis; however, this transformation may distort experimental errors, thus necessitating the use of computer software which can model release kinetics without necessarily transforming non-linear data to linear form (COSTA & LOBO, 2001; ZUO *et al.*, 2014). Table 15 shows the non-linear kinetics model parameters of all tested models.

Table 15: Non-linear release kinetics parameters of IST-DLX polymeric nanoparticles

	Parameters		
Models	**k_0/k_1/kH/kKP**	**Adjusted R^2**	**n**
Zero order	0.569	0.9670	-
First order	0.008	0.9779	-
Higuchi	5.190	0.9928	-
Korsmeyer-Peppas	6.303	0.9926	0.450

Rate constants: k_0, zero order; k_1, first order (t^{-1}); kH, Higuchi; kKP, Korsmeyer-Peppas

The modeling result shows that the release of IST from IST-DLX polymeric nanoparticles did not follow zero nor first order models with R^2 values being 0.9670 and 0.9779 respectively. This perceived non-fitting to zero and first order models might be due to the non-linear approach used in evaluating the models (COSTA & LOBO, 2001) and the initial non-linear burst release of IST from the surface of IST-DLX polymeric nanoparticles. The release of IST from IST-DLX polymeric nanoparticles however adequately fits the Higuchi model with R^2

= 0.9928. The Higuchi model has been used extensively in describing drug release based on fick's law from diverse modified release dosage forms including transdermal systems (COSTA & LOBO, 2001). The Korsmeyer-Peppas release exponent n = 0.45 shows that the release of IST from IST-DLX polymeric nanoparticles is based on a Fickian diffusion mechanism through the DLX polymer matrix (COSTA & LOBO, 2003; DASH *et al.*, 2010).

Subjecting the latter phase of the release to a linear modeling (without the burst release) however fits zero order release model with k = 0.493 and adjusted R^2 = 0.9944. This suggests that, after the initial burst release, the release of IST from IST-DLX polymeric nanoparticles was probably dependent on other mechanisms not related to the concentration of IST, thereby sustaining the release of IST for over 48 h. Hydrophilic polymers such as DLX polymer are known to generally swell and form a gel-like layer on their surface which can retard fluid ingress into the polymer core, thereby controlling the rate of drug release (SARMAH *et al.*, 2011); this mechanism might have dictated the sustained release of IST from IST-DLX polymeric nanoparticles after the initial burst release.

5.8.3 **Skin resistivity parameters: influence of PBS/ethanol**

The stratum corneum integrity in dermatomed skins were determined by calculating the resistivity as described in previous studies (TANG *et al.*, 2001). Table 16 shows the resistivity parameter of dermatomed skins used in the skin penetration experiments as a function of time.

Table 16: Pig ear skin resistivity parameters

Time (h)	Skin resistivity ($K\Omega.cm^2$)
0.5	91 ± 6
1	88 ± 10
2	72 ± 6
3	70 ± 7
4	70 ± 7
5	71 ± 13
6	62 ± 5
7	69 ± 11
12	64 ± 5

The result shows that the presence of PBS/ethanol (7:3) in the receiver compartment of the model Franz diffusion cells did not negatively affect the skin integrity even up to 12 h as values were higher than 35 $K\Omega.cm^2$. Moreover, skin resistivity parameters determined at the end of each expanerimental time involving IST-DLX polymer solution or IST-DLX polymeric nanoparticles in the donor compartment and PBS/ethanol (7:3) in the receiver compartment did not go below 35 $K\Omega.cm^2$ throughout the experiment time of 12 h.

5.8.4 *In vitro* BODIPY-DLX polymeric nanoparticles skin penetration/distribution

Pig skin cryo-sections, 10 µm thick, exposed to 1 and 6 h lipophilic BODIPY-DLX polymer solution or BODIPY-DLX polymeric nanoparticles were visualized using the Leica TCS SP8 Confocal microscope (Leica, Germany). It should be noted that the size of these nanoparticles was not statistically different from the size of the IST-DLX nanoparticles (One Way ANOVA, $p > 0.05$). Figure 33 shows BODIPY distribution when skins were exposed to BODIPY-DLX polymer solution or BODIPY-DLX polymeric nanoparticles.

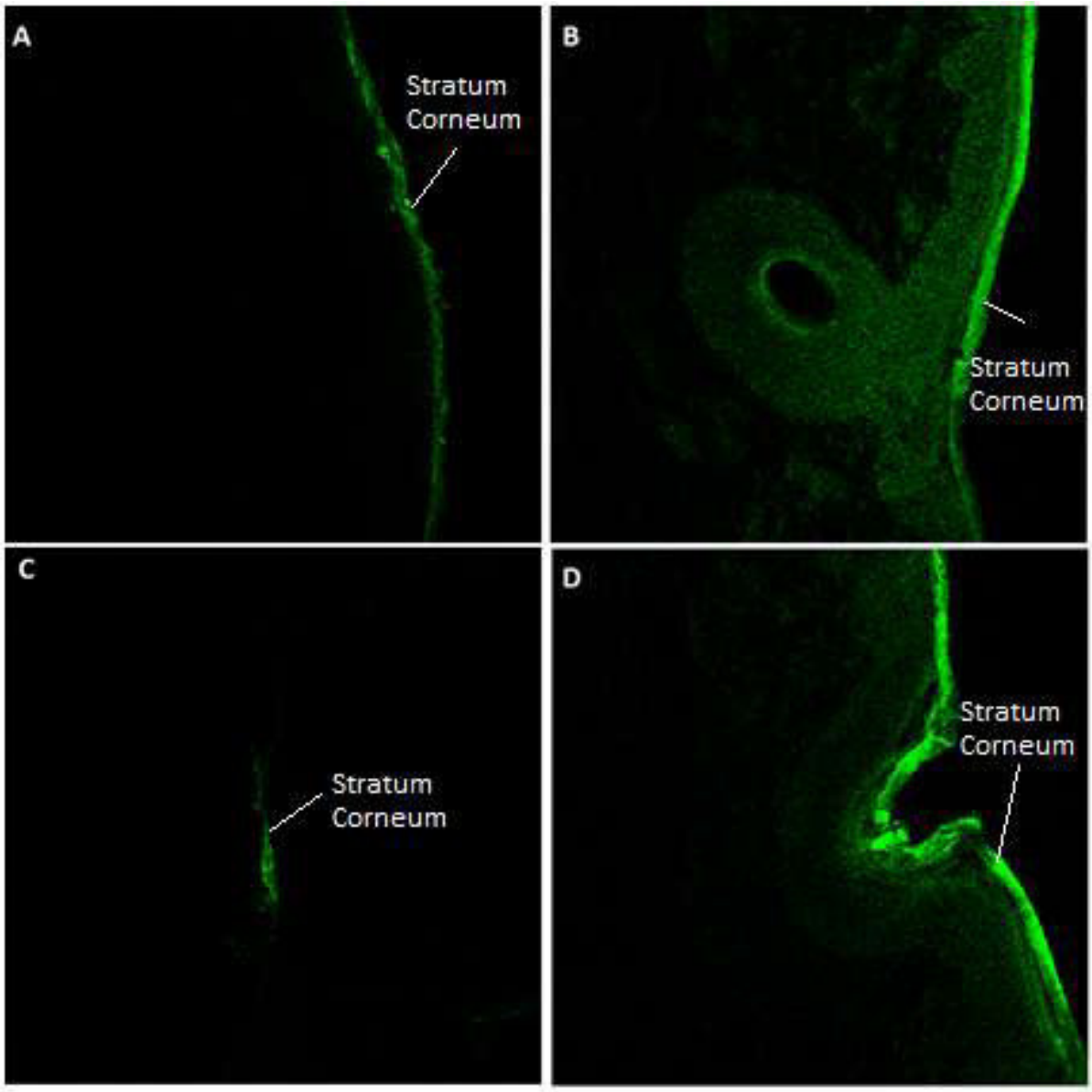

Figure 33: Confocal photomicrograph: BODIPY distribution in skin. BODIPY-DLX polymer solution (A) 1 h (B) 6 h; BODIPY-DLX polymeric nanoparticles (C) 1 h (D) 6 h

The result shows that minimal amount of BODIPY penetrated into the stratum corneum after 1 h when BODIPY-DLX polymeric nanoparticles were used as compared to the BODIPY-DLX polymer solution which showed prominent homogeneous fluorescence on the stratum corneum (Figure 33A). The same trend was observed after 6 h of application as free BODIPY in

DLX polymer solution penetrated into the deeper skin layers (225.8 µm) as compared to lesser penetration (134.7 µm) observed when BODIPY-DLX polymeric nanoparticles was used. The result suggests that BODIPY-DLX polymeric nanoparticles accumulated in the hair follicle and stratum corneum, evidenced by the higher intensity of BODIPY observed after 6 h of application as compared to BODIPY-DLX solution. This accumulation of polymeric nanoparticles in the hair follicles has been previously demonstrated in other studies (ALVAREZ-ROMÁN *et al.*, 2004; MITTAL *et al.*, 2013).

5.8.5 *In vitro* IST-DLX polymeric nanoparticles skin penetration

Several toxicities due to oral IST usage (ERTURAN *et al.*, 2012; FERGUSON *et al.*, 2005) have been reported prompting the need for local topical therapies that are beneficial. The pathogenesis of acne is multifactorial involving blockade of pilosebaceous follicles and hyperkeratinization, androgen stimulation of sebaceous gland leading to over secretion of sebum, colonization of the pilosebaceous unit by *Propiobacterium acnes* and inflammatory responses due to the activation of pro-inflammatory cytokines, suggesting that the disease is localized in the polisebaceous units of the skin (RIGOPOULOS *et al.*, 2010; TOYODA & MOROHASHI, 2001; ZOUBOULIS *et al.*, 2005). Moreover, the mechanism of IST in acne is not completely known, but IST has been shown to normalize follicular keratinization (WILLIAMS *et al.*, 2012), reduce *P. acnes (COATES et al., 1997; RAZA, SINGH, SINGLA, et al., 2013),* inhibit comedogenesis and sebaceous lipid synthesis(ZOUBOULIS, 2006), and elicit indirect and direct anti-inflammatory responses (COATES *et al.*, 2005; RAZA, SINGH, SINGLA*, et al.*, 2013; RIGOPOULOS *et al.*, 2010; ZOUBOULIS, 2006). Thus, any local therapy that would be beneficial and effective will be such that it can deliver the drug, IST, in optimum concentrations

to the disease site but still avoid systemic penetration, thereby preventing known side effects and toxicities associated with oral IST use.

Using an *in vitro* pig skin model and differential tape stripping technique, the amount of IST that accumulated in each layer of the pig skin and receiver medium was calculated. Table 17 show the distribution/accumulation of IST in the skin layers when dermatomed pig skin was treated with 1 mL IST-DLX polymer solution or IST-DLX polymeric nanoparticles at 400 µg/mL, while Table 18 shows IST differential skin penetration when IST-DLX polymeric nanoparticles at 800 µg/mL were put in contact with the skin.

Table 17: IST differential skin penetration of IST-DLX solution and IST-loaded DLX polymeric nanoparticles (dose: 400 µg/mL)

	Stratum Corneum (µg/cm^2)		Follicle (µg/cm^2)		Viable Epidermis (µg/cm^2)		Dermis (µg/cm^2)		Receiver médium (µg/cm^2)	
Time (h)	IST-DLX Sol	IST-DLX	IST-DLX Sol	IST-DLX	IST-DLX Sol	IST-DLX	IST-DLX Sol	IST-DLX	IST-DLX Sol	IST-DLX
1	14.6 ± 3.2	0.68 ± 0.04	1.7 ± 0.9	0.34 ± 0.05	0.3 ± 0.2	0.08 ± 0.02	0.42 ± 0.06	0.18 ± 0.02	1.2 ± 0.1	-
3	16.9 ± 6.6	0.73 ± 0.07	3.2 ± 1.2	0.32 ± 0.05	1.8 ± 1.1	0.09 ± 0.02	2.75 ± 1.05	0.19 ± 0.02	2.2 ± 0.3	-
6	29.6 ± 3.7	0.72 ± 0.05	2.4 ± 0.9	0.35 ± 0.09	2.3 ± 0.9	0.09 ± 0.01	3.17 ± 0.15	0.18 ± 0.02	3.0 ± 0.9	-
12	33.3 ± 12.3	0.79 ± 0.09	4.1 ± 1.3	0.36 ± 0.05	3.9 ± 0.6	0.13 ± 0.01	7.05 ± 0.92	0.18 ± 0.01	4.1 ± 3.2	-

- IST concentration was lower than the limit of quantification of HPLC method

Table 18: IST differential skin penetration of IST-loaded DLX polymeric nanoparticles (double dose: 800 µg/mL)

Time (h)	Stratum Corneum (µg/cm^2)	Follicle (µg/cm^2)	Viable Epidermis (µg/cm^2)	Dermis (µg/cm^2)	Receiver médium (µg/cm^2)
1	1.2 ± 0.1	0.14 ± 0.02	0.056 ± 0.009	0.12 ± 0.02	-
3	1.3 ± 0.1	0.31 ± 0.00	0.101 ± 0.009	0.19 ± 0.02	-
6	1.4 ± 0.1	2.08 ± 0.31	0.273 ± 0.081	0.28 ± 0.06	-
12	1.4 ± 0.1	2.01 ± 0.58	0.222 ± 0.017	0.27 ± 0.08	-
12**	1.4 ± 0.1	2.02 ± 0.39	0.217 ± 0.083	0.27 ± 0.08	-

** Formulation was removed from donor compartment after 6 hours; - IST concentration was lower than the limit of quantification of HPLC method

Results show significantly higher and uncontrolled accumulation of IST in different layers of the skin when IST-DLX polymer solution was employed as compared to lower and controlled accumulation of IST when IST-DLX polymeric nanoparticles was used up to 12 h of experimental time. This could be due to the influence of the DLX polymeric nanoparticles which controlled the diffusion of IST into the skin even though the polymer cannot penetrate into the skin. Also, substantial amount of IST was quantified in the receptor medium at each experimental time using IST-DLX polymer solution as compared to IST-DLX polymeric nanoparticles which has no IST in the reception medium up to 12 h.

The result also shows that a controlled amount of IST (about 200 ng/cm^2) penetrated into the dermis when IST-DLX polymeric nanoparticles were used as compared to about 7000 ng/cm^2 recovered from the dermis when IST-DLX polymer solution was employed. This is actually a positive as it will be possible to avoid the systemic presence of high IST concentration, thereby preventing known IST toxicities when IST-DLX polymeric nanoparticles are employed.

Doubling the dose of IST by doubling the amount of IST-DLX polymeric nanoparticles (Table 18) showed a controlled release and follicular accumulation of IST previously demonstration but with almost double the amount IST recovered from the skin layers. The amount of IST recovered from the skin layers was constant even after the removal of IST-DLX polymeric nanoparticles at 6 h. This could be due to the accumulation of more IST-DLX polymeric nanoparticles within follicles, which will be discussed in detail below.

To evaluate the propensity for follicular targeting by IST-DLX polymeric nanoparticles, IST-DLX polymer solution and IST-DLX polymeric nanoparticles were removed from the donor compartment in some specific experimental setups after 6 h of permeation, and the amount of

IST in the skin layers were thereafter quantified after 12 h (Figure 34 and last row of Table 18). A significant reduction (Figure 34A) in IST in the stratum corneum, viable epidermis and follicle were observed except in the dermis (which might have benefited from the continuous flux of IST already accumulated in the stratum corneum) when IST-DLX polymer solution was employed. This suggests that, upon removal of IST-DLX polymer solution from the donor compartment, there was a concomitant reduction in IST concentration gradient, thereby reducing the penetration of IST into the skin.

However, a constant amount of IST (Figure 34B) was recovered from the layers of the skin after 12 h when IST-DLX polymeric nanoparticles were removed from the donor compartment. This could be due to the deposition or accumulation of IST-DLX polymeric nanoparticles in the skin follicle, from where it continued to release its encapsulated IST content. The accumulation of polymeric nanoparticles in hair follicle has been demonstrated in other studies (ALVAREZ-ROMÁN *et al.*, 2004; MITTAL *et al.*, 2013). This results further affirms the confocal photomicrographs (Figure 33) reported initially; thus, IST-DLX polymeric nanoparticles can accumulate within the follicle, continuously release IST for up to 12 h and probably allow the application of the formulation once within 12 h.

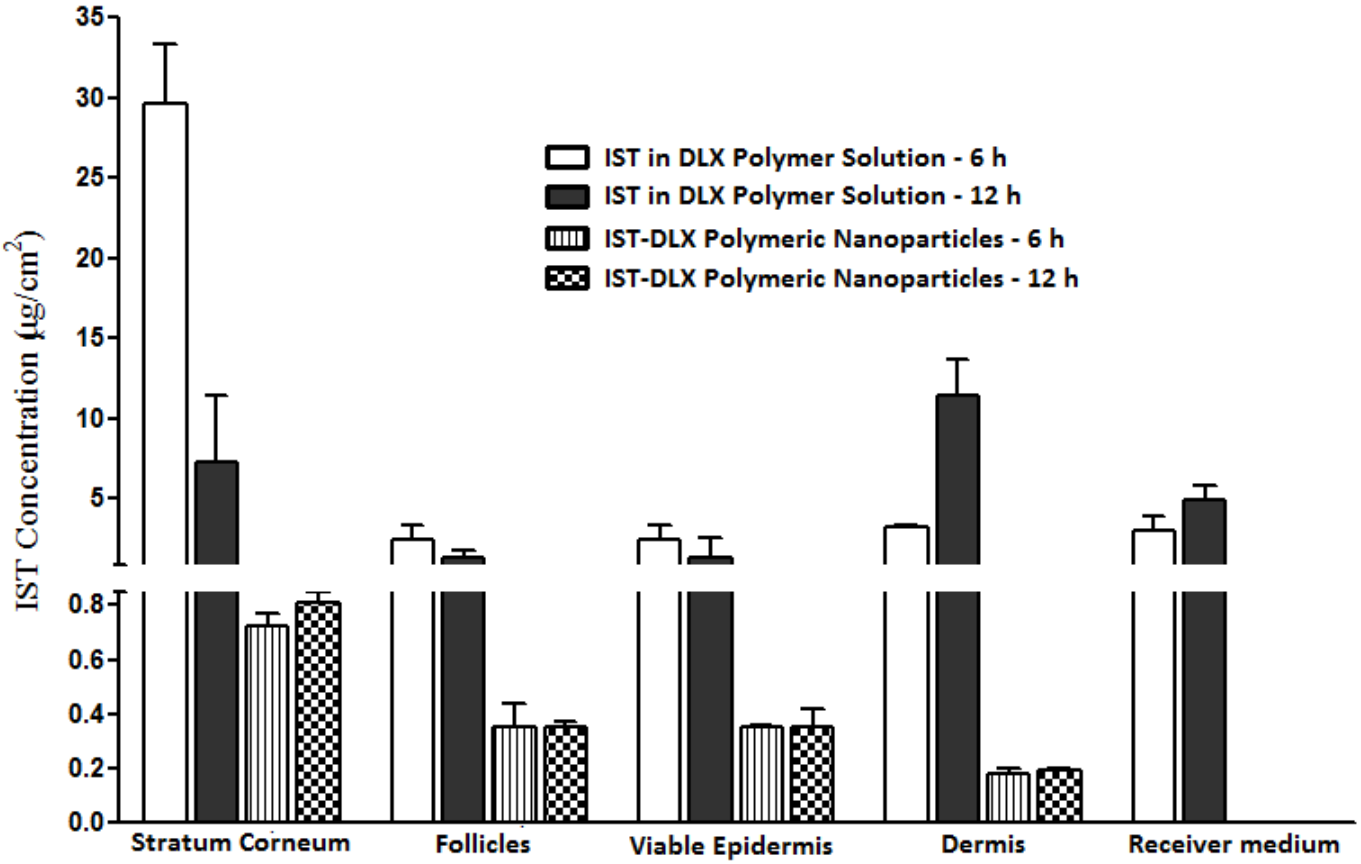

Figure 34: IST quantified in different pig skin layer at 6 h and 12 h after removal of formulation.

Figure 35 shows the % IST recovered as a function of total IST in skin layers. The result shows that IST-DLX polymeric nanoparticles significantly targeted the hair follicle (26%) as compared to IST-DLX polymer solution (6.5%). Thus, it may be possible to apply IST-DLX polymeric nanoparticles and target the pilosebaceous follicular unit where acne is located. In addition, the sustained release of IST from DLX polymeric nanoparticles may allow single application of IST-DLX polymeric nanoparticles, which elicit its effects for longer period of time.

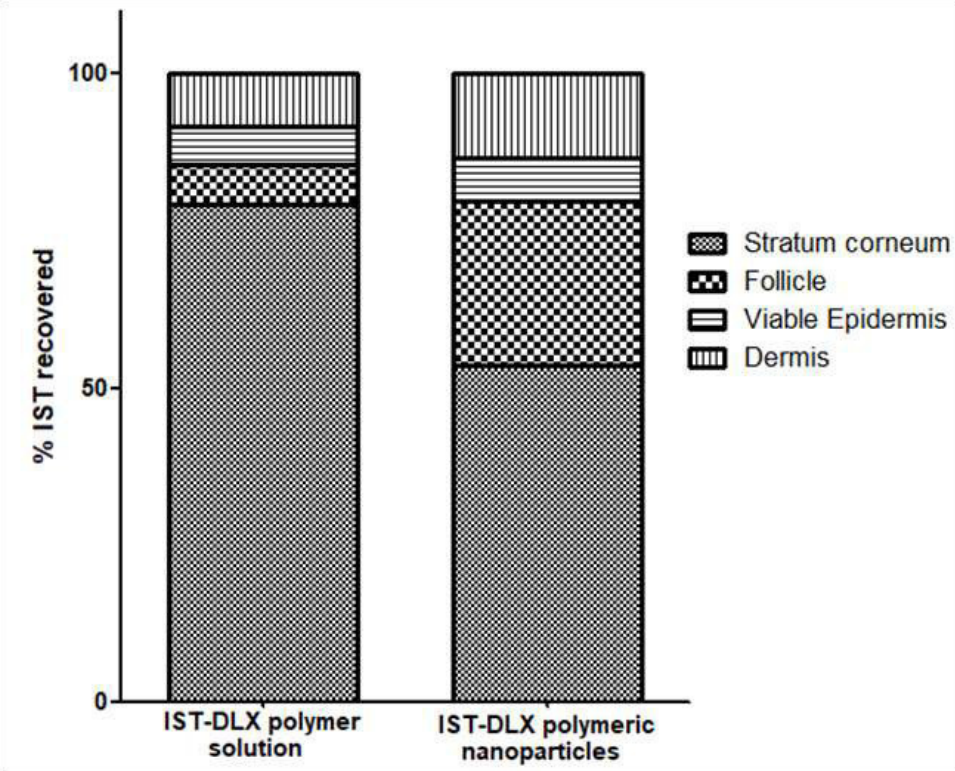

Figure 35: Percent IST distribution in pig ear skin as a function of total permeated IST

5.8.6 *In vitro* phototoxicity study

The phototoxicity of IST and other retinoic acid derivatives have been well documented (FU *et al.*, 2003; SPIEWAK *et al.*, 2012) while topical irritations have also been observed when commercial IST or retinoic acid derivative gels are used (IOANNIDES *et al.*, 2002). It is therefore important that an effective acne topical therapy should prevent known photo-toxicity and irritation associated with IST. The OECD test guideline 432, *3T3 neutral red phototoxicity assay* was employed in evaluating the influence of DLX polymeric nanoparticles in the reduction/prevention of IST photo-irritation (CERIDONO *et al.*, 2012; OECD, 2004).

The rationale of the study is based on the comparison of the cytotoxicity of a substance in the presence and absence of a non-cytotoxic dose of UVA light, with cytotoxicity being measured in terms of the capacity of the cell to take up neutral red (OECD, 2004).

Figure 36 shows fibroblast cell viability when treated with free IST and IST-DLX polymeric nanoparticles. It can be observed that free IST in culture medium has an +UVA EC_{50} of 88.71 µg/mL, PIF of 1.128 and a MPE of 0.124 which affirms the phototoxicity of free IST on 3T3 Balbc Fibroblast cells (OECD, 2004). However, IST-DLX polymeric nanoparticles did not show any trend of cyto- nor photo-toxicity with EC_{50} not achieved in the presence nor absence of UVA, PIF = 1 and MPE = 0.01. This result thus confirms that DLX polymeric nanoparticles could probably prevent direct IST contact with the fibroblast cells and thus, mitigated the observed phototoxicity/irritation with free IST within the concentration and experimental time tested.

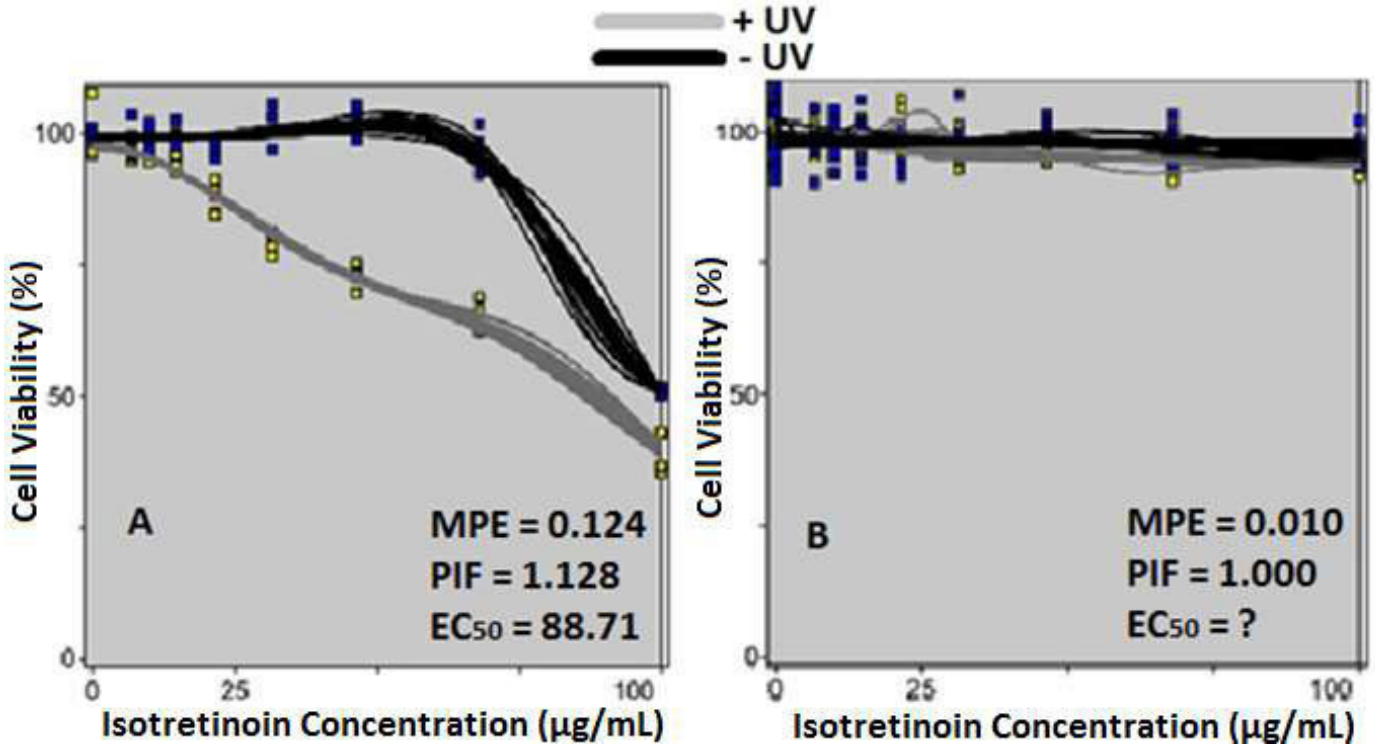

Figure 36: Fibroblast cell Viability when treated with (A) free IST (B) IST-DLX polymeric nanoparticles; MPE - Mean Photo Effect, PIF - Photo Irritancy Factor; ? – EC_{50} not detectable

5.8.7 *In vitro* inflammatory response

Inflammation is a prominent process and one of the pathogenic factors in acnegenesis. Retinoids, including IST have been shown to suppress inflammation in different models. Studies have demonstrated the ability of IST in suppressing pro and anti-inflammatory cytokines including IL-1, IL-6 and TNF-α (AHMED *et al.*, 2000; BERGLER-CZOP & BRZEZIŃSKA-WCISŁO, 2014; NOZAKI *et al.*, 2006; WOLF, 2002). Our study aimed to assess how IST-DLX polymeric nanoparticles could improve inflammatory responses in comparison to free IST in solution. Thus, ***AMJ–2 macrophage cells*** were stimulated by LPS to produce inflammatory cytokines and the effect of free IST or IST-DLX polymeric nanoparticles on IL-6, IL-10 and TNF-α production was assessed using ELISA technique. Figure 37 shows the inflammatory response of treated cells.

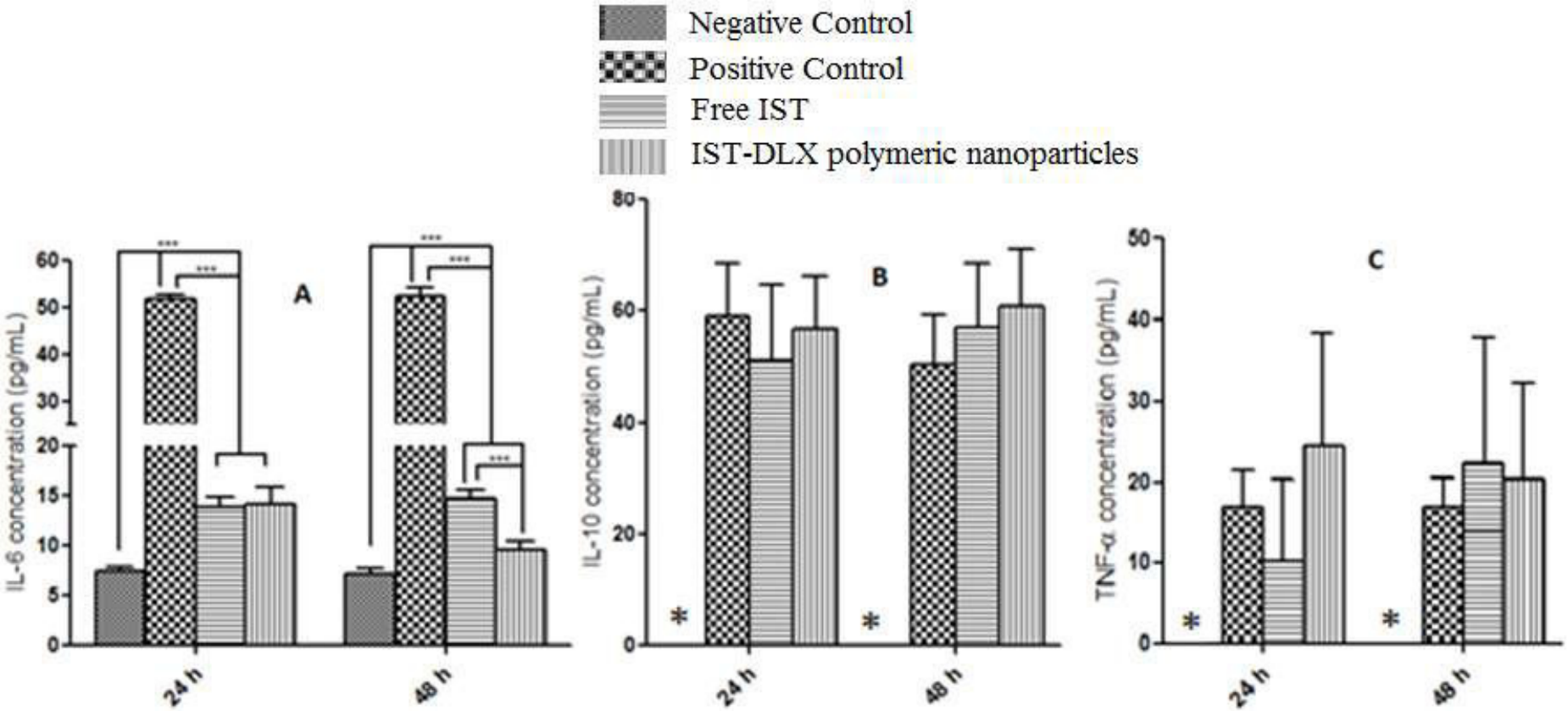

Figure 37: Inflammatory response of treated cells (A) IL-6, (B) IL-10, (C) TNF-α. * LPS non-treated control cells did not produce IL-10 and TNF in detectable amounts.

Cells treated with LPS stimulated the production of IL-6, IL-10 and TNF-α when compared to untreated cells ($p < 0.0001$) suggesting that LPS actually stimulated their production in the macrophages (Figure 37). Likewise, there was a significantly ($p < 0.0001$) higher IL-6 concentration in the positive control at 24 and 48 h as compared to the cells treated with free IST and IST-DLX polymeric nanoparticles. This could be due to the suppression effect of IST, a retinoid, on the production of IL-6 which has been demonstrated in other studies (NOZAKI *et al.*, 2006; WOLF, 2002). Free IST or IST-DLX polymeric nanoparticles suppressed the production of IL-6 to different extents. At 24 h, there was no significant difference in IL-6 concentration quantified in the free IST or IST-DLX polymeric nanoparticles treated cells, however, there was a significantly ($p < 0.0001$) lower IL-6 concentration after 48 h in cells treated with IST-DLX polymeric nanoparticles. Probably, within 24 h, the burst release of IST from IST-DLX polymeric nanoparticles elicited same degree of effect as free IST, thus suppressing IL-6 production; however, due to IST sustained release from IST-DLX polymeric nanoparticles, its effect might have been prolonged, leading to lower IL-6 concentration after 48 h. We have previously demonstrated the sustained release of IST and follicular targeting of IST-DLX polymeric nanoparticles (Figure 32), thus, it could be possible that IST in IST-DLX polymeric nanoparticles can elicit its action and also mediate in acne related inflammatory processes for longer hours.

For IL-10, however, at 24 and 48 h, there was no significant difference in the concentration of IL-10 between the positive control and cells treated with free IST or IST-DLX polymeric nanoparticles (Figure 37B). Other study have also suggested no significant difference in IL-10 concentrations between untreated and all-trans-retinoic acid treated cells, probably suggesting retinoids may not interfer in IL-10 suppression (NOZAKI *et al.*, 2006). TNF-α

concentration showed a similar trend. Although after 48 h, TNF-α concentration in IST-DLX polymeric nanoparticles treated cells was slightly lower than those of free IST treated cells, the reduction was not significantly different. There was also no significantly different TNF-α concentration between positive control and treated cells at 24 and 48 h. Although, some studies have demonstrated significant suppression of TNF-α by retinoids (BERGLER-CZOP & BRZEZIŃSKA-WCISŁO, 2014; KELHÄLÄ), our experiments did not show same result. However, these studies, which were performed in human acne patients, did not involve stimulation by LPS and results were based on comparison of baseline TNF-α levels between healthy individuals and oral IST treated acne patients over a period of time.

5.8.8 *In vitro* antibacterial activity on *P. acnes*

The survival/growth of *P. acnes* in treated and untreated wells were evaluated based on the irreversible reduction of blue Resazurin dye to pink in the presence of microbes. Our result shows complete change of color from blue to pink color in all wells treated with free IST and IST-DLX polymeric nanoparticles at all concentrations and negative control wells after 24 and 48 h of anaerobic incubation. No change in color was observed in the wells that were not inoculated with *P. acnes* suggesting no contamination in the BHI medium nor in the experimental process.

Significant reduction in *P. acnes* population is generally observed during oral IST therapies, prompting suggestions that IST could have some antimicrobial properties against *P. acnes*. IST has been shown to have an indirect antimicrobial action by exerting a marked reduction in sebum excretion rate (SER) and pilosebaceous duct size (DEL ROSSO, 2012; LAYTON, 2009). Although the possibility of a direct antimicrobial effect of IST on *P. acnes* had

been demonstrated (RAZA, SINGH, SINGLA*, et al.*, 2013), our results suggests that IST may not have any direct antimicrobial activity against *P. acnes* within the concentration range of IST tested, further supporting the assertions that IST anti-bacterial action may be an indirect one earlier suggested by other researchers (LAYTON, 2009)

5.9 *In vivo* topical IST administration studies

5.9.1 IST quantification in Wistar rat skin

The amount of IST recovered from the treated Wistar rat skin is as shown in Figure 38. There was significantly (unpaired *t-test*; $p = 0.0005$) higher IST amount recovered from the stratum corneum of Wistar rats treated with free IST in HEC gel (1.797 ± 0.4387 µg/cm^2) as compared to 0.57 ± 0.39 µg/cm^2 IST recovered from Wistar rats treated with IST-DLX polymeric nanoparticles. Likewise, significantly (unpaired *t-test*; $p = 0.0106$) higher IST amounts was recovered from the deeper skin layers when free IST in HEC gel (0.42 ± 0.26 µg/cm^2) was applied as compared to 0.066 ± 0.028 µg/cm^2 IST recovered when IST-DLX polymeric nanoparticles were applied.

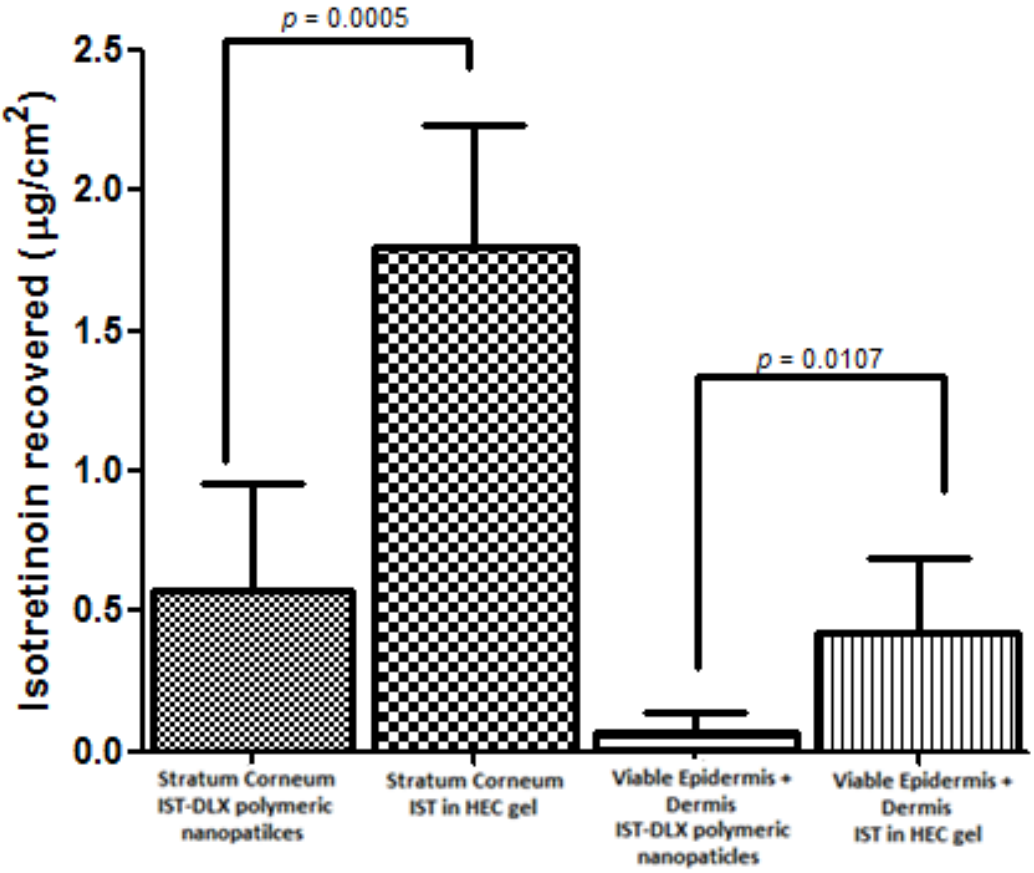

Figure 38: IST recovered from Wistar rat skin

The lower amount of IST observed with IST-DLX polymeric nanoparticles could be due to the controlled release of IST previously observed in the *in vitro* release and skin penetration studies. No amount of IST was however detected in the blood of the rats when both formulations were used.

5.9.2 **Cutaneous irritation**

Skin irritation is a prominent side effect of topically applied retinoids, including IST (BRELSFORD & BEUTE, 2008; IOANNIDES *et al.*, 2002). An effective topical IST formulation should be one that effectively deliver its medicament to the desired skin sites and

suppress irritation so as to improve compliance by patients. Wistar rats were treated with HEC gels with or without IST, blank DLX polymeric nanoparticles or IST-DLX polymeric nanoparticles and the skin at the application sites were evaluated macroscopically and microscopically after histology processing. Additionally, some treated animals were exposed to UVA irradiation for 3 mins. Figure 39 shows the macroscopic photo of Wistar rat skins treated with different HEC gel formulations with or without IST, blank DLX polymeric nanoparticles or IST-DLX polymeric nanoparticles, with or without UVA irradiation.

Figure 39: Macroscopic photomicrographs of Wister rat skin treated with (A) HEC gel (B) Blank DLX polymeric nanoparticles in HEC gel (C) IST-DLX polymeric nanoparticles in HEC gel (D) IST in HEC gel (E) UVA + HEC gel (F) UVA+ Blank DLX polymeric nanoparticles in HEC gel (G) UVA + IST-DLX polymeric nanoparticles in HEC gel (H) UVA + IST in HEC gel. Red arrows show inflammatory erythema

After the treatment periods, there was no conspicuous sign of irritation in the skin of animals treated with HEC gel (Figure 39A), blank DLX polymeric nanoparticles in HEC gel (Figure 39B) and IST-DLX polymeric nanoparticles in HEC gel (Figure 39C). However, there was a slight sign of erythema (red arrows) in the skin of Wistar rats treated with free IST in HEC gel (Figure 39D). The result suggests that blank DLX polymeric nanoparticles did not produce inflammatory erythema, but did protect the encapsulated IST from direct contact with the Wistar rat skin, thereby preventing IST skin inflammatory eythema observed with Wistar rats treated with free IST in HEC gel which might have been caused by the direct exposure of the skin to IST.

Upon exposure of treated animals to UVA irradiation, there was no noticeable sign of inflammatory erythema in the skin of animals treated with HEC gel (Figure 39E), DLX polymeric nanoparticles in HEC gel (Figure 39F) or IST-DLX polymeric nanoparticles in HEC gel (Figure 39G). However, a very conspicuous sign of inflammatory erythema was observed in animals treated with IST in HEC gel after UVA irradiation (Figure 39H). IST is a known photo-irritant and as such in the presence of UVA, it may have irritated the rat skin. On the contrary, it could be said that DLX polymeric nanoparticles protected IST from having direct contact with the skin and thus protected the rat skin from UVA associated inflammatory erythema.

Figure 40 shows the photomicrograph of Wistar rat skins treated with different HEC gel formulations with or without IST, blank DLX polymeric nanoparticles or IST-DLX polymeric nanoparticles, with or without UVA irradiation after histological staining with hematoxylin and eosin. Epidermal thickness of the skin histological cuts was measured using Fiji software (ImageJ, NIH, USA) and results are shown in Table 19 and Figure 41.

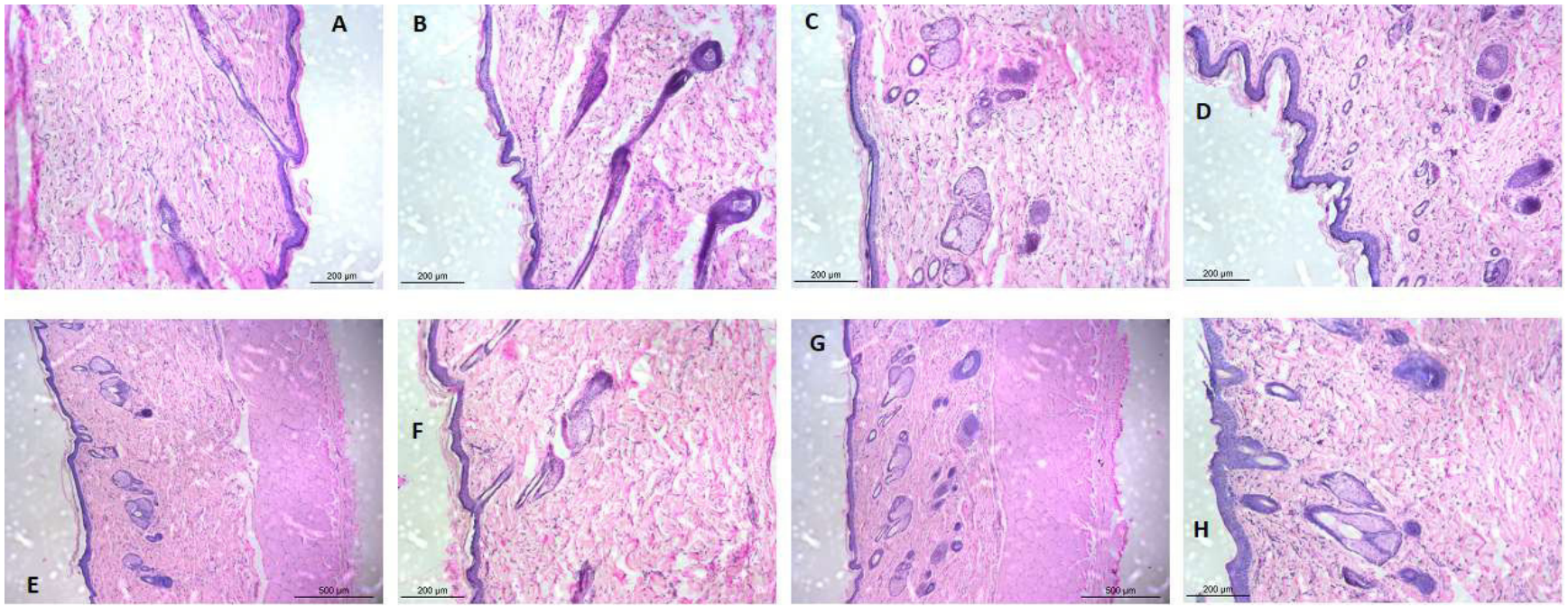

Figure 40: Histological photomicrographs of Wister rat skin treated with (A) HEC gel (B) Blank DLX polymeric nanoparticles in HEC gel (C) IST-DLX polymeric nanoparticles in HEC gel (D) IST in HEC gel (E) UVA + HEC gel (F) UVA+ Blank DLX polymeric nanoparticles in HEC gel (G) UVA + IST-DLX polymeric nanoparticles in HEC gel (H) UVA + IST in HEC gel

Table 19: Epidermal thickness of rat skin treated with different HEC gel formulations

Formulation	Epidermal thickness (µm)
HEC gel	24 ± 5
DLX-HEC gel	23± 5
IST-DLX HEC gel	46 ± 9
IST-HEC gel	26 ± 7
UV HEC gel	25 ± 6
UV DLX-HEC gel	25 ± 7
UV IST-DLX HEC gel	66 ± 11
UV IST-HEC gel	31 ± 7

DLX-HEC gel - Blank DLX polymeric nanoparticles in HEC gel; IST-DLX HEC gel - IST-DLX polymeric nanoparticles in HEC gel; IST-HEC gel - Free IST in HEC gel; UV - with application of UVA irradiation

The result showed no significant difference in the epidermal thickness of Wistar rats treated with blank HEC gel, blank DLX polymeric nanoparticles in HEC gel and IST-DLX polymeric nanoparticles in HEC gel even after irradiation with UVA. However, there was significant increase in the epidermal thickness of animals treated with free IST in HEC gel with and without UVA irradiation. Retinoids, including IST induces epidermal thickness and as thus been used in the management of photo-aging (VARANI *et al.*, 2003). This significant increase in the epidermal thickness could be due to the uncontrolled release of free IST from HEC gel as compared to the lower amount and controlled release of IST from IST-DLX polymeric nanoparticles in HEC gel. Studies demonstrating epidermal thickening due to retinoids application involves the treatment of study animal skins with formulations containing these retinoids without the application of UVA irradiation (CASTRO *et al.*, 2011). In our study, free IST in HEC gel and other formulations were applied for 15 days without UVA irradiation while the experiments involving UVA irradiation using same formulations were applied for a shorter period of 5 days.

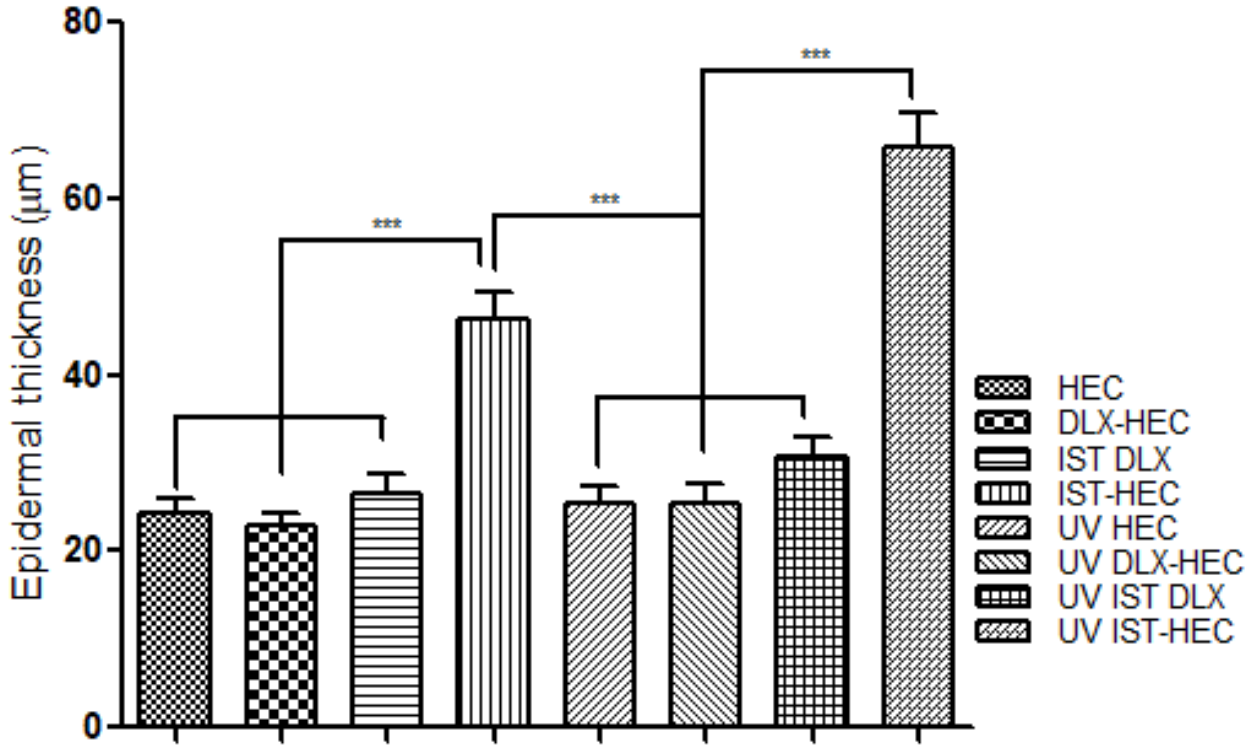

Figure 41: Epidermal thickness of rat skin treated with difrerent HEC gel formulations

The significantly higher epidermal thickness of Wistar rats treated with IST in HEC gel with UVA irradiation as compared to those not irradiated with UVA or IST-DLX polymeric nanoparticles treated Wistar rats may suggest that, order than the known epidermal thickening effect associated with retinoids such as IST, exposure of Wistar rats treated with free IST in HEC gel to UVA might have actually increased the propensity for inflammatroy erythema observed. In fact, Wistar rats treated with IST-DLX polymeric nanoparticles in HEC gel and exposed to UVA irradiation had a higher, but statistically insignificant epidermal thickness when compared to those not exposed to UVA irradiation; while Wistar rats treated with blank HEC or DLX polymeric nanoparticles in HEC gel with or without UVA irradiation had similar epidermal

thickness, suggesting that the epidermal thickening observed may be independent of only UVA irradiation, but may be dependent on UVA irradiation interactions with IST.

Thus, it could be hypthesized that DLX polymeric nanoparticles may prevent IST-related skin inflammatory irritations evidenced by no physical sign of erythema and reduced epidermal thickening as compared to free IST in HEC gel which produced visible signs of inflammatory erythema and significant epidermal thickening as epidermal thickening (hyperplasia) may also be due to inflammatory factors which has been previously demonstrated (BONNET *et al.*, 2011; GROVES *et al.*, 1996)

5.10 **DLX polymer versatility studies**

DLX polymer is an underutilized polymer in drug delivery but with documented properties that could be beneficial in drug delivery. These properties include mucoadhesion (DEVKAR *et al.*, 2014), sustained release (ADETOGUN & ALEBIOWU, 2007; ADETOGUN & ALEBIOWU, 2009), and microencapsulation (BETANCUR-ANCONA *et al.*, 2011). Thus, its usability in diverse delivery routes is of interest. In this work, the potential of DLX polymeric nanoparticles as a topical or intravitreal drug delivery system for ocular administration was evaluated.

5.10.1 **Characteristics and stability of DLX polymeric nanoparticles in SLF components**

The osmolarity of tear fluid is very important as it can dictate the integrity of the cornea. The normal osmolarity of normal tears varies between 290 to 310 mOsm/kg (MARQUES *et al.*, 2011). The osmolarity of DLX polymeric nanoparticles dispersion determined was 220 mOsm/L, showing that DLX polymeric nanoparticles is not hyperosmolar and can be employed as an ocular delivery polymer.

The stability of colloidal biomaterials in biological fluids which generally contains ample amount of enzymes and proteins is very crucial (LAZZARI *et al.*, 2012; OGUNJIMI *et al.*, 2017) while the biomaterial particles size could play an important role in interaction with mucosal surfaces including ocular mucosa (ALBANESE *et al.*, 2012). Thus, in order to evaluate the stability of DLX polymeric nanoparticles in the presence of simulated ocular fluid components, the nanoparticles were incubated with lysozyme, SLF and mucin; lysozyme and mucin being two major components of the precorneal fluid.

The particle size and zeta potential of DLX polymeric nanoparticles upon incubation with or without lysozyme, evaluated as a function of time is shown in Figure 42.

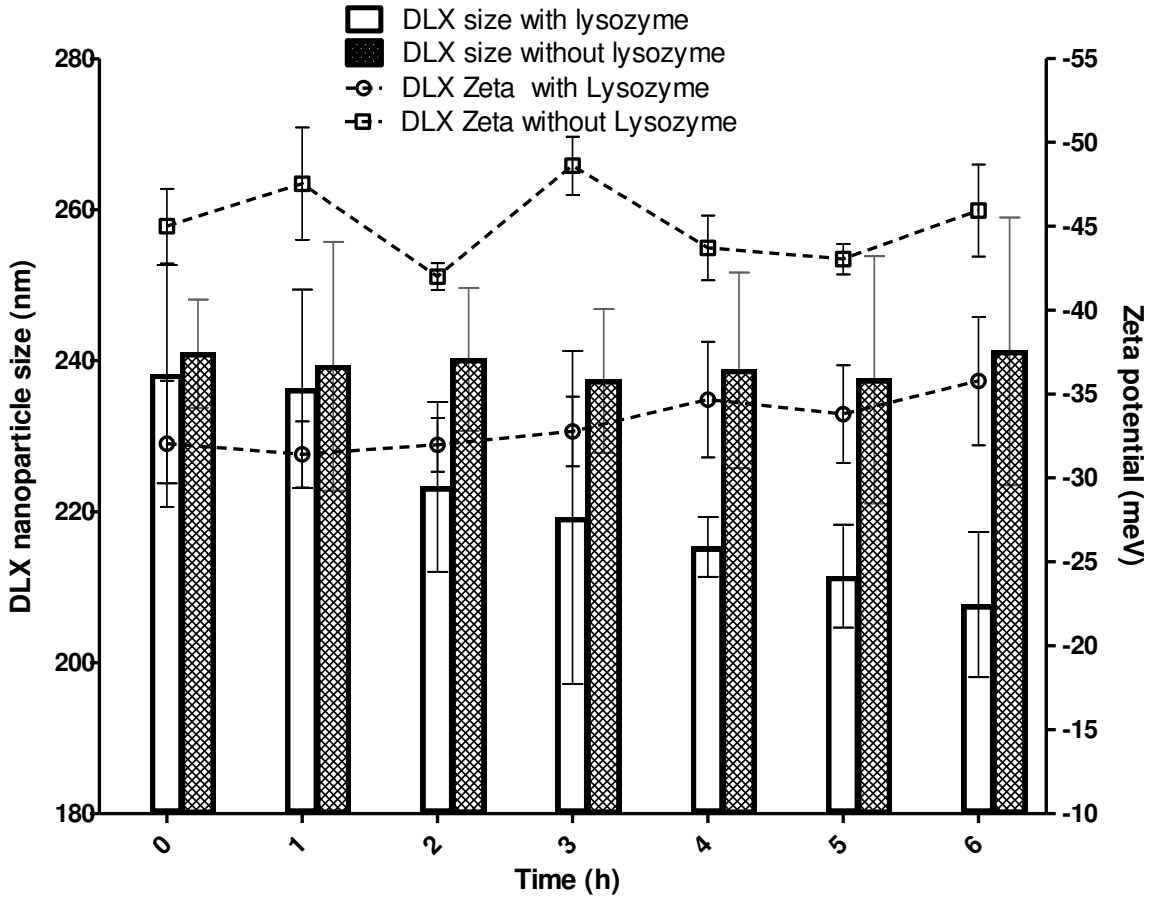

Figure 42: Influence of lysozyme on DLX polymeric nanoparticles size and zeta potential as a function of time.

Figure 42 shows that DLX polymeric nanoparticles size reduced upon incubation with lysozyme as compared to the control without lysozyme. The size reduction could be attributed to the partial hydrolysis of the glycosidic bonds in DLX polysaccharide structure which could result in minute break-off on the nanoparticles surface (DE CAMPOS *et al.*, 2005; HU *et al.*, 2010). This result further suggests that DLX polymer is biodegradable, an important characteristic for biomedical polymers; however, there was minimal nanoparticle size reduction (13%) over the period of 6 h, suggesting that DLX polymeric nanoparticles will be capable of holding to its payload despite its biodegradability. In addition, the size reduction of DLX polymeric nanoparticles in the presence of lysozyme can also be due to some electrostatic interactions between the negatively charged nanoparticles and cationic lysozyme enzyme. In fact, a significant reduction in the zeta potential of the DLX polymeric nanoparticles (Figure 42) was observed; however, this reduction in zeta potential might not adversely affect the nanoparticle stability as the values were larger than -30 mV. This stability is an advance in comparison to poly-ε-caprolactone nanocapsules which aggregate upon contact with lysozyme (CALVO *et al.*, 1997; DE CAMPOS *et al.*, 2005).

Table 20 shows the influence of SLF on DLX polymeric nanoparticles size and zeta potential as a function of time. The SLF has no significant ($p > 0.05$) effect on the nanoparticle size and PdI, however there was a significant reduction ($p < 0.05$) in the zeta potential of the DLX polymeric nanoparticles. This is understandable as the presence of mono and multivalent ions in the SLF could lead to the compression of electrical double layer and consequently a reduction in the negative charge on the nanoparticles surface (CARNEIRO-DA-CUNHA *et al.*, 2011; MCCONAUGHY *et al.*, 2008). Despite the reduction in zeta potential, no alterations in the

size and in the PdI of nanoparticles were observed. This is an important advantage compared to chitosan nanoparticles, that are instable in phosphate buffer pH 7.4 (DE CAMPOS *et al.*, 2005).

Table 20: Properties of DLX polymeric nanoparticles incubated with SLF

	DLX polymeric nanoparticles size (nm)		Zeta potential (mV)	
Time (h)	Control	In SLF	Control	In SLF
0	209.6 ± 13.5	211.4 ± 15.5	-45.0 ± 2.2	-5.4 ± 0.5
1	206.6 ± 9.2	204.5 ± 14.6	-47.5 ± 3.4	-5.9 ± 0.3
2	203.0 ± 12.3	205.0 ± 8.9	-42.0 ± 0.8	-6.3 ± 1.3
3	207.5 ± 8.9	206.2 ± 8.5	-48.6 ± 1.7	-6.0 ± 0.7
4	205.1 ± 10.1	205.4 ± 13.3	-43.7 ± 1.9	-6.2 ± 0.4
5	204.8 ± 11.1	206.9 ± 10.0	-43.0 ± 0.9	-6.2 ± 0.9
6	203.4 ± 8.0	205.4 ± 7.7	-45.9 ± 2.7	-6.1 ± 0.7

The addition of mucin to DLX polymeric nanoparticles dispersion did not significantly change ($p > 0.05$) the zeta potential of the DLX nanoparticle dispersion (DLX polymeric nanoparticles -42.3 ± 2.8 mV; DLX polymeric nanoparticles dispersion with mucin -38.1 ± 0.3 mV); however, there was a significant difference ($p < 0.05$) between the zeta potential of the mucin dispersion (-15.5 ± 0.5 mV) as compared to that containing DLX polymeric nanoparticles. Interactions between nanoparticles and mucin in terms of surface charge could be an indirect way of predicting mucoadhesion. Although, there was no significant interaction between the DLX polymeric nanoparticles and mucin in terms of charges, biopolymers mucoadhesion to surfaces is a multi-mechanism process which does not only involve interactions between surface charges; adsorption, wetting and diffusion have also been proposed as possible mechanism for mucoadhesion (KHUTORYANSKIY, 2011; SMART, 2005). While it might be interesting to conduct an *in vivo* ocular study to evaluate mucoadhesion prowess of DLX polymeric

nanoparticles in addition to understanding its probable mechanism of mucoadhesion (SERRA *et al.*, 2009; SMART, 2005), study have already reported its use as a mucoadhesion enhancer (DEVKAR *et al.*, 2014).

5.10.2 *In vitro* cytotoxicity of DLX polymeric nanoparticles

Cell viability is a well-recognized assay to evaluate *in vitro* cytotoxicity of nano-materials (BRUNNER *et al.*, 2006; VOIGT *et al.*, 2014) Cell viability in this study was assessed using NRU and MTT uptake assays. The MTT assay is a rapid colorimetric and quantitative method based on the conversion of a yellow tetrazolium salt to insoluble purple formazan crystals in the mitochondrial of viable cells while neutral red is a dye taken up by viable cells and internalized within the lysosomes (BOUALLAGUI *et al.*, 2011). The combination of these two assay methods have a benefit of adding reliability to cytotoxicity results of tested materials.

A nanoparticulate system with prospect for ocular use must be capable of delivering optimum quantity of active agents without compromising the viability of the host cells. The result of MTT and NRU assays (Figure 43) suggest that DLX polymeric nanoparticles are non-toxic on both ARPE-19 and HCE cells at all tested concentrations (100 to 1483.3 µg/mL) within 24 h. ARPE-19 however showed reduction in cell viability after 48 and 72 h, but the reduction was only significantly different ($p < 0.05$) at DLX polymeric nanoparticles concentration of 1483.3 µg/mL. Both MTT and NRU assay demonstrated same result giving reliability to the study. The HCE showed reduced cell viability after 48 and 72 h but the reduction was significantly different only at 1483.3 µg/mL ($p < 0.05$) after 48 h; after 72 h, there was significant difference in cell viability at 1009 ($p < 0.05$) and 1483.3 µg/mL ($p < 0.001$). The MTT and NRU assay on HCE cells suggest same results.

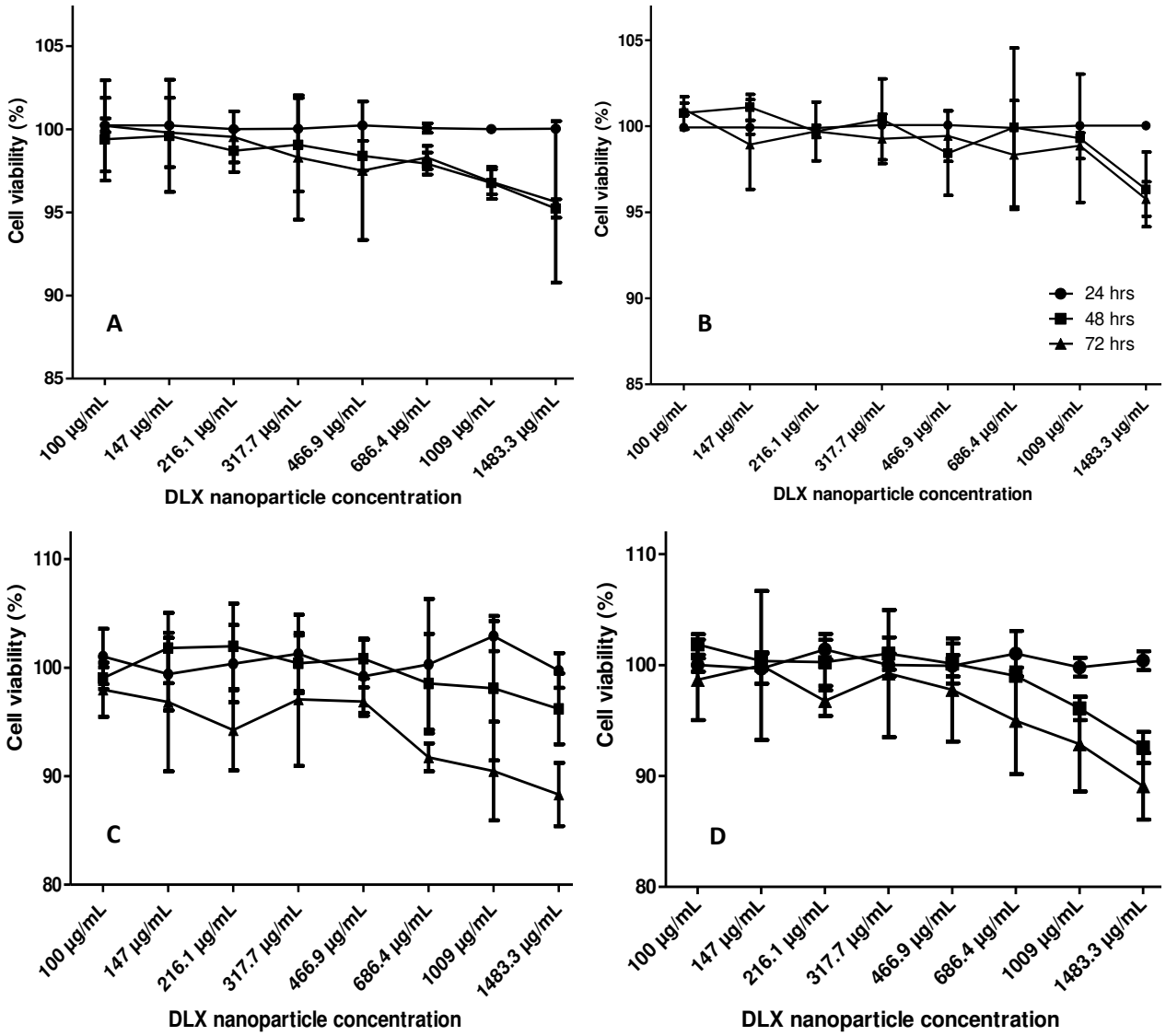

Figure 43: In vitro cytotoxicity of DLX polymeric nanoparticles on ARPE-19 and HCE cells as measured by MTT and NRU assay. (A) ARPE-19 cells MTT assay (B) ARPE-19 cells NRU assay (C) HCE cells MTT assay (D) HCE cells NRU assay

Based on this result, it could be said that DLX polymeric nanoparticles use on ARPE-19 and HCE cells did not show obvious toxic effects within the concentration limits of this study.

5.10.3 **Cellular uptake: Flow Cytometry**

Cellular uptake is an important prerequisite for nanoparticles efficacy and effectiveness, and physicochemical characteristics such as size, surface charge and hydrophobicity dictates the extent of uptake of nanoparticles by cells (GUSTAFSON *et al.*, 2015; MURUGAN *et al.*, 2015) For uptake to occur, it is considered that there is an adhesion process followed by internalization. Cellular uptake of nanoparticles apart from dictating efficacy, could also give insight into the toxicity propensity of nanoparticles (ZHAO *et al.*, 2011). Two methods were employed to assess the uptake of BODIPY-DLX polymeric nanoparticles by ARPE-19 and HCE cell lines; flow cytometry and confocal microscopy. Figure 44 shows flow cytometry results for hydrophilic BODIPY-DLX polymeric nanoparticles in contact with ARPE-19 and HCE cells.

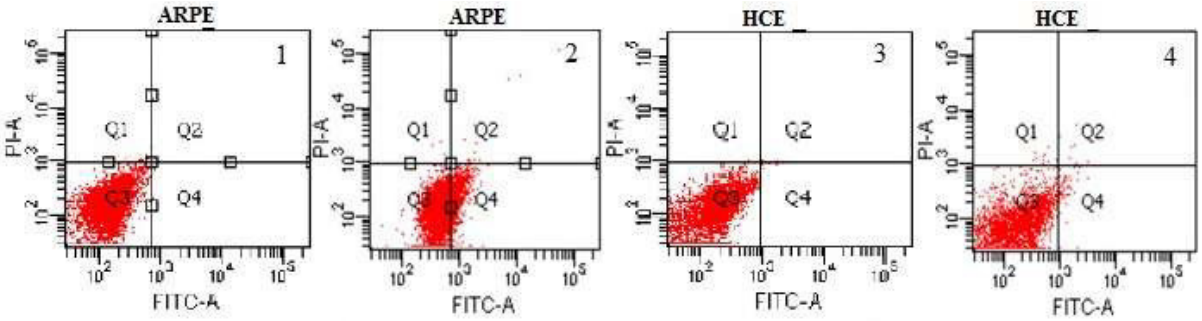

Figure 44: Flow Cytometry analysis: Dot plots showing uptake by ARPE-19 and HCE cells incubated for 24 h with BODIPY-DLX polymeric nanoparticles (2 and 4) and blank DLX polymeric nanoparticles (1 and 3)

Flow cytometry result depicted by the dot plots in Figure 44-2, Q4, suggests a 17.45 ± 1.14% uptake of BODIPY-DLX polymeric nanoparticles by the ARPE-19 cells after 24 h of incubation while there is almost no uptake of the nanoparticles by the HCE cells (Figure 44-4). The low or no cellular uptake by the HCE cells could be due to the morphological tight junction

conformation of the cells after adherence and confluence (IMAYASU *et al.*, 2008; KIMURA *et al.*, 2008; YI *et al.*, 2000).

5.10.4 **Cellular uptake: Confocal**

Figure 45 shows confocal photomicrographs of ARPE-19 cells incubated with BODIPY solution (4-6), blank DLX polymeric nanoparticles (1-3) and BODIPY-DLX polymeric nanoparticles (7-9). Confocal photomicrographs showed significant uptake of BODIPY-DLX polymeric nanoparticles by ARPE-19 cells (Figure 45-9) after 24 h with no uptake observed in the HCE cells in 24 h prompting a further incubation of HCE cells for 48 h (Figure 45-C3).

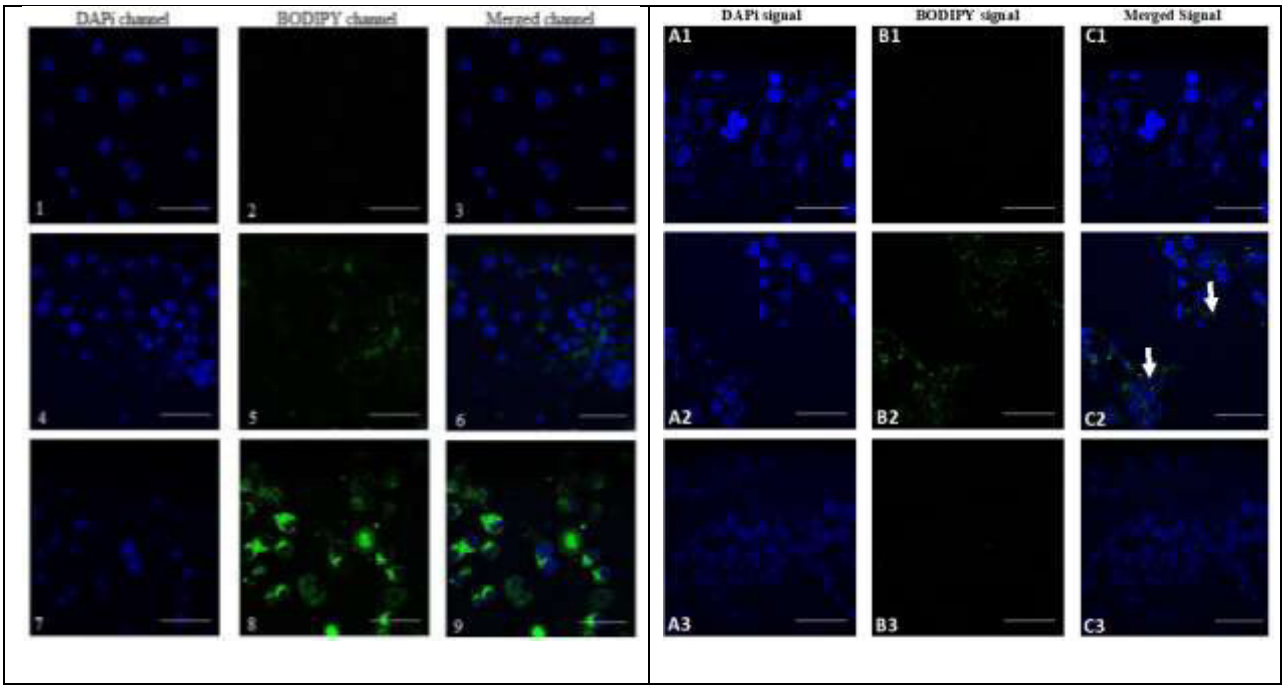

Figure 45: Confocal micrographs of ARPE-19 cells incubated for 24 h with blank DLX polymeric nanoparticles (1 - 3), 5 mg/mL BODIPY solution (4 - 6) and BODIPY-loaded DLX polymeric nanoparticles (7 - 9) and HCE cells incubated for 48 h with blank DLX polymeric nanoparticles (A1 - C1), 5 mg/mL BODIPY solution (A2 – C2) and BODIPY-loaded DLX polymeric nanoparticles (A3 – C3). Cell nuclei are stained blue with DAPi; BODIPY solution or BODIPY-loaded DLX polymeric nanoparticles appears green. White arrows show faint green BODIPY color (x 63 mag with immersion oil). *Scale bar: 20 μm*

Confocal photomicrographs show a minimal uptake of BODIPY (faint green) by ARPE-19 (Figure 45 - 5) or uptake by HCE cells treated with free BODIPY solution as compared to the ARPE-19 cells treated with BODIPY-DLX polymeric nanoparticles, which showed bright green colors (Figure 45 - 8) of the florescent BODIPY after 24 h. Confocal result of BODIPY-DLX polymeric nanoparticles uptake by ARPE-19 further corroborated the flow cytometry results (Figure 44). Studies have suggested nanoparticles are effectively taken up by cells when compared to their free drug solutions (AHN *et al.*, 2013). Thus, the DLX polymeric nanoparticles improved the uptake of BODIPY by the ARPE-19 cells in contrast to control BODIPY solution, implying a possibility of using DLX polymeric nanoparticles as a potential drug carrier for retina related ocular disorders. Furthermore, differences between the uptake of BODIPY in solution and in DLX polymeric nanoparticles suggest that the dye visualized inside the cells are not due to only passive diffusion of BODIPY from the DLX polymeric nanoparticles carrier. It is also important to consider the hydrophilicity of the BODIPY used in these experiments, which should hamper its passive redistribution, thus further confirming the high possibility for the dye observed within the cells being a result of the DLX polymeric nanoparticles uptake. This uptake noticed even after 24 h of experiment suggests that DLX polymeric nanoparticles may be useful for a sustained delivery of hydrophilic drugs in the posterior region of the eye.

Confocal results showed no uptake of BODIPY-DLX polymeric nanoparticles by HCE cells even after 48 h of treatment which further corroborates the flow cytometry results. However, there was a minute uptake of the BODIPY solution by the cells after 48 h treatment (Figure 45 - B2). The low uptake of BODIPY solution and no uptake of BODIPY-DLX polymeric nanoparticles could be due to the morphological tight junctions of the HCE cells as

previously described (IMAYASU *et al.*, 2008; KIMURA *et al.*, 2008; YI *et al.*, 2000). The low uptake of BODIPY solution could also be due to BODIPY metabolism as a function of the long experimental time. Therefore, if fluorescent dyes were taken up after 5 to 15 min incubation, as shown in other study using HCE cells (PRETOR *et al.*, 2015), the probability of BODIPY degradation might be higher after cellular uptake considering the long experimental time. Thus, it can be hypothesized that DLX polymer's mucoadhesive (DEVKAR *et al.*, 2014) and sustained release ability could favor its use topically in the eye, increasing residence time and sustaining drug release.

6 Conclusions

DLX polymer was successfully extracted and purified from the endosperm of Delonix plant. Characteristics of a DLX polymer dispersion in aqueous medium was not detrimentally affected by alkali medium and sonication process. Composition of this dispersion was determined to be a mixture of mannose and galactose at a ratio of 6.3:1 with a Mw between 170 and 185 kDa.

Optimized DLX polymeric nanoparticles were prepared with the sonicated alkali DLX polymeric dispersion. DLX polymeric nanoparticles presented sizes ranged between 215 and 360 nm, adequate polydispersibility and stability. DLX polymer concentration and surfactant mix ratio significantly influenced DLX polymeric nanoparticles sizes, with Tween 80 and Span 80 mix ratio of 3:2 giving the desired DLX polymeric nanoparticles sizes.

The HPLC method developed for the quantification of IST from DLX polymer solution, pig and Wistar rat skin, and commercial Roacutane® capsule was adequate, presenting selectivity, linearity, accuracy and precision values within acceptable quantification and detection limits.

IST and fluorescent BODIPY dyes were successfully loaded into DLX polymeric nanoparticles with approximately 6, 69 and 27 % of lipophilic BODIPY, hydrophilic BODIPY and IST loaded respectively. IST-loaded DLX polymeric nanoparticles sustained the release of IST over 48 h with about 37 % IST released. IST release profile from these nanoparticles presented a burst release followed by a sustained zero order release state.

Lipophilic BODIPY loaded into DLX polymeric nanoparticles showed accumulation in hair follicle in a pig ear skin penetration model. IST-loaded DLX polymeric nanoparticles significantly targeted the hair follicles (26 %) as compared to IST solution (6.5 %) and prevented IST permeation through the skin.

IST-loaded DLX polymeric nanoparticles prevented photo-irritation of Balbc 3T3 Fibroblast cells *in vitro* as compared to IST in DLX polymer solution. IST-loaded DLX polymeric nanoparticles successfully modulated inflammatory response by significantly reducing IL-6 production *in vitro* in *AMJ–2* macrophage cells even after 48 h as compared to free IST in solution.

IST and IST-*loaded DLX polymeric* nanoparticles did not have a direct antibacterial effect against *P. acnes*, suggesting other indirect mechanism of action are involved in the reduction of *P. acnes* in patients treated with IST.

In vivo, IST-loaded DLX polymeric nanoparticles in HEC gel delivered lower but adequate amount of IST to the deeper dermis of Wistar rats, prevented photo-irritation and produced significantly lower epidermal thickness of Wistar rat skin as compared to free IST in HEC gel.

Therefore, in summary, IST-loaded into DLX polymeric nanoparticles can successful target the skin layers where acne is located, deliver adequate IST concentrations for longer period of time, avoid systemic penetration, modulate inflammatory pathogenic stage of acne and also prevent topical irritation associated with IST.

Also, DLX polymeric nanoparticles stability was not affected negatively in simulated ocular fluid components and was non-toxic *in vitro* to ARPE-19 and HCE ocular cell lines. ARPE-19 cells successfully uptake BODIPY-loaded DLX polymeric nanoparticles confirming their probable use for diseases associated with the posterior part of the eye.

In conclusion, DLX polymer could be a promising polymer in drug delivery and DLX polymeric nanoparticles could have prospects as a nano-carrier in the treatment of acne and for ocular delivery purposes.

7 References

ABD, E.; YOUSEF, S. A.; PASTORE, M. N.; TELAPROLU, K.; MOHAMMED, Y. H.; NAMJOSHI, S.; GRICE, J. E., & ROBERTS, M. S. (2016). Skin models for the testing of transdermal drugs. *Clinical pharmacology: advances and applications, 8*, 163.

ADETOGUN, G. E., & ALEBIOWU, G. (2007). Influence of Delonix regia seed gum on the compressional characteristics of paracetamol tablet formulations. *Journal of Drug Delivery Science and Technology, 17*(6), 443-445. doi: 10.1016/s1773-2247(07)50086-9

ADETOGUN, G. E., & ALEBIOWU, G. (2009). Properties of Delonix regia seed gum as a novel tablet binder. *Acta Pol Pharm, 66*(4), 433-438.

AGNIHOTRI, S. A.; MALLIKARJUNA, N. N., & AMINABHAVI, T. M. (2004). Recent advances on chitosan-based micro-and nanoparticles in drug delivery. *Journal of Controlled Release, 100*(1), 5-28.

AHMED, N.; SAMMONS, J.; KHOKHER, M., & HASSAN, H. (2000). Retinoic acid suppresses interleukin 6 production in normal human osteoblasts. *Cytokine, 12*(3), 289-293.

AHMED, T. A., & KHALID, M. (2014). Development of alginate-reinforced chitosan nanoparticles utilizing W/O nanoemulsification/internal crosslinking technique for transdermal delivery of rabeprazole. *Life sciences, 110*(1), 35-43.

AHN, S.; SEO, E.; KIM, K., & LEE, S. J. (2013). Controlled cellular uptake and drug efficacy of nanotherapeutics. *Sci Rep, 3*, 1997. doi: 10.1038/srep01997

ALBANESE, A.; TANG, P. S., & CHAN, W. C. (2012). The effect of nanoparticle size, shape, and surface chemistry on biological systems. *Annual review of biomedical engineering, 14*, 1-16.

ALEXIS, F.; PRIDGEN, E.; MOLNAR, L. K., & FAROKHZAD, O. C. (2008). Factors affecting the clearance and biodistribution of polymeric nanoparticles. *Mol Pharm, 5*(4), 505-515.

ALI, M. E., & LAMPRECHT, A. (2013). Polyethylene glycol as an alternative polymer solvent for nanoparticle preparation. *Int J Pharm, 456*(1), 135-142. doi: 10.1016/j.ijpharm.2013.07.077

ALVAREZ-ROMÁN, R.; NAIK, A.; KALIA, Y. N.; GUY, R. H., & FESSI, H. (2004). Skin penetration and distribution of polymeric nanoparticles. *Journal of Controlled Release, 99*(1), 53-62. doi: https://doi.org/10.1016/j.jconrel.2004.06.015

ANDERSON, J. M., & SHIVE, M. S. (2012). Biodegradation and biocompatibility of PLA and PLGA microspheres. *Advanced Drug Delivery Reviews, 64*, 72-82. doi: 10.1016/j.addr.2012.09.004

ARCHER, C. (2010). Functions of the skin. *Rook's Textbook of Dermatology, Eighth Edition*, 1-11.

AROWOJOLU, A. O.; GALLO, M. F.; LOPEZ, L. M., & GRIMES, D. A. (2012). Combined oral contraceptive pills for treatment of acne. *Cochrane Database Syst Rev, 7*(11).

BARRY, B. (2002). Drug delivery routes in skin: a novel approach. *Advanced Drug Delivery Reviews, 54*, S31-S40.

BASAVARAJ, K.; JOHNSY, G.; NAVYA, M., & RASHMI, R. (2010). Biopolymers as transdermal drug delivery systems in dermatology therapy. *Critical Reviews™ in Therapeutic Drug Carrier Systems, 27*(2).

BENEVENUTO, C. G.; GUERRA, L. O., & GASPAR, L. R. (2015). Combination of retinyl palmitate and UV-filters: Phototoxic risk assessment based on photostability and in vitro and in vivo phototoxicity assays. *European journal of pharmaceutical sciences, 68*, 127-136. doi: 10.1016/j.ejps.2014.12.007

BENTO, J. F.; MAZZARO, I.; DE ALMEIDA SILVA, L. M.; DE AZEVEDO MOREIRA, R.; FERREIRA, M. L. C.; REICHER, F., & DE OLIVEIRA PETKOWICZ, C. L. (2013). Diverse patterns of cell wall mannan/galactomannan occurrence in seeds of the Leguminosae. *Carbohydrate Polymers, 92*(1), 192-199.

BERGLER-CZOP, B., & BRZEZIŃSKA-WCISŁO, L. (2014). Pro-inflammatory cytokines in patients with various kinds of acne treated with isotretinoin. *Advances in Dermatology and Allergology/Postępy Dermatologii i Alergologii, 31*(1), 21.

BETANCUR-ANCONA, D.; PACHECO-AGUIRRE, J.; CASTELLANOS-RUELAS, A., & CHEL-GUERRERO, L. (2011). Microencapsulation of papain using carboxymethylated flamboyant (Delonix regia) seed gum. *Innovative Food Science & Emerging Technologies, 12*(1), 67-72. doi: 10.1016/j.ifset.2010.11.002

BHAMBRI, S.; DEL ROSSO, J. Q., & BHAMBRI, A. (2009). Pathogenesis of acne vulgaris: recent advances. *J Drugs Dermatol, 8*(7), 615-618.

BHARDWAJ, S.; SHUKLA, A., & COLLINS, C. (1995). Effect of varying drug loading on particle size distribution and drug release kinetics of verapamil hydrochloride microspheres prepared with cellulose esters. *J Microencapsul, 12*(1), 71-81.

BHOWMIK, M.; KUMARI, P.; SARKAR, G.; BAIN, M. K.; BHOWMICK, B.; MOLLICK, M. M.; MONDAL, D.; MAITY, D.; RANA, D.; BHATTACHARJEE, D., & CHATTOPADHYAY, D. (2013). Effect of xanthan gum and guar gum on in situ gelling ophthalmic drug delivery system based on poloxamer-407. *Int J Biol Macromol, 62*, 117-123. doi: 10.1016/j.ijbiomac.2013.08.024

BILATI, U.; ALLEMANN, E., & DOELKER, E. (2005). Development of a nanoprecipitation method intended for the entrapment of hydrophilic drugs into nanoparticles. *Eur J Pharm Sci, 24*(1), 67-75. doi: 10.1016/j.ejps.2004.09.011

BOLOGNIA, J. L.; JORIZZO, J. L., & RAPINI, R. P. (2003). Pyoderma gangrenosum. *Dermatology, 1*, 415-418.

BONNET, M. C.; PREUKSCHAT, D.; WELZ, P.-S.; VAN LOO, G.; ERMOLAEVA, M. A.; BLOCH, W.; HAASE, I., & PASPARAKIS, M. (2011). The adaptor protein FADD protects epidermal keratinocytes from necroptosis in vivo and prevents skin inflammation. *Immunity, 35*(4), 572-582.

BOUALLAGUI, Z.; HAN, J.; ISODA, H., & SAYADI, S. (2011). Hydroxytyrosol rich extract from olive leaves modulates cell cycle progression in MCF-7 human breast cancer cells. *Food Chem Toxicol, 49*(1), 179-184. doi: 10.1016/j.fct.2010.10.014

BRADFORD, M. M., & WILLIAMS, W. L. (1977). Protein-assay reagent and method: Google Patents.

BRELSFORD, M., & BEUTE, T. C. (2008). *Preventing and managing the side effects of isotretinoin.* Paper presented at the Seminars in cutaneous medicine and surgery.

BRUNNER, T. J.; WICK, P.; MANSER, P.; SPOHN, P.; GRASS, R. N.; LIMBACH, L. K.; BRUININK, A., & STARK, W. J. (2006). In vitro cytotoxicity of oxide nanoparticles: comparison to asbestos, silica, and the effect of particle solubility. *Environmental science & technology, 40*(14), 4374-4381.

CALVO, P.; VILA-JATO, J., & ALONSO, M. (1997). Effect of lysozyme on the stability of polyester nanocapsules and nanoparticles: stabilization approaches. *Biomaterials, 18*(19), 1305-1310.

CARNEIRO-DA-CUNHA, M. G.; CERQUEIRA, M. A.; SOUZA, B. W. S.; TEIXEIRA, J. A., & VICENTE, A. A. (2011). Influence of concentration, ionic strength and pH on zeta potential and mean hydrodynamic diameter of edible polysaccharide solutions envisaged for multinanolayered films production. *Carbohydrate Polymers, 85*(3), 522-528. doi: 10.1016/j.carbpol.2011.03.001

CASTRO, G.; OLIVEIRA, C.; MAHECHA, G., & FERREIRA, L. (2011). Comedolytic effect and reduced skin irritation of a new formulation of all-trans retinoic acid-loaded solid lipid nanoparticles for topical treatment of acne. *Archives of dermatological research, 303*(7), 513-520.

CERIDONO, M.; TELLNER, P.; BAUER, D.; BARROSO, J.; ALÉPÉE, N.; CORVI, R.; DE SMEDT, A.; FELLOWS, M. D.; GIBBS, N. K., & HEISLER, E. (2012). The 3T3 neutral red uptake phototoxicity test: Practical experience and implications for phototoxicity testing–The report of an ECVAM–EFPIA workshop. *Regulatory Toxicology and Pharmacology, 63*(3), 480-488.

CHARAKIDA, A.; MOUSER, P., & CHU, A. (2004). Safety and side effects of the acne drug, oral isotretinoin. *Expert opinion on drug safety, 3*(2), 119-129.

CIUCANU, I., & KEREK, F. (1984). A simple and rapid method for the permethylation of carbohydrates. *Carbohydrate Research, 131*(2), 209-217.

CLINICALGATEIKNOWLEDGE. (2015). Topical and transdermal drug delivery. from https://clinicalgate.com/topical-and-transdermal-drug-delivery/https://clinicalgate.com/topical-and-transdermal-drug-delivery/https://clinicalgate.com/topical-and-transdermal-drug-delivery/

COATES, P.; ADAMS, C.; CUNLIJFE, W.; MCGINLEY, K.; EADY, E.; LEYDEN, J.; RAVENSCROFT, J.; VYAKRNAM, S., & VOWELS, B. (1997). Does oral isotretinoin prevent Propionibacterium acnes resistance? *Dermatology, 195*(Suppl. 1), 4-9.

COATES, P.; VYAKRNAM, S.; RAVENSCROFT, J.; STABLES, G.; CUNLIFFE, W.; LEYDEN, J.; JOHNSON, J.; EADY, E., & COVE, J. (2005). Efficacy of oral isotretinoin in the control of skin and nasal colonization by antibiotic-resistant propionibacteria in patients with acne. *British Journal of Dermatology, 153*(6), 1126-1136.

COSTA, P., & LOBO, J. (2003). Evaluation of mathematical models describing drug release from estradiol transdermal systems. *Drug development and industrial pharmacy, 29*(1), 89-97.

COSTA, P., & LOBO, J. M. S. (2001). Modeling and comparison of dissolution profiles. *European journal of pharmaceutical sciences, 13*(2), 123-133.

CUNLIFFE, W. (1998). The sebaceous gland and acne–40 years on. *Dermatology, 196*(1), 9-15.

DASH, S.; MURTHY, P. N.; NATH, L., & CHOWDHURY, P. (2010). Kinetic modeling on drug release from controlled drug delivery systems. *Acta Pol Pharm, 67*(3), 217-223.

DE CAMPOS, A. M.; DIEBOLD, Y.; CARBALHO, E. L.; SÁNCHEZ, A., & JOSÉ ALONSO, M. (2005). Chitosan Nanoparticles as New Ocular Drug Delivery Systems: In Vitro Stability, in Vivo Fate, and Cellular Toxicity. *Pharmaceutical Research, 22*(6), 1007-1007.

DE ROSA, F. S.; TEDESCO, A. C.; LOPEZ, R. F. V.; PIERRE, M. B. R.; LANGE, N.; MARCHETTI, J. M.; ROTTA, J. C. G., & BENTLEY, M. V. L. B. (2003). In vitro skin permeation and retention of 5-aminolevulinic acid ester derivatives for photodynamic therapy. *Journal of Controlled Release, 89*(2), 261-269.

DEL ROSSO, J. Q. (2012). Face to face with oral isotretinoin: a closer look at the spectrum of therapeutic outcomes and why some patients need repeated courses. *The Journal of clinical and aesthetic dermatology, 5*(11), 17.

DEVKAR, T. B.; TEKADE, A. R., & KHANDELWAL, K. R. (2014). Surface engineered nanostructured lipid carriers for efficient nose to brain delivery of ondansetron HCl using Delonix regia gum as a natural mucoadhesive polymer. *Colloids Surf B Biointerfaces, 122*, 143-150. doi: 10.1016/j.colsurfb.2014.06.037

DIAS, S. F. L.; NOGUEIRA, S. S.; DE FRANÇA DOURADO, F.; GUIMARÃES, M. A.; DE OLIVEIRA PITOMBEIRA, N. A.; GOBBO, G. G.; PRIMO, F. L.; DE PAULA, R. C. M.; FEITOSA, J. P. A., & TEDESCO, A. C. (2016). Acetylated cashew gum-based nanoparticles for transdermal delivery of diclofenac diethyl amine. *Carbohydrate Polymers, 143*, 254-261.

DUBOIS, M.; GILLES, K. A.; HAMILTON, J. K.; REBERS, P., & SMITH, F. (1956). Colorimetric method for determination of sugars and related substances. *Analytical chemistry, 28*(3), 350-356.

DUNN, J. A.; COBURN, R. A.; EVANS, R. T.; GENCO, R. J., & WALTERS, K. A. (2007). Novel Topically Active Antimicrobial and Anti-inflammatory Compounds for Acne. *Dermatologic, Cosmeceutic, and Cosmetic Development: Therapeutic and Novel Approaches*, 243.

EADY, A. E.; COVE, J. H., & LAYTON, A. M. (2003). Is antibiotic resistance in cutaneous propionibacteria clinically relevant? *American journal of clinical dermatology, 4*(12), 813-831.

ELZOGHBY, A. O.; EL-FOTOH, W. S., & ELGINDY, N. A. (2011). Casein-based formulations as promising controlled release drug delivery systems. *J Control Release, 153*(3), 206-216. doi: 10.1016/j.jconrel.2011.02.010

ERTURAN, İ.; NAZıROĞLU, M., & AKKAYA, V. B. (2012). Isotretinoin treatment induces oxidative toxicity in blood of patients with acne vulgaris: a clinical pilot study. *Cell biochemistry and function, 30*(7), 552-557.

FAKHOURI, T.; YENTZER, B. A., & FELDMAN, S. R. (2009). Advancement in benzoyl peroxide-based acne treatment: methods to increase both efficacy and tolerability. *Journal of drugs in dermatology: JDD, 8*(7), 657-661.

FDA. BENEFITS OF ACCUTANE. from https://www.fda.gov/ohrms/dockets/ac/00/backgrd/3639b1c_04.pdf

FERGUSON, S. A.; CISNEROS, F. J.; GOUGH, B. J., & ALI, S. F. (2005). Four weeks of oral isotretinoin treatment causes few signs of general toxicity in male and female Sprague–Dawley rats. *Food and chemical toxicology, 43*(8), 1289-1296.

FRAUNFELDER, F. T.; FRAUNFELDER, F. W., & EDWARDS, R. (2001). Ocular side effects possibly associated with isotretinoin usage. *American Journal of Ophthalmology, 132*(3), 299-305. doi: https://doi.org/10.1016/S0002-9394(01)01024-8

FRIEDMAN, A. J.; PHAN, J.; SCHAIRER, D. O.; CHAMPER, J.; QIN, M.; PIROUZ, A.; BLECHER-PAZ, K.; OREN, A.; LIU, P. T., & MODLIN, R. L. (2013). Antimicrobial and anti-inflammatory activity of chitosan–alginate nanoparticles: A targeted therapy for cutaneous pathogens. *Journal of Investigative Dermatology, 133*(5), 1231-1239.

FU, P.; CHENG, S.-H.; COOP, L.; XIA, Q.; CULP, S.; TOLLESON, W.; WAMER, W., & HOWARD, P. (2003). Photoreaction, phototoxicity, and photocarcinogenicity of retinoids. *Journal of Environmental Science and Health, Part C, 21*(2), 165-197.

GELFUSO, G. M.; GRATIERI, T.; DELGADO-CHARRO, M. B.; GUY, R. H., & VIANNA LOPEZ, R. F. (2013). Iontophoresis-targeted, follicular delivery of minoxidil sulfate for the treatment of alopecia. *J Pharm Sci, 102*(5), 1488-1494.

GELFUSO, G. M.; GRATIERI, T.; SIMAO, P. S.; DE FREITAS, L. A., & LOPEZ, R. F. (2011). Chitosan microparticles for sustaining the topical delivery of minoxidil sulphate. *J Microencapsul, 28*(7), 650-658. doi: 10.3109/02652048.2011.604435

GIRI, A.; BHUNIA, T.; MISHRA, S. R.; GOSWAMI, L.; PANDA, A. B.; PAL, S., & BANDYOPADHYAY, A. (2013). Acrylic acid grafted guargum–nanosilica membranes for transdermal diclofenac delivery. *Carbohydrate Polymers, 91*(2), 492-501.

GOLMOHAMMADZADEH, S.; MORTEZANIA, S., & JAAFARI, M. R. (2012). Improved photostability, reduced skin permeation and irritation of isotretinoin by solid lipid nanoparticles. *Acta pharmaceutica, 62*(4), 547-562.

GRATIERI, T.; GELFUSO, G. M.; ROCHA, E. M.; SARMENTO, V. H.; DE FREITAS, O., & LOPEZ, R. F. (2010). A poloxamer/chitosan in situ forming gel with prolonged retention time for ocular delivery. *Eur J Pharm Biopharm, 75*(2), 186-193. doi: 10.1016/j.ejpb.2010.02.011

GRENHA, A.; REMUÑÁN-LÓPEZ, C.; CARVALHO, E. L., & SEIJO, B. (2008). Microspheres containing lipid/chitosan nanoparticles complexes for pulmonary delivery of therapeutic proteins. *European Journal of Pharmaceutics and Biopharmaceutics, 69*(1), 83-93.

GRIFFITHS, C.; BARKER, J.; BLEIKER, T.; CHALMERS, R., & CREAMER, D. (2016). *Rook's Textbook of Dermatology, 4 Volume Set*: John Wiley & Sons.

GROVES, R. W.; RAUSCHMAYR, T.; NAKAMURA, K.; SARKAR, S.; WILLIAMS, I. R., & KUPPER, T. S. (1996). Inflammatory and hyperproliferative skin disease in mice that express elevated levels of the IL-1 receptor (type I) on epidermal keratinocytes. Evidence that IL-1-inducible secondary cytokines produced by keratinocytes in vivo can cause skin disease. *Journal of Clinical Investigation, 98*(2), 336.

GUO, H.; LAI, Q.; WANG, W.; WU, Y.; ZHANG, C.; LIU, Y., & YUAN, Z. (2013). Functional alginate nanoparticles for efficient intracellular release of doxorubicin and hepatoma carcinoma cell targeting therapy. *Int J Pharm, 451*(1), 1-11.

GÜRBÜZ, A.; ÖZHAN, G.; GÜNGÖR, S., & ERDAL, M. S. (2015). Colloidal carriers of isotretinoin for topical acne treatment: skin uptake, ATR-FTIR and in vitro cytotoxicity studies. *Archives of dermatological research, 307*(7), 607-615.

GUSTAFSON, H. H.; HOLT-CASPER, D.; GRAINGER, D. W., & GHANDEHARI, H. (2015). Nanoparticle uptake: the phagocyte problem. *Nano today, 10*(4), 487-510.

HAFNER, A.; LOVRIĆ, J.; PEPIĆ, I., & FILIPOVIĆ-GRČIĆ, J. (2011). Lecithin/chitosan nanoparticles for transdermal delivery of melatonin. *J Microencapsul, 28*(8), 807-815.

HOLZHÜTTER, H.-G. (1997). A general measure of in vitro phototoxicity derived from pairs of dose-response curves and its use for predicting the in vivo phototoxicity of chemicals. *ATLA. Alternatives to laboratory animals, 25*(4), 445-462.

HU, B.; SU, Q.; LU, P., & WANG, Y. (2012). BODIPY modified 9-cycloheptatrienylidene fluorene derivatives: Fluorescent "turn-on" for detecting Cu2+ with acidity independence. *Sensors and Actuators B: Chemical, 168*, 310-317. doi: 10.1016/j.snb.2012.04.028

HU, R.; CHEN, Y. Y., & ZHANG, L. M. (2010). Synthesis and characterization of in situ photogelable polysaccharide derivative for drug delivery. *Int J Pharm, 393*(1-2), 96-103. doi: 10.1016/j.ijpharm.2010.04.011

HUANG, S., & FU, X. (2010). Naturally derived materials-based cell and drug delivery systems in skin regeneration. *J Control Release, 142*(2), 149-159. doi: 10.1016/j.jconrel.2009.10.018

HUGHES, B.; NORRIS, J., & CUNLIFFE, W. (1992). A double-blind evaluation of topical isotretinoin 0.05%, benzoyl peroxide gel 5% and placebo in patients with acne. *Clinical and experimental dermatology, 17*(3), 165-168.

ICH. (2005). VALIDATION OF ANALYTICAL PROCEDURES: TEXT AND METHODOLOGY Q2(R1) *ICH HARMONISED TRIPARTITE GUIDELINE*.

IMAYASU, M.; SHIRAISHI, A.; OHASHI, Y.; SHIMADA, S., & CAVANAGH, H. D. (2008). Effects of Multipurpose Solutions on Corneal Epithelial Tight Junctions. *Eye & Contact Lens, 34*(1), 50-55. doi: 10.1097/ICL.0b013e318073cbdb

IOANNIDES, D.; RIGOPOULOS, D., & KATSAMBAS, A. (2002). Topical adapalene gel 0· 1% vs. isotretinoin gel 0· 05% in the treatment of acne vulgaris: a randomized open-label clinical trial. *British Journal of Dermatology, 147*(3), 523-527.

JACOB, C. I.; DOVER, J. S., & KAMINER, M. S. (2001). Acne scarring: A classification system and review of treatment options. *Journal of the American Academy of Dermatology, 45*(1), 109-117. doi: https://doi.org/10.1067/mjd.2001.113451

JAIN, S. K.; GUPTA, Y.; JAIN, A.; SAXENA, A. R.; KHARE, P., & JAIN, A. (2008). Mannosylated gelatin nanoparticles bearing an anti-HIV drug didanosine for site-specific delivery. *Nanomedicine: Nanotechnology, Biology and Medicine, 4*(1), 41-48.

KANITAKIS, J. (2002). Anatomy, histology and immunohistochemistry of normal human skin. *European journal of dermatology: EJD, 12*(4), 390-399; quiz 400-391.

KAPOOR, V. (1972). A galactomannan from the seeds of Delonix regia. *Phytochemistry, 11*(3), 1129-1132.

KATSAMBAS, A., & PAPAKONSTANTINOU, A. (2004). Acne: systemic treatment. *Clinics in dermatology, 22*(5), 412-418.

KELHÄLÄ, H.-L. THE EFFECT OF SYSTEMIC TREATMENT ON IMMUNE RESPONSES AND SKIN MICROBIOTA IN ACNE.

KHOEE, S., & YAGHOOBIAN, M. (2009). An investigation into the role of surfactants in controlling particle size of polymeric nanocapsules containing penicillin-G in double emulsion. *Eur J Med Chem, 44*(6), 2392-2399. doi: 10.1016/j.ejmech.2008.09.045

KHUTORYANSKIY, V. V. (2011). Advances in mucoadhesion and mucoadhesive polymers. *Macromolecular bioscience, 11*(6), 748-764.

KIM, J.-H.; KIM, Y.-S.; PARK, K.; KANG, E.; LEE, S.; NAM, H. Y.; KIM, K.; PARK, J. H.; CHI, D. Y., & PARK, R.-W. (2008). Self-assembled glycol chitosan nanoparticles for the sustained and prolonged delivery of antiangiogenic small peptide drugs in cancer therapy. *Biomaterials, 29*(12), 1920-1930.

KIMURA, K.; TERANISHI, S.; FUKUDA, K.; KAWAMOTO, K., & NISHIDA, T. (2008). Delayed disruption of barrier function in cultured human corneal epithelial cells induced by tumor necrosis factor-alpha in a manner dependent on NF-kappaB. *Invest Ophthalmol Vis Sci, 49*(2), 565-571. doi: 10.1167/iovs.07-0419

KLIGMAN, A. M., & CHRISTOPHERS, E. (1963). Preparation of isolated sheets of human stratum corneum. *Archives of Dermatology, 88*(6), 702-705.

KUMARI, A.; YADAV, S. K., & YADAV, S. C. (2010a). Biodegradable polymeric nanoparticles based drug delivery systems. *Colloids and Surfaces B: Biointerfaces, 75*(1), 1-18.

KUMARI, A.; YADAV, S. K., & YADAV, S. C. (2010b). Biodegradable polymeric nanoparticles based drug delivery systems. *Colloids Surf B Biointerfaces, 75*(1), 1-18. doi: 10.1016/j.colsurfb.2009.09.001

LADEMANN, J.; RICHTER, H.; SCHAEFER, U.; BLUME-PEYTAVI, U.; TEICHMANN, A.; OTBERG, N., & STERRY, W. (2006). Hair follicles–a long-term reservoir for drug delivery. *Skin pharmacology and physiology, 19*(4), 232-236.

LAYTON, A. (2009). The use of isotretinoin in acne. *Dermato-endocrinology, 1*(3), 162-169.

LAZZARI, S.; MOSCATELLI, D.; CODARI, F.; SALMONA, M.; MORBIDELLI, M., & DIOMEDE, L. (2012). Colloidal stability of polymeric nanoparticles in biological fluids. *Journal of Nanoparticle Research, 14*(6), 920. doi: 10.1007/s11051-012-0920-7

LEE, S. J.; KOO, H.; JEONG, H.; HUH, M. S.; CHOI, Y.; JEONG, S. Y.; BYUN, Y.; CHOI, K.; KIM, K., & KWON, I. C. (2011). Comparative study of photosensitizer loaded and conjugated glycol chitosan nanoparticles for cancer therapy. *Journal of Controlled Release, 152*(1), 21-29.

LEHMANN, H. P.; ROBINSON, K. A.; ANDREWS, J. S.; HOLLOWAY, V., & GOODMAN, S. N. (2002). Acne therapy: A methodologic review. *Journal of the American Academy of Dermatology, 47*(2), 231-240. doi: https://doi.org/10.1067/mjd.2002.120912

LI, L.; HAN, J.; NGUYEN, B., & BURGESS, K. (2008). Syntheses and spectral properties of functionalized, water-soluble BODIPY derivatives. *The Journal of organic chemistry, 73*(5), 1963-1970.

LIEBSCH, M., & SPIELMANN, H. (2002a). Currently available in vitro methods used in the regulatory toxicology. *Toxicology letters, 127*(1), 127-134.

LIEBSCH, M., & SPIELMANN, H. (2002b). INVITTOX Protocol No. 78: 3T3 NRU Phototoxicity Assay. European Commission DG-JRC,. *ECVAM, SIS Database, 1998*.

LIN, A.; LIU, Y.; HUANG, Y.; SUN, J.; WU, Z.; ZHANG, X., & PING, Q. (2008). Glycyrrhizin surface-modified chitosan nanoparticles for hepatocyte-targeted delivery. *Int J Pharm, 359*(1), 247-253.

LIU, J.; HU, W.; CHEN, H.; NI, Q.; XU, H., & YANG, X. (2007). Isotretinoin-loaded solid lipid nanoparticles with skin targeting for topical delivery. *Int J Pharm, 328*(2), 191-195.

LOH, J. W.; SAUNDERS, M., & LIM, L. Y. (2012). Cytotoxicity of monodispersed chitosan nanoparticles against the Caco-2 cells. *Toxicol Appl Pharmacol, 262*(3), 273-282. doi: 10.1016/j.taap.2012.04.037

LYONS, R. E. (1978). Comparative effectiveness of benzoyl peroxide and tretinoin in acne vulgaris. *International journal of dermatology, 17*(3), 246-251.

MAGIN, P.; ADAMS, J.; POND, C., & SMITH, W. (2006). Topical and oral CAM in acne: a review of the empirical evidence and a consideration of its context. *Complementary therapies in medicine, 14*(1), 62-76.

MARPLES, R. R.; DOWNING, D. T., & KLIGMAN, A. M. (1971). Control of free fatty acids in human surface lipids by Corynebacterium acnes. *Journal of Investigative Dermatology, 56*(2), 127-131.

MARQUES, M. R.; LOEBENBERG, R., & ALMUKAINZI, M. (2011). Simulated biological fluids with possible application in dissolution testing. *Dissolution Technol, 18*(3), 15-28.

MCCONAUGHY, S. D.; STROUD, P. A.; BOUDREAUX, B.; HESTER, R. D., & MCCORMICK, C. L. (2008). Structural Characterization and Solution Properties of a Galacturonate Polysaccharide Derived from Aloe vera Capable of in Situ Gelation∆. *Biomacromolecules, 9*(2), 472-480.

MCLANE, J. (2001). Analysis of common side effects of isotretinoin. *Journal of the American Academy of Dermatology, 45*(5), S188-S194.

MENG, J.; STURGIS, T. F., & YOUAN, B.-B. C. (2011). Engineering tenofovir loaded chitosan nanoparticles to maximize microbicide mucoadhesion. *European journal of pharmaceutical sciences, 44*(1), 57-67.

MIRSHAHPANAH, P., & MAIBACH, H. I. (2007). Models in acnegenesis. *Cutaneous and ocular toxicology, 26*(3), 195-202.

MITCHELL, D. J., & NINHAM, B. W. (1981). Micelles, vesicles and microemulsions. *Journal of the Chemical Society, Faraday Transactions 2: Molecular and Chemical Physics, 77*(4), 601-629. doi: 10.1039/F29817700601

MITTAL, A.; RABER, A. S.; SCHAEFER, U. F.; WEISSMANN, S.; EBENSEN, T.; SCHULZE, K.; GUZMÁN, C. A.; LEHR, C.-M., & HANSEN, S. (2013). Non-invasive delivery of nanoparticles to hair follicles: A perspective for transcutaneous immunization. *Vaccine, 31*(34), 3442-3451. doi: https://doi.org/10.1016/j.vaccine.2012.12.048

MIYAZAKI, S.; SUZUKI, S.; KAWASAKI, N.; ENDO, K.; TAKAHASHI, A., & ATTWOOD, D. (2001). In situ gelling xyloglucan formulations for sustained release ocular delivery of pilocarpine hydrochloride. *Int J Pharm, 229*(1), 29-36.

MURUGAN, K.; CHOONARA, Y. E.; KUMAR, P.; BIJUKUMAR, D.; DU TOIT, L. C., & PILLAY, V. (2015). Parameters and characteristics governing cellular internalization and trans-barrier trafficking of nanostructures. *Int J Nanomedicine, 10*, 2191.

NAGARWAL, R. C.; KANT, S.; SINGH, P. N.; MAITI, P., & PANDIT, J. K. (2009). Polymeric nanoparticulate system: a potential approach for ocular drug delivery. *J Control Release, 136*(1), 2-13. doi: 10.1016/j.jconrel.2008.12.018

NAIK, A.; KALIA, Y. N., & GUY, R. H. (2000). Transdermal drug delivery: overcoming the skin's barrier function. *Pharmaceutical science & technology today, 3*(9), 318-326.

NG, C. H.; TAM, M. M.; CELI, E.; TATE, B., & SCHWEITZER, I. (2002). Prospective study of depressive symptoms and quality of life in acne vulgaris patients treated with isotretinoin compared to antibiotic and topical therapy. *Australasian journal of dermatology, 43*(4), 262-268.

NITTA, S. K., & NUMATA, K. (2013). Biopolymer-based nanoparticles for drug/gene delivery and tissue engineering. *International journal of molecular sciences, 14*(1), 1629-1654.

NOZAKI, Y.; YAMAGATA, T.; SUGIYAMA, M.; IKOMA, S.; KINOSHITA, K., & FUNAUCHI, M. (2006). Anti-inflammatory effect of all-trans-retinoic acid in inflammatory arthritis. *Clinical Immunology, 119*(3), 272-279.

NWOKOCHA, L. M.; WILLIAMS, P. A., & YADAV, M. P. (2017). Physicochemical characterisation of the galactomannan from Delonix regia seed. *Food Hydrocolloids*.

OBEREMOK, S. S., & SHALITA, A. R. (2002). Acne vulgaris, I: pathogenesis and diagnosis. *CUTIS-NEW YORK-, 70*(2), 101-105.

OECD. (2004). OECD GUIDELINE FOR TESTING OF CHEMICALS: In Vitro 3T3 NRU phototoxicity test *OECD*.

OGUNJIMI, A. T.; MELO, S. M.; VARGAS-RECHIA, C. G.; EMERY, F. S., & LOPEZ, R. F. (2017). Hydrophilic polymeric nanoparticles prepared from Delonix galactomannan with low cytotoxicity for ocular drug delivery. *Carbohydrate Polymers, 157*, 1065-1075.

OPENSTAX. (2017). Anatomy and Physiology. from http://cnx.org/contents/14fb4ad7-39a1-4eee-ab6e-3ef2482e3e22@8.108

ÖZCAN, İ.; AZIZOĞLU, E.; ŞENYIĞIT, T.; ÖZYAZıCı, M., & ÖZER, Ö. (2013). Enhanced dermal delivery of diflucortolone valerate using lecithin/chitosan nanoparticles: in-vitro and in-vivo evaluations. *Int J Nanomedicine, 8*, 461.

OZOLINS, M.; EADY, E. A.; AVERY, A. J.; CUNLIFFE, W. J.; PO, A. L. W.; O'NEILL, C.; SIMPSON, N. B.; WALTERS, C. E.; CARNEGIE, E., & LEWIS, J. B. (2004). Comparison of five antimicrobial regimens for treatment of mild to moderate inflammatory facial acne vulgaris in the community: randomised controlled trial. *The Lancet, 364*(9452), 2188-2195.

PRAJAPAT, A. L., & GOGATE, P. R. (2015). Depolymerization of guar gum solution using different approaches based on ultrasound and microwave irradiations. *Chemical Engineering and Processing: Process Intensification, 88*, 1-9.

PRAUSNITZ, M. R., & LANGER, R. (2008). Transdermal drug delivery. *Nature biotechnology, 26*(11), 1261-1268.

PRAUSNITZ, M. R.; MITRAGOTRI, S., & LANGER, R. (2004). Current status and future potential of transdermal drug delivery. *Nature reviews Drug discovery, 3*(2), 115-124.

PRETOR, S.; BARTELS, J.; LORENZ, T.; DAHL, K.; FINKE, J. H.; PETERAT, G.; KRULL, R.; AL-HALHOULI, A. T.; DIETZEL, A.; BUTTGENBACH, S.; BEHRENDS, S.; REICHL, S., & MULLER-GOYMANN, C. C. (2015). Cellular uptake of coumarin-6 under microfluidic conditions into HCE-T cells from nanoscale formulations. *Mol Pharm, 12*(1), 34-45. doi: 10.1021/mp500401t

PROKSCH, E.; BRANDNER, J. M., & JENSEN, J. M. (2008). The skin: an indispensable barrier. *Experimental dermatology, 17*(12), 1063-1072.

PROW, T. W.; GRICE, J. E.; LIN, L. L.; FAYE, R.; BUTLER, M.; BECKER, W.; WURM, E. M.; YOONG, C.; ROBERTSON, T. A., & SOYER, H. P. (2011). Nanoparticles and microparticles for skin drug delivery. *Advanced Drug Delivery Reviews, 63*(6), 470-491.

QUEILLE-ROUSSEL, C.; PONCET, M.; MESAROS, S.; CLUCAS, A.; BAKER, M., & SOLOFF, A.-M. (2001). Comparison of the cumulative irritation potential of adapalene gel and cream with that of erythromycin/tretinoin solution and gel and erythromycin/isotretinoin gel. *Clinical therapeutics, 23*(2), 205-212.

RAZA, K.; SINGH, B.; SINGAL, P.; WADHWA, S., & KATARE, O. P. (2013). Systematically optimized biocompatible isotretinoin-loaded solid lipid nanoparticles (SLNs) for topical treatment of acne. *Colloids and Surfaces B: Biointerfaces, 105*, 67-74.

RAZA, K.; SINGH, B.; SINGLA, S.; WADHWA, S.; GARG, B.; CHHIBBER, S., & KATARE, O. P. (2013). Nanocolloidal Carriers of Isotretinoin: Antimicrobial Activity against Propionibacterium acnes and Dermatokinetic Modeling. *Mol Pharm, 10*(5), 1958-1963. doi: 10.1021/mp300722f

RIGOPOULOS, D.; LARIOS, G., & KATSAMBAS, A. D. (2010). The role of isotretinoin in acne therapy: why not as first-line therapy? facts and controversies. *Clinics in dermatology, 28*(1), 24-30.

ROHRS, B. R. (2001). Dissolution Method Development for Poorly Soluble Compounds. *Dissolution Technologies, 8*(3), 6-12. doi: 10.14227/dt080301p6

SAIED, N. M., & HAMZA, A. A. (2014). Selenium ameliorates isotretinoin-induced liver injury and dyslipidemia via antioxidant effect in rats. *Toxicology mechanisms and methods, 24*(6), 433-437.

SAKAMOTO, F. H.; LOPES, J. D., & ANDERSON, R. R. (2010). Photodynamic therapy for acne vulgaris: a critical review from basics to clinical practice: part I. Acne vulgaris: when and why consider photodynamic therapy? *Journal of the American Academy of Dermatology, 63*(2), 183-193.

SARMAH, J. K.; MAHANTA, R.; BHATTACHARJEE, S. K.; MAHANTA, R., & BISWAS, A. (2011). Controlled release of tamoxifen citrate encapsulated in cross-linked guar gum nanoparticles. *Int J Biol Macromol, 49*(3), 390-396. doi: 10.1016/j.ijbiomac.2011.05.020

SASSAKI, G. L.; GORIN, P. A.; SOUZA, L. M.; CZELUSNIAK, P. A., & IACOMINI, M. (2005). Rapid synthesis of partially O-methylated alditol acetate standards for GC–MS: Some relative activities of hydroxyl groups of methyl glycopyranosides on Purdie methylation. *Carbohydrate Research, 340*(4), 731-739.

SERRA, L.; DOMENECH, J., & PEPPAS, N. A. (2009). Engineering design and molecular dynamics of mucoadhesive drug delivery systems as targeting agents. *Eur J Pharm Biopharm, 71*(3), 519-528. doi: 10.1016/j.ejpb.2008.09.022

SHAM, J. O.-H.; ZHANG, Y.; FINLAY, W. H.; ROA, W. H., & LÖBENBERG, R. (2004). Formulation and characterization of spray-dried powders containing nanoparticles for aerosol delivery to the lung. *Int J Pharm, 269*(2), 457-467.

SMART, J. D. (2005). The basics and underlying mechanisms of mucoadhesion. *Adv Drug Deliv Rev, 57*(11), 1556-1568. doi: 10.1016/j.addr.2005.07.001

SOPPIMATH, K. S.; AMINABHAVI, T. M.; KULKARNI, A. R., & RUDZINSKI, W. E. (2001). Biodegradable polymeric nanoparticles as drug delivery devices. *Journal of Controlled Release, 70*(1), 1-20.

SPIEWAK, R.; GREGORIUS, A., & SZNELEWSKI, P. (2012). A new in vitro protocol for assessing phototoxic effects of xenobiotics on human keratinocytes. *Estetol Med Kosmetol, 2*, 110-114.

STRAHAN, J. E., & RAIMER, S. (2006). Isotretinoin and the controversy of psychiatric adverse effects. *International journal of dermatology, 45*(7), 789-799.

TAMAKI, Y.; TERUYA, T., & TAKO, M. (2010). The chemical structure of galactomannan isolated from seeds of Delonix regia. *Biosci Biotechnol Biochem, 74*(5), 1110-1112. doi: 10.1271/bbb.90935

TAN, J., & BHATE, K. (2015). A global perspective on the epidemiology of acne. *British Journal of Dermatology, 172*(S1), 3-12.

TAN, Q.; LIU, W.; GUO, C., & ZHAI, G. (2011). Preparation and evaluation of quercetin-loaded lecithin-chitosan nanoparticles for topical delivery. *Int J Nanomedicine, 6*, 1621.

TANG, H.; MITRAGOTRI, S.; BLANKSCHTEIN, D., & LANGER, R. (2001). Theoretical description of transdermal transport of hydrophilic permeants: Application to low-frequency sonophoresis. *J Pharm Sci, 90*(5), 545-568.

TEICHMANN, A.; JACOBI, U.; OSSADNIK, M.; RICHTER, H.; KOCH, S.; STERRY, W., & LADEMANN, J. (2005). Differential stripping: determination of the amount of topically applied substances penetrated into the hair follicles. *Journal of General Internal Medicine, 20*(5), 264-269.

TEKADE, A. R., & GATTANI, S. G. (2009). Development and evaluation of pulsatile drug delivery system using novel polymer. *Pharm Dev Technol, 14*(4), 380-387.

TEKADE, A. R., & GATTANI, S. G. (2010). Development and evaluation of a pulsatile drug delivery system using novel polymer. Part II: In vivo radio imaging study. *Pharm Dev Technol, 15*(6), 666-668.

THIBOUTOT, D.; GOLLNICK, H.; BETTOLI, V.; DRÉNO, B.; KANG, S.; LEYDEN, J. J.; SHALITA, A. R.; LOZADA, V. T.; BERSON, D.; FINLAY, A.; GOH, C. L.; HERANE, M. I.; KAMINSKY, A.; KUBBA, R.; LAYTON, A.; MIYACHI, Y.; PEREZ, M.; MARTIN, J. P.; RAMOS-E-SILVA, M.; SEE, J. A.; SHEAR, N., & WOLF, J. (2009). New insights into the management of acne: An update from the Global Alliance to Improve Outcomes in Acne Group. *Journal of the American Academy of Dermatology, 60*(5, Supplement 1), S1-S50. doi: https://doi.org/10.1016/j.jaad.2009.01.019

TOYODA, M., & MOROHASHI, M. (2001). Pathogenesis of acne. *Medical Electron Microscopy, 34*(1), 29-40.

TUCKER, S. B.; ROGERS, R. S.; WINKELMANN, R.; PRIVETT, O. S., & JORDON, R. E. (1980). Inflammation in acne vulgaris: leukocyte attraction and cytotoxicity by comedonal material. *Journal of Investigative Dermatology, 74*(1), 21-25.

VARANI, J.; FLIGIEL, H.; ZHANG, J.; ASLAM, M. N.; LU, Y.; DEHNE, L. A., & KELLER, E. T. (2003). Separation of retinoid-induced epidermal and dermal thickening from skin irritation. *Archives of dermatological research, 295*(6), 255-262.

VERONOVSKI, N.; ANDREOZZI, P.; LA MESA, C., & SFILIGOJ-SMOLE, M. (2010). Stable TiO2 dispersions for nanocoating preparation. *Surface and Coatings Technology, 204*(9-10), 1445-1451. doi: 10.1016/j.surfcoat.2009.09.041

VOIGT, N.; HENRICH-NOACK, P.; KOCKENTIEDT, S.; HINTZ, W.; TOMAS, J., & SABEL, B. A. (2014). Toxicity of polymeric nanoparticles in vivo and in vitro. *Journal of Nanoparticle Research, 16*(6), 2379.

WANG, A. Z.; LANGER, R., & FAROKHZAD, O. C. (2012). Nanoparticle delivery of cancer drugs. *Annual review of medicine, 63*, 185-198.

WANG, J. J.; ZENG, Z. W.; XIAO, R. Z.; XIE, T.; ZHOU, G. L.; ZHAN, X. R., & WANG, S. L. (2011). Recent advances of chitosan nanoparticles as drug carriers. *Int J Nanomedicine, 6*, 765.

WEBMDRESOURCES. An Overview of the Skin. from https://www.webmd.com/beauty/cosmetic-procedures-overview-skin#1

WILLIAMS, A. (2003). *Transdermal and topical drug delivery: from theory to clinical practice*: Pharmaceutical Press London.

WILLIAMS, A. C., & BARRY, B. W. (2012). Penetration enhancers. *Advanced Drug Delivery Reviews, 64*, 128-137.

WILLIAMS, H. C.; DELLAVALLE, R. P., & GARNER, S. (2012). Acne vulgaris. *The Lancet, 379*(9813), 361-372. doi: https://doi.org/10.1016/S0140-6736(11)60321-8

WIN, K. Y., & FENG, S.-S. (2005). Effects of particle size and surface coating on cellular uptake of polymeric nanoparticles for oral delivery of anticancer drugs. *Biomaterials, 26*(15), 2713-2722.

WOLF, J. E. (2002). Potential anti-inflammatory effects of topical retinoids and retinoid analogues. *Advances in therapy, 19*(3), 109-118.

YENTZER, B. A.; MCCLAIN, R. W., & FELDMAN, S. R. (2009). Do topical retinoids cause acne to" flare"? *Journal of drugs in dermatology: JDD, 8*(9), 799-801.

YI, X.-J.; WANG, Y., & FU-SHIN, X. Y. (2000). Corneal epithelial tight junctions and their response to lipopolysaccharide challenge. *Investigative ophthalmology & visual science, 41*(13), 4093-4100.

ZAENGLEIN, A. L.; PATHY, A. L.; SCHLOSSER, B. J.; ALIKHAN, A.; BALDWIN, H. E.; BERSON, D. S.; BOWE, W. P.; GRABER, E. M.; HARPER, J. C.; KANG, S.; KERI, J. E.; LEYDEN, J. J.; REYNOLDS, R. V.; SILVERBERG, N. B.; STEIN GOLD, L. F.; TOLLEFSON, M. M.; WEISS, J. S.; DOLAN, N. C.; SAGAN, A. A.; STERN, M.; BOYER, K. M., & BHUSHAN, R. (2016). Guidelines of care for the management of acne vulgaris. *Journal of the American Academy of Dermatology, 74*(5), 945-973.e933. doi: https://doi.org/10.1016/j.jaad.2015.12.037

ZAHOOR, A.; SHARMA, S., & KHULLER, G. (2005). Inhalable alginate nanoparticles as antitubercular drug carriers against experimental tuberculosis. *International journal of antimicrobial agents, 26*(4), 298-303.

ZHANG, Y.; HUO, M.; ZHOU, J.; ZOU, A.; LI, W.; YAO, C., & XIE, S. (2010). DDSolver: An Add-In Program for Modeling and Comparison of Drug Dissolution Profiles. *The AAPS Journal, 12*(3), 263-271. doi: 10.1208/s12248-010-9185-1

ZHANG, Z.; TSAI, P. C.; RAMEZANLI, T., & MICHNIAK-KOHN, B. B. (2013). Polymeric nanoparticles-based topical delivery systems for the treatment of dermatological diseases. *Wiley Interdisciplinary Reviews: Nanomedicine and Nanobiotechnology, 5*(3), 205-218.

ZHAO, F.; ZHAO, Y.; LIU, Y.; CHANG, X.; CHEN, C., & ZHAO, Y. (2011). Cellular uptake, intracellular trafficking, and cytotoxicity of nanomaterials. *Small, 7*(10), 1322-1337. doi: 10.1002/smll.201100001

ZOUBOULIS, C.; EADY, A.; PHILPOTT, M.; GOLDSMITH, L.; ORFANOS, C.; CUNLIFFE, W., & ROSENFIELD, R. (2005). What is the pathogenesis of acne? *Experimental dermatology, 14*(2), 143-143.

ZOUBOULIS, C. C. (2006). Isotretinoin revisited: pluripotent effects on human sebaceous gland cells. *Journal of Investigative Dermatology, 126*(10), 2154-2156.

ZOUBOULIS, C. C.; XIA, L.; AKAMATSU, H.; SELTMANN, H.; FRITSCH, M.; HORNEMANN, S.; RÜHL, R.; CHEN, W.; NAU, H., & ORFANOS, C. (1998). The human sebocyte culture model provides new insights into development and management of seborrhoea and acne. *Dermatology, 196*(1), 21-31.

ZUO, J.; GAO, Y.; BOU-CHACRA, N., & LÖBENBERG, R. (2014). Evaluation of the DDSolver software applications. *BioMed research international, 2014*.

ANNEX

UNIVERSIDADE DE SÃO PAULO
Faculdade de Ciências Farmacêuticas de Ribeirão Preto
COMISSÃO DE ÉTICA NO USO DE ANIMAIS

AUTORIZAÇÃO

Certificamos que a proposta intitulada "Toxicidade e segurança de nanopartículas de Delonix contendo isotretinoína administrada por via tópica e oral", registrada sob nº 17.5.213.60.3, sob a responsabilidade de Abayomi Tolulope Ogunjimi e Renata Fonseca Vianna Lopez, que envolve a manutenção e utilização de animais pertencentes ao filo Chordata, subfilo Vertebrata (exceto o homem) para fins de pesquisa científica encontra-se de acordo com os preceitos da Lei nº 11.794, de 8 de outubro de 2008, do Decreto º 6.899, de 15 de julho de 2009, e com as normas editadas pelo Conselho Nacional de Controle da Experimentação Animal (CONCEA), foi aprovada na reunião de 26/10/2017 pela Comissão de Ética no Uso de Animais da Faculdade de Ciências Farmacêuticas de Ribeirão Preto (CEUA FCFRP).

Lembramos da obrigatoriedade de apresentação do relatório de atividades, em modelo da CEUA, para emissão do certificado, como disposto nas Resoluções Normativas do CONCEA.

Finalidade	( ) Ensino (x) Pesquisa Científica
Vigência da Autorização	15/11 a 21/12/2017
Espécie/Linhagem/Raça	Rato heterogênico Wistar
Nº de animais	96
Peso/Idade	180-220g/ 6-8 semanas
Sexo	Macho
Origem	Biotério Central do Campus USP RP

Ribeirão Preto, 27 de outubro de 2017.

Ana Patrícia Yatsuda Natsui
Coordenadora da CEUA-FCFRP

Avenida do Café S/N° - Monte Alegre - CEP: 14040-903 - Ribeirão Preto – SP
Comissão de Ética no Uso de Animais – ceua@fcfrp.usp.br
Fone: (16) 3315-8559 – Fax: (16) 33152-4892

Histology Preparation bench set-up